COMPUTATIONAL DESIGN OF SMALL ORGANIC MOLECULES AS ENZYME MIMICS: SPIROCYCLIC ORGANOCATALYSTS WITH HIGH-LEVEL STRUCTURAL AND ELECTROSTATIC PREORGANIZATION FOR TRANSESTERIFICATION REACTIONS

by
Zahide Merve Tanyeri

Submitted to Graduate School of Natural and Applied Sciences
in Partial Fulfillment of the Requirements
for the Degree of Master of Science in
Chemical Engineering

Yeditepe University
2019

COMPUTATIONAL DESIGN OF SMALL ORGANIC MOLECULES AS ENZYME MIMICS: SPIROCYCLIC ORGANOCATALYSTS WITH HIGH-LEVEL STRUCTURAL AND ELECTROSTATIC PREORGANIZATION FOR TRANSESTERIFICATION REACTIONS

APPROVED BY:

Assoc. Prof. Nihan Çelebi Ölçüm ..... ncelebi .....
(Thesis Supervisor)
(Yeditepe University)

Assoc. Prof. Tuğba Davran Candan .....
(Yeditepe University)

Assist. Prof. Burcu Dedeoğlu .....
(Gebze Technical University)

DATE OF APPROVAL: ..../..../2019

ACKNOWLEDGEMENTS

It is with immense gratitude that I acknowledge the support and help of my Professor Nihan Çelebi-Ölçüm. Pursuing my thesis under her supervision has been an experience which broadens the mind and presents an unlimited source of learning.

This study was supported by TUBITAK 1001 (116Z514). The calculations reported in this thesis were completely performed at TUBITAK ULAKBIM, High Performance and Grid Computing Center.

I would like to thank my lovely friends Sezen Alsancak and Yeşim Çamlısoy for their support and warm friendship.

Finally, I would like to thank my family for their endless love and support, which makes everything more beautiful.

ABSTRACT

COMPUTATIONAL DESIGN OF SMALL ORGANIC MOLECULES AS ENZYME MIMICS: SPIROCYCLIC ORGANOCATALYSTS WITH HIGH-LEVEL STRUCTURAL AND ELECTROSTATIC PREORGANIZATION FOR TRANSESTERIFICATION REACTIONS

Natural enzymes are proficient catalysts. In the past few years, chemists have tried to mimic enzymes and synthesized amino-acid based catalysts to optimize efficiency of many different transformations. Recently, new transesterification catalysts were developed called "spiroligozymes", by placing the catalytic machinery of esterase enzymes onto modular spiro-fused bispeptides with the help of quantum mechanical transition state calculations using the "inside-out" approach. Molecular dynamics simulations showed that, in contrast to the observed behavior in naturally evolved enzymes, the catalytic groups in spiroligozymes sample numerous alternative conformations and the H-bond between the nucleophilic dyad essential for catalysis is not maintained. These computational results suggest that the activities of spiroligozymes can be significantly improved by providing a high-level preorganization of the catalytic functional groups. For this purpose, the structural modifications that eliminate non-reactive conformations of spiroligozymes and fix the active conformation of catalytic groups were identified. Medchem transformations were used to obtain spiroligozyme derivatives. Conformational library for each spirologozyme derivative was generated with the MMFF force field using lowmodeMD sampling procedure. The conformers of selected derivatives were evaluated by quantum mechanical calculations. Molecular dynamics (MD) simulations were performed to evaluate whether the designed catalytic contacts were maintained in a dynamic environment in the presence of explicit solvent molecules. This work constitutes an important step towards the computational design of organocatalysts with preorganized functional groups as well as reaching an enzyme-like activity with small organic molecules.

ÖZET

ENZİMLERİ MİMİK EDEN KÜÇÜK ORGANİK MOLEKÜLLERİN HESAPSAL TASARIMI: TRANSESTERİFİKASYON TEPKİMELERİ İÇİN YÜKSEK SEVİYE YAPISAL VE ELEKTROSTATİK ÖN ORGANİZASYONA SAHİP SPİROSİKLİK ORGANOKATALİZÖRLER

Doğanın usta katalizörleri olan enzimlerin katalitik gücünü taşıyan yeni yeşil katalizörlerin geliştirilmesi son yıllarda üzerinde en çok çalışılan konulardan biridir. Yakın geçmişte, esteraz enzimlerinin katalitik mekanizması "içten-dışa" tasarım yaklaşımı kullanarak, kuantum mekaniksel geçiş konumu modelleri yardımıyla modüler spiro-birleşik bispeptidlerin üzerine yerleştirerek "spiroligozim" adı verilen yeni transesterifikasyon katalizörleri geliştirildi. Ancak moleküler dinamik simülasyonları, doğal olarak evrimleşen enzimlerde gözlenenin aksine, spiroligozimlerdeki katalitik grupların aktif konformasyonun yanında birçok alternatif konformasyonu da örneklediğini ve alkol-piridil ikilisi arasındaki hidrojen bağının korunmadığını ortaya koymuştur. Bu hesapsal sonuçlar, spiroligozimlerin aktivitelerinin, katalitik fonksiyonel grupların ön-organizasyonlarının sağlanması yoluyla büyük ölçüde artırılabileceğini göstermektedir. Bu amaçla, hesapsal modeller kullanılarak, spiroligozmlerin reaktif olmayan konformasyonları saf dışı ederek katalitik grupların aktif konformasyonlarının molekül için hidrojen bağları yardımıyla sabitlenmesi için gerekli yapısal değişiklikler belirlenmiştir. Böylece transesterifikasyon spiroligozimlerinin katalitik etkilerinin artırılması hedeflenmiştir. Spiroligozim türevlerini elde etmek için Medchem dönüşümleri kullanılmıştır. MMFF kuvvet alanı ile her bir spirologozim türevi için konformasyon kütüphanesi oluşturulmuştur. Seçilen konformerler kuantum mekaniksel hesaplamalar ile değerlendirilmiştir. Moleküler dinamik (MD) simülasyonları ile tasarlanan katalitik ikili arasındaki bağın açık bir çözücü molekülü varlığında dinamik bir ortamda muhafaza edilip edilmediği değerlendirilmiştir. Bu çalışma, gerek ön-organizasyona sahip organokatalizörlerin hesapsal tasarımında gerekse küçük organik moleküller ile enzim benzeri aktiviteye ulaşılmasında önemli bir adımdır.

TABLE OF CONTENTS

LIST OF FIGURES

LIST OF TABLES

LIST OF SYMBOLS/ABBREVIATIONS

A	Helmholtz free energy
Å	Angstrom
⟨A⟩	Ensemble average value of property A
D	Distance / Chirality center points to the right
E	Electronic energy
$\hat{H}$	Hamiltonian operator
K	Kelvin
k_i	Force constant
$l_i, l_{i,0}$	Bond length
L	Chirality center points to the left
M	Number of nuclei
N	Number of particles in system
p^N	Momenta of the N particles in the system
R	Gas constant
r_{ij}	Distances between two particles i and j
r^N	Positions of the N particles in the system
q_i	Partial charge on atom i
q_j	Partial charge on atom j
T	Temperature
V_n	Barrier height
α	Alpha
β	Beta
γ	Phase factor
ε_0	Dielectric constant in vacuo
ε_{ij}	Well depth parameter in Lennard-Jones pairwise potential function
$\theta, \theta_i, \theta_{i,0}$	Bond angle
σ_{ij}	Collision diameter used in Lennard-Jones function

ψ	Wavefunction
ω	Torsion angle
ΔE	The change in internal energy of a system

3-D	Three dimensional
Asn	Asparagine
Asp	Aspartate
Atm	Atmosphere
Cos	Cosinus
Cys	Cystine
BF3	Bifunctional spiroligozyme
DFT	Density functional theory
FFA	Free fatty acid
Fs	Femtosecond
GAFF	General amber force field
Glu	Glutamate
HF	Hartree-fock
His	Histidine
IEF-PCM	Integral-equation-formalism polarizable continuum model
Kcal/mol	Kilocalorie per mol
MD	Molecular dynamics
MM	Molecular mechanics
MMFF94x	Merck molecular force field
MOE	Molecular operating environment
NPT	Isotermic isobaric ensemble
Ns	Nanosecond
PE	Total potential energy of system
RESP	Restrained electrostatic potential
QM	Quantum mechanics
Ser	Serine
SMD	Solvation model based on electron density
TF3	Trifunctional spiroligozyme

1. INTRODUCTION

Enzymes are biological catalysts that are used in many reactions of living organisms [1]. There are more than 5000 biological processes catalyzed by enzymes. They have excellent activity in aqueous media under ambient conditions [2]. Enzymes are also preferred in industrial applications instead of the synthetic catalysts because they are environmentally friendly. There are many different large scale industrial applications of enzymes such as; production of drugs, detergents, drinks and sugars [1], [3].

Enzymes are good catalyst alternatives to eliminate problems of acid or base catalyzed transesterification processes. For example, acid catalysts used in the transesterification reactions can be inhibited by water but enzymes are not adversely affected by the presence of water. Moreover, enzymes can convert free fatty acids (FFA) to fatty acid alkyl esters completely, which makes it possible to use low cost raw materials such as waste oil or lard. Immobilization of enzymes leads to facilitation of the seperation process. As such, products can be seperated easily and it is possible to obtain high quality glycerol. Additionally, immobilization enables the reuse of catalyst [1], [4], [5].

Some advantages of using enzymes instead of acid and alkali catalysts are [1], [6], [7], [8];

- Prevention of soap formation.
- Esterification of FFA's and triglycerides in one step and no requirement for a washing process.
- Increase in the quality of glycerol.
- Toleration to the raw material with different quality like waste oils, animal fat. Different types of waste oils and animal fat with high FFA and water content can be catalyzed successfully using enzymes.
- Catalysis with less energy consumption.
- Lower alcohol to oil ratio requirement.

There are several disadvantages in enzymatic transesterification [1], [5], [8];

- Reaction time is longer than the reaction with acid or alkali catalyst.
- Higher catalyst concentration is required.

- Enzymes are more expensive compared to alkali catalyst. For example, usage of lipase in a process has higher cost compared to sodium hydroxide.
- Reuse of enzyme is possible but after 100 days of application it loses activity.

Hydrolytic enzymes (hydrolases) such as, esterases, proteases and lipases are used to catalyze hydrolysis reactions to maintain our metabolism [9], [10]. Esterases and proteases are proficient enzymes that catalyze the hydrolysis of carboxyl esters and amides, respectively [10]. For example, serine protease is a natural well-understood enzyme, which plays a vital role in living organisms. This enzyme accelerates peptide hydrolysis approximately 10^{10}- fold compared to the uncatalyzed reaction [11], [12]. Lipases are naturally evolved catalysts efficient in catalysis of transesterification reactions [13]. They also help to resolve problems resourced from chemical catalysts for both esterification and transesterification reactions [14], [15], [16].

Hydrolases function via formation of a covalent bond between enzyme and substrate through nucleophilic catalysis mechanism. Figure 1.1 represents the catalytic mechanism of hydrolase enzymes. After the formation of enzyme-substrate complex, in order to initiate catalysis, a nucleophile must be activated in the enzyme active site. This is achieved via proton shuttle mechanism in a so-called “catalytic triad” or alternatively “nucleophilic triad”. A catalytic triad is composed of three amino-acid residues interacting with each other via a well-maintained H-bond network. The most common catalytic triads occurring in natural proteins are Ser-His-Asp, Ser-His-Glu, Cys-His-Asp, Ser-His-His, and Ser-Glu-Asp [9]. As a specific example, serine proteases use Ser-His-Asp triad as the nucleophile [17], [18], [19].

The presence of aspartate increases the basicity of histidine, and in turn histidine activates serine as a nucleophile by abstracting the proton from the hydroxyl group [9], [20], [21]. The activated serine through this proton shuttle mechanism attacks ester or peptide bond of the substrate forming a tetrahedral oxyanionic intermediate. This intermediate is stabilized by a number of H-bonding interactions in a region called the “oxyanion hole” [22], [23]. These key catalytic elements of hydrolase enzymes are shown in Figure 1.2. As such, protein binds the substrate covalently and formation of this acyl-enzyme intermediate is known as the acylation step. Now protonated histidine acts as the acid and activates the C terminal fragment of ester on peptide as a leaving group. A water (for esterases or

proteases) or an alcohol (for lipases) bound in the active site attacks the ester bond between serine and the substrate breaking the covalent bond. As a result, product is released and free enzyme is regenerated. This process is called the deacylation step in the catalytic cycle [24].

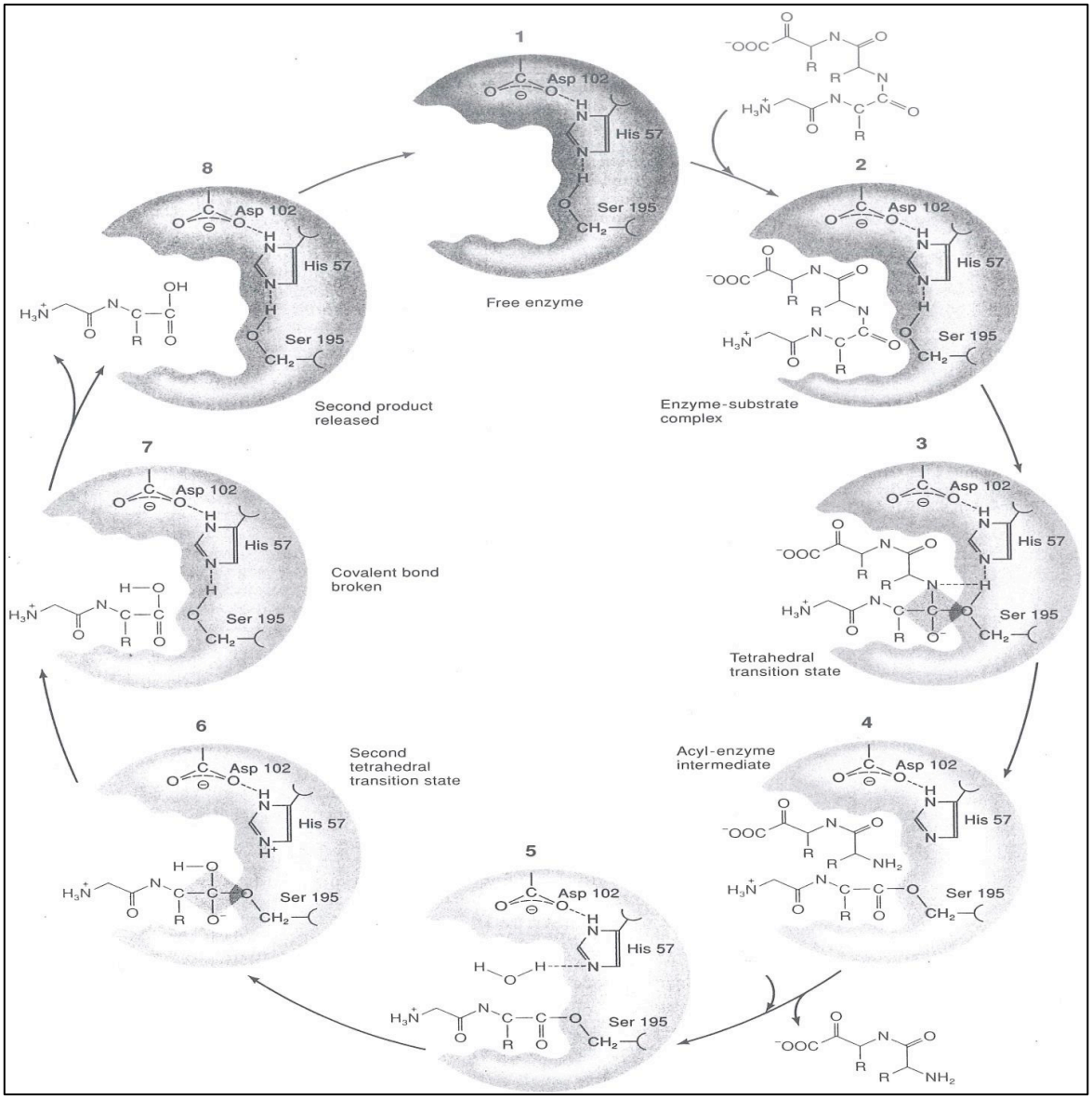

Figure 1.1. Representation of catalytic mechanism of hydrolases [24]

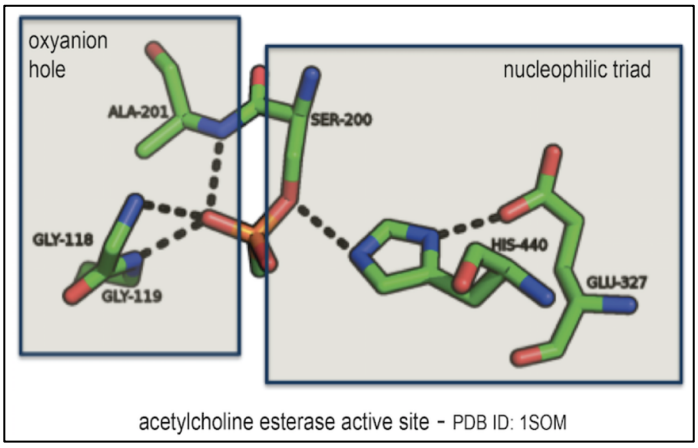

Figure 1.2. Key catalytic elements of acetylcholine esterase as taken form the crystal structure with PDB ID: 1SOM

Even though H-bond is weaker than a covalent bond [25], it is primarily essential underlying many kinds of chemical processes. Especially, preorganized H-bond networks in a catalytic active site enable catalysis. Hydrolases have high-level structural and electrostatic preorganization through a well-maintained H-bond network in their active site and this provides high proficiency in hydrolysis during multiple chemical steps [10]. Indeed, molecular dynamics (MD) simulations showed that hydrogen bonds between the catalytic triad, which are essential for the proton shuttle mechanism, were tightly maintained in a solvated dynamic environment [26].

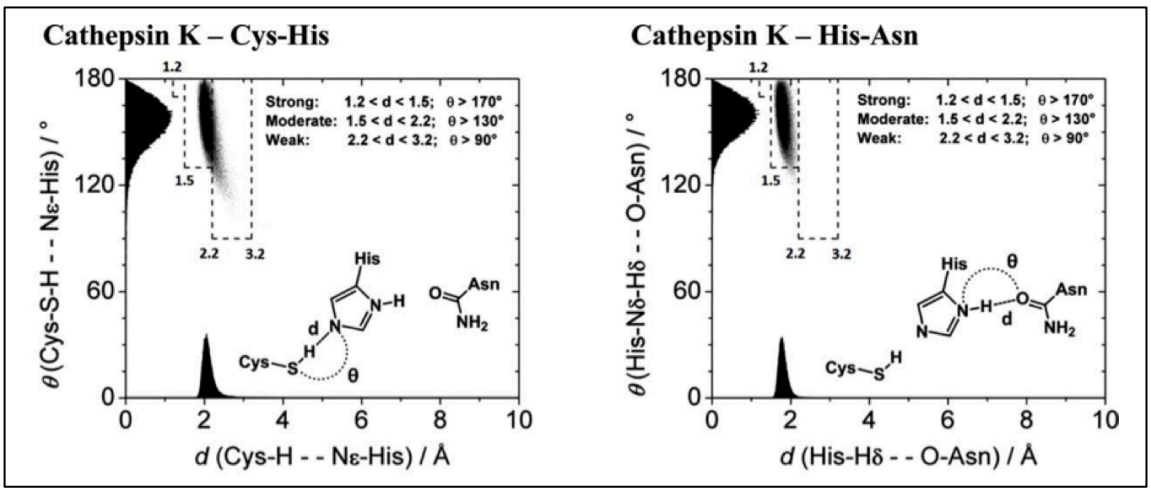

Figure 1.3. MD results of natural enzyme Cathepsin K - angle vs. distance graph of the relation between catalytic triad [26]

MD population is a term that is used to define cumulation of MD snapshots in the H-bond region ($1.2 < d < 3.2$; $90 < \theta < 180$) in the H-bond angle (θ) - distance (d) plot. Figure 1.3 shows the H-bond distance-angle graphs of the catalytic triad of Cathepsin K, a naturally evolved enzyme, obtained by molecular dynamics simulations [26]. This figure shows that the hydrogen bond lengths between cysteine-histidine and histidine-asparagine are densely cumulated in the moderate H-bond region ($1.5 < d < 2.2$; $\theta > 130$). In this respect, H-bond plays an important role in the design of new enzymes and catalytic active sites [27].

Chemical modification of a natural enzyme enables the design of new enzymes for different reactions [28]. However, the number of parameters to be handled and controlled to develop new enzymes is exceedingly high and design of such a structurally complex molecule is still a challenging task. Development of small molecule catalysts that mimic the catalytic properties of enzymes is a field of study that has emerged with the concept of biomimetic chemistry [29], [7]. Biomimetic chemistry is a term that is used to describe the imitation of natural biological processes and reactions by creating new processes or molecules [30]. In biomimetic catalysis, excellence in enzyme-substrate active site relationship, high turnover rate at catalytic reactions and significant increase in reaction rate relative to the background reaction are targeted [31], [32].

In recent years, much effort has been devoted to the identification and development of small molecule organic catalyst for transesterification reactions that mimic the functional group richness of enzyme active sites [33].

Miller has identified oligopeptides that perform acyl transfer reactions enantioselectively by screening small peptide libraries. The oligopeptide shown in Figure 1.4 is the most reactive catalyst, which displayed a 51-fold increase in the reaction rate compared to the control catalyst with no secondary structure [34].

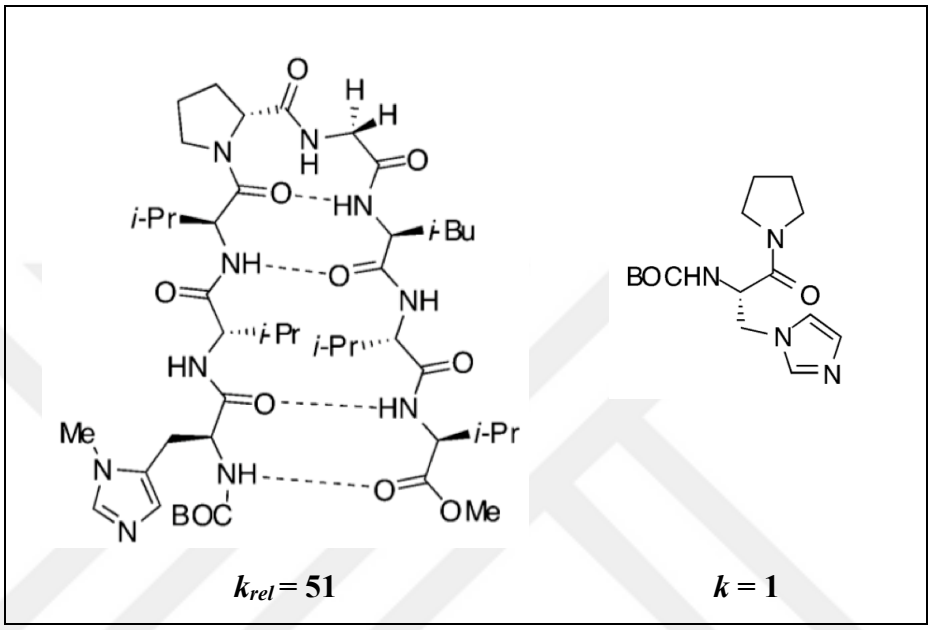

Figure 1.4. Oligopeptide developed by Miller for catalysis of acyl transfer reactions [34]

Sakai and coworkers have developed trifuctional organocatalysts that mimic serine esterase catalytic active site. The catalyst shown in Figure 1.5 accelerated acyl-transfer reactions from vinyl trifluoroacetate to alcohol up to 1.9×10^5-fold [35].

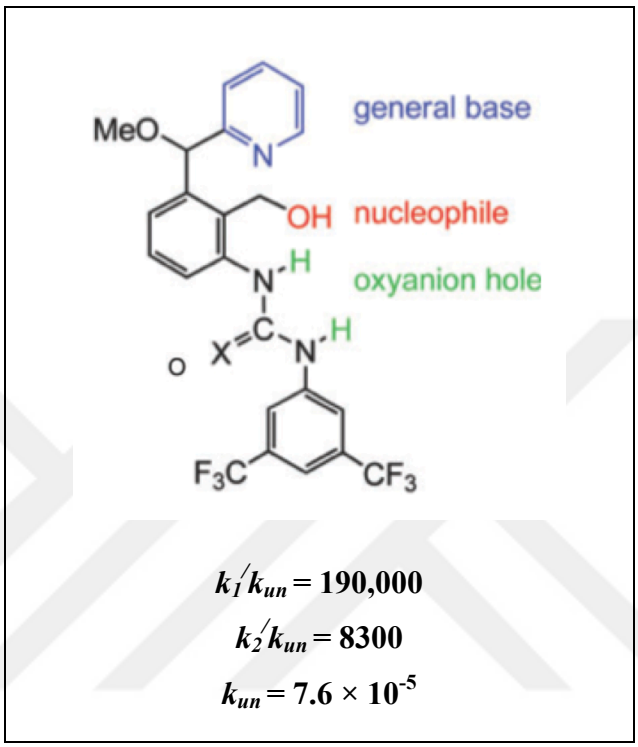

Figure 1.5. Trifunctional organocatalyst developed by Sakai et al. for catalysis of acyl transfer reactions [35]

Matsumoto et al. have analyzed histidine containing β-hairpin libraries to develop strategies to accelerate acyl- and phosphonyl-transfer reactions. In their work, rate accelerations in organic solvents of up to 2.4×10^8 were observed for the oligopeptide shown in Figure 1.6 [36].

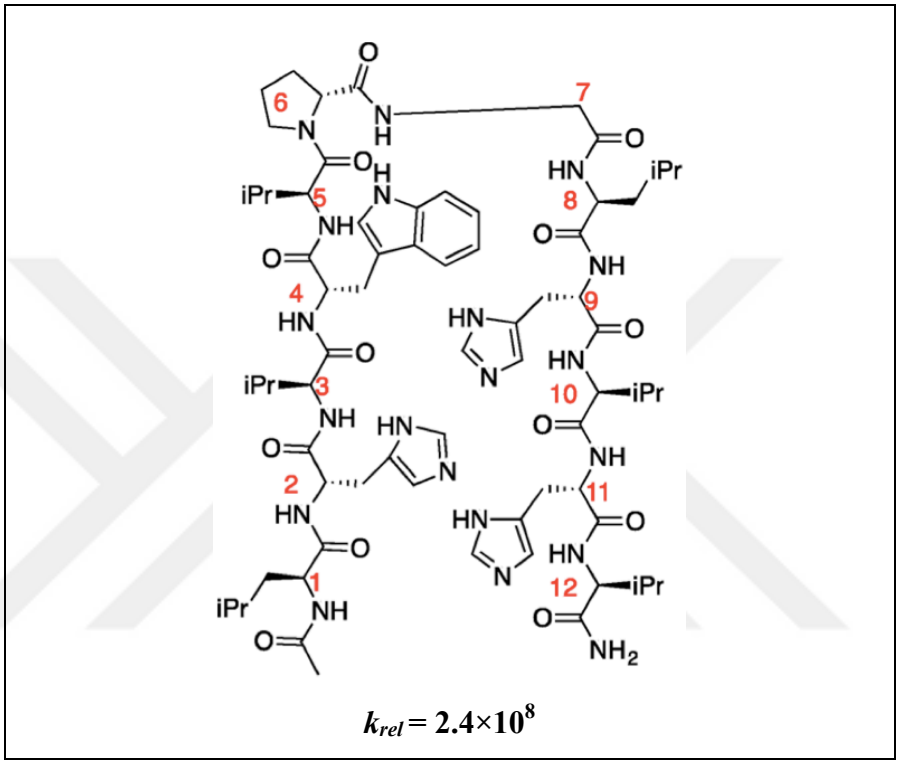

Figure 1.6. Oligopeptide developed by Matsumoto et al. for catalysis of acyl- and phosphonyl- transfer reactions [36]

Matsui and co-workers assembled oligopeptides with protease/esterase (CP4) activity with hydrophobic pockets to mimic the tertiary structures of enzyme active sites. The fused oligopeptide (CP4)-Aβ assembly accelerated the hydrolysis of *p*-nitrophenyl acetate 4-fold compared to CP4 (Figure 1.7) [37].

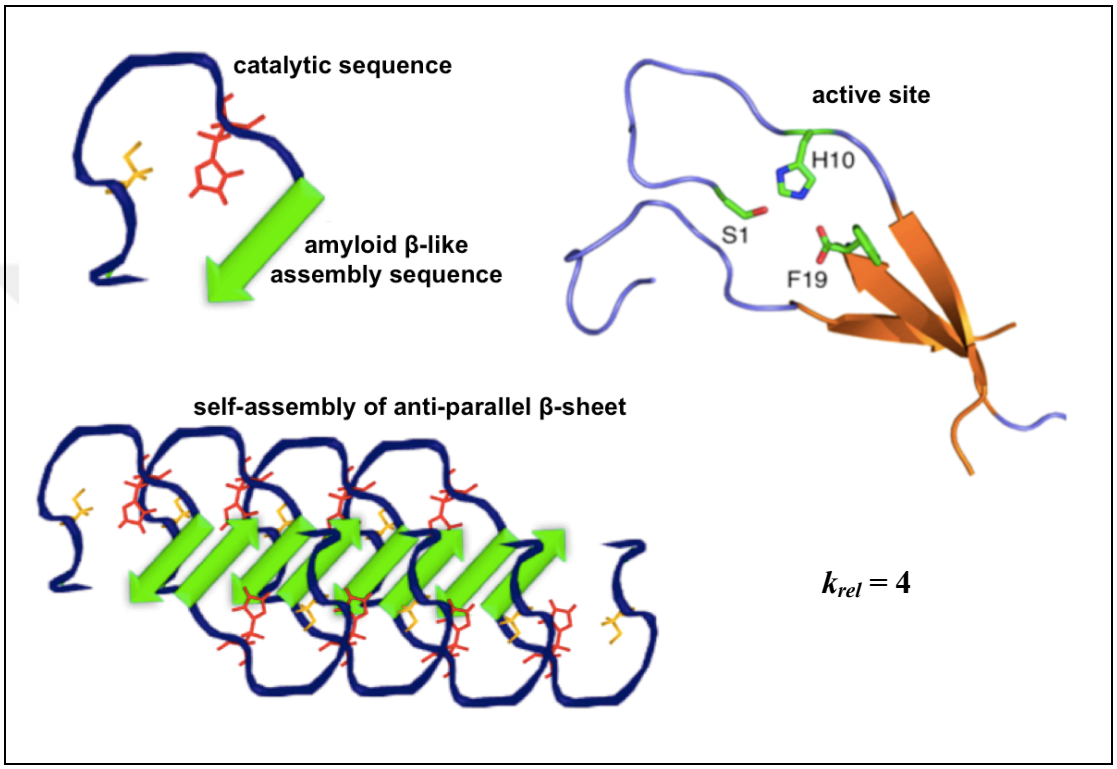

Figure 1.7. Polypeptide designed by Matsui et al. for hydrolysis of *p*-nitrophenyl acetate [37]

Goyal et al. have designed a β-hairpin polypeptide consisting of twenty L- and D- α-amino-acid residues that mimics hydrolase enzyme. The designed enzymes were used in the hydrolysis reaction of *p*-nitrophenyl acetate [38], [39]. The designed polypeptide has a k_{cat} of $(20.04\pm0.21)\times10^{-5}$ s^{-1} (Figure 1.8). This catalyst showed modest activity but it is found structurally promising for the future designs of artificial enzymes.

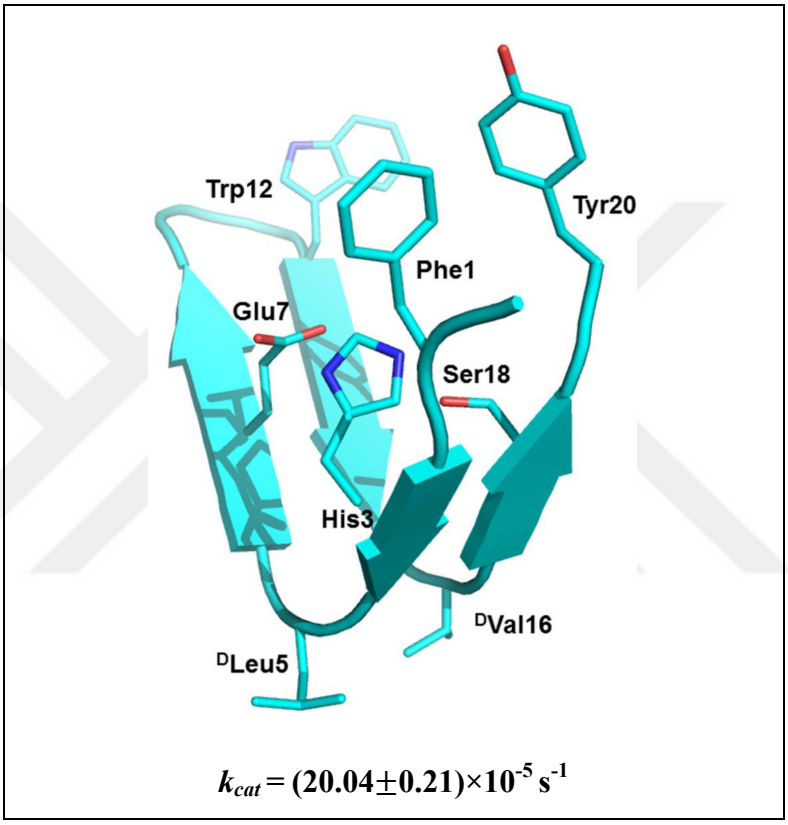

Figure 1.8. The polypeptide designed by Goyal et al. for catalysis of *p*-nitrophenyl acetate [39]

Horng and co-workers designed an oligopeptide based on a polyproline scaffold for hydrolysis of *p*-nitrophenyl acetate. Figure 1.9 shows the designed catalyst and representation of the catalytic active site of protease with a k_{cat} of (1.76±0.16) $\times 10^{-3}$ s^{-1} and k_{cat}/K_m of 1.23±0.20 $M^{-1}s^{-1}$ [40].

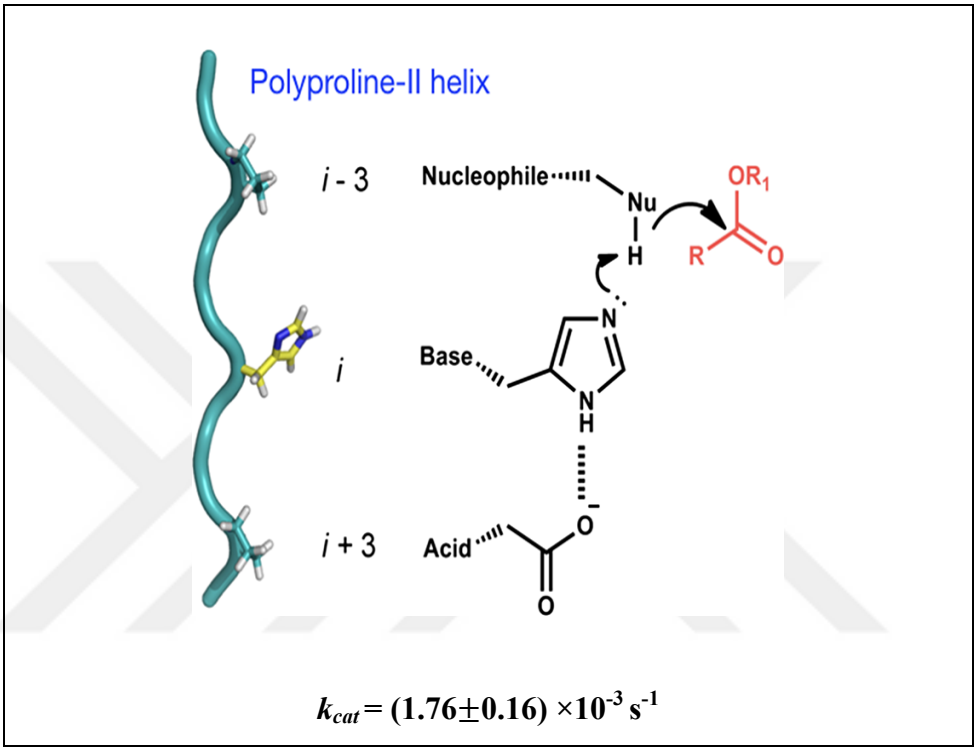

Figure 1.9. Polyproline II helix developed by Horng et al. for catalysis of *p*- nitrophenyl acetate [40]

Connal and co-workers designed a catalyst immobilized on Merrifield resin, based on the catalytic triad of hydrolases which, hydrolyzed *p*-nitrophenyl butyrate with a k_{cat} of 98 hr^{-1} and k_{cat}/K_m of 136.1 min^{-1} M^{-1}. Figure 1.10 shows the designed catalyst. These results showed that better arrangement of functional groups could significantly enhance the catalytic activity [41].

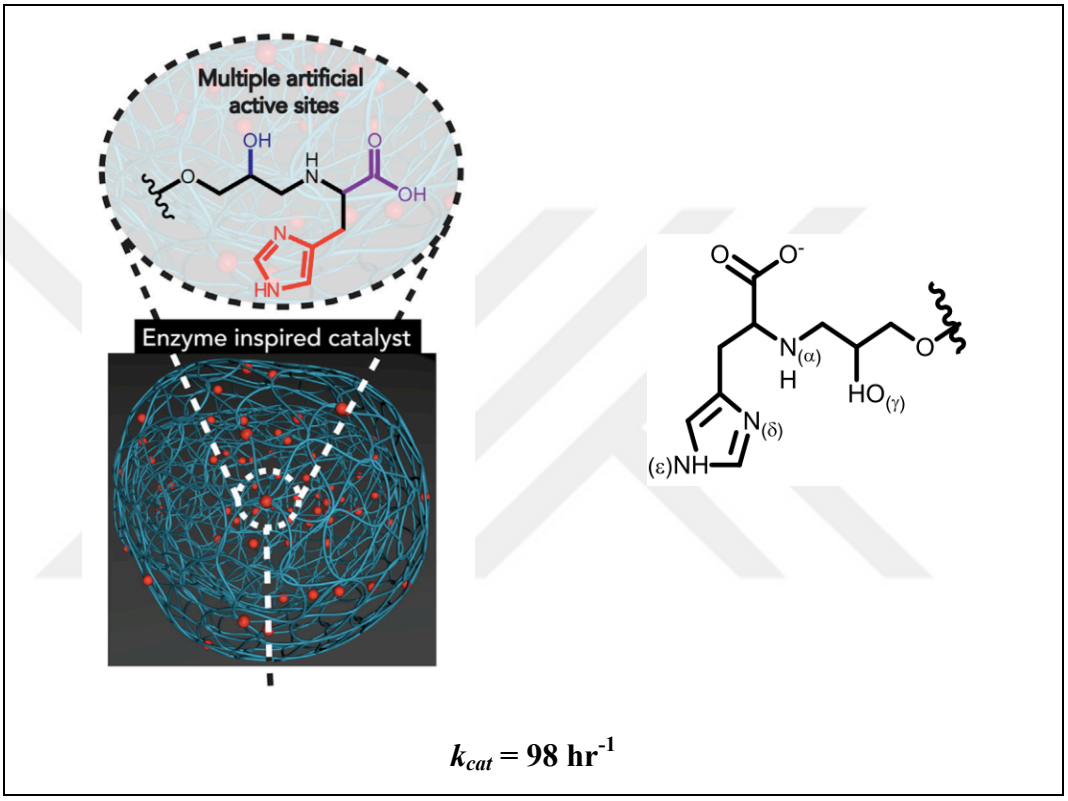

Figure 1.10. Merrifield resin designed by Connal et al. for catalysis of *p*-nitrophenyl butyrate [41]

Liang and coworkers developed a nanofiber with catalytic centers consisting of histidine and arginine residues to catalyze hydrolysis of *p*-nitrophenyl acetate (Figure 1.11). Value of the k_{cat} of this nanofiber catalyst was calculated as 2.64×10^{-3} s^{-1} and also k_{cat}/K_m was found as 0.15 $M^{-1}s^{-1}$ [42].

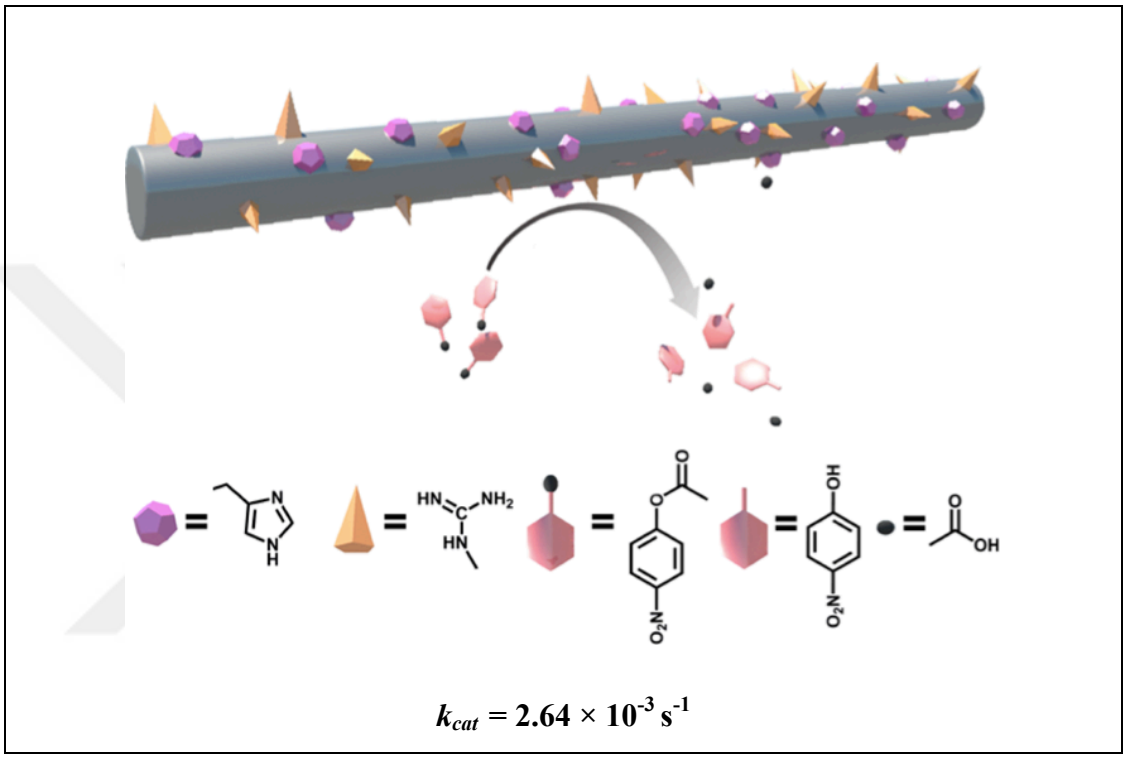

Figure 1.11. Nanofiber developed by Liang et al. for catalysis of *p*-nitrophenyl acetate hydrolysis [42]

Zhang et al. developed an artificial hydrolase by attaching short peptides and actives sites onto carbon nanotubes. The catalyst shown in Figure 1.12 has a k_{cat} of 1.67×10^{-3} s^{-1} and k_{cat}/K_m of 0.58 $M^{-1}s^{-1}$ [43].

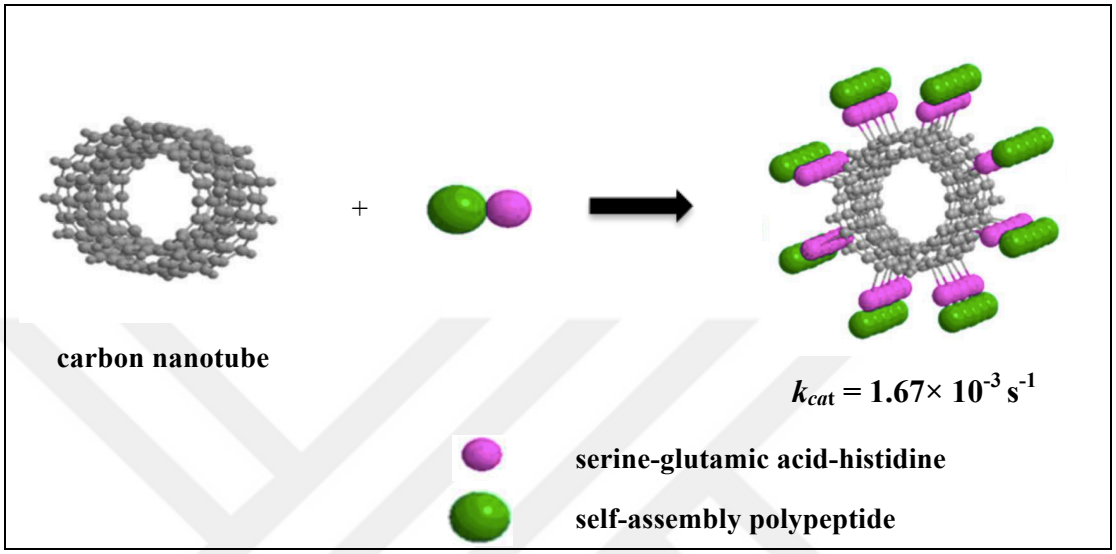

Figure 1.12. The hydrophobic carbon nanotube designed by Zhang et al. for catalysis of *p*-nitrophenyl acetate [43]

All this effort for the design of small molecule mimics of hydrolase enzymes is based on experimental findings and chemical intuition and largely relies on a costly experimental trial and error process [44]. A rational *in-silico* design approach based on the computational insights on key catalytic elements would significantly accelerate this process.

Approximately 50 years ago, it was not possible to use computational methods to simulate a chemical before synthesis. Release of minicomputers and development of density functional theory (DFT) enabled computational design processes of new molecules and reactions. Quantum mechanical (QM) calculations allow many predictions and the selected predictions can be supported by experimental work. This helps the researches to save time and money. [45].

A computational design strategy, known as "inside-out" approach and has successfully used in the *de-novo* design of artificial enyzmes [46], [47], [48], [49]. The same strategy was applied to the design of new transesterification catalysts, which are called "spiroligozymes", mimicking the catalytic machinery of hydrolase enzymes [10]. The catalytic triad of esterase enzymes is mimicked with a catalytic dyad consisting of pyridine and alcohol. The oxyanion hole is mimicked by urea. Figure 1.13 represents the catalytic active sites of esterase and spiroligozyme.

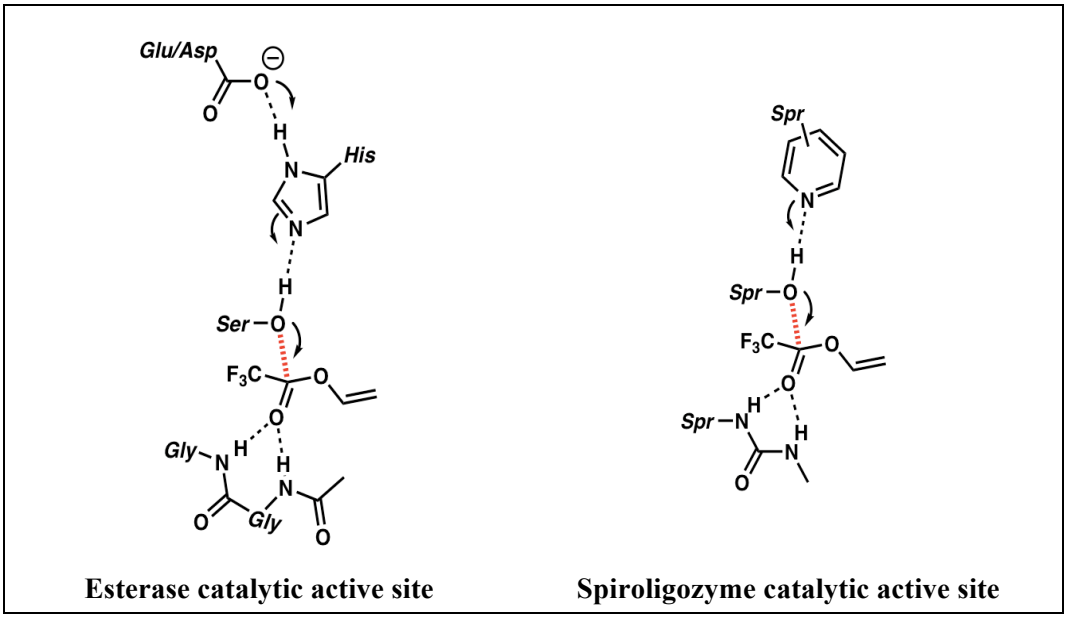

Figure 1.13. Catalytic active sites of esterase and spiroligozyme [10]

The “inside-out” design strategy, summarized in Figure 1.14, is based on a theoretical active site model (theozyme), which gives optimal positions of catalytic functional groups (pyridine, alcohol and urea) around the transition state. A theozyme describes the three-dimensional (3-D) layouts of catalytic functional groups that could best stabilize the transition state of the target reaction identified using quantum mechanical calculations [45], [50].

In the next step, a chiral skeleton, which could provide the stereochemically 3-D arrangement of the catalytic groups determined in QM-theozyme, is generated by combining the appropriate bis-amino acid building blocks with peptide bond pairs. The process of the placement of predicted geometry of the functional groups, which are carried by bis-amino acid building blocks, in the QM-theozyme is called “molecular lego” (Figure 1.15).

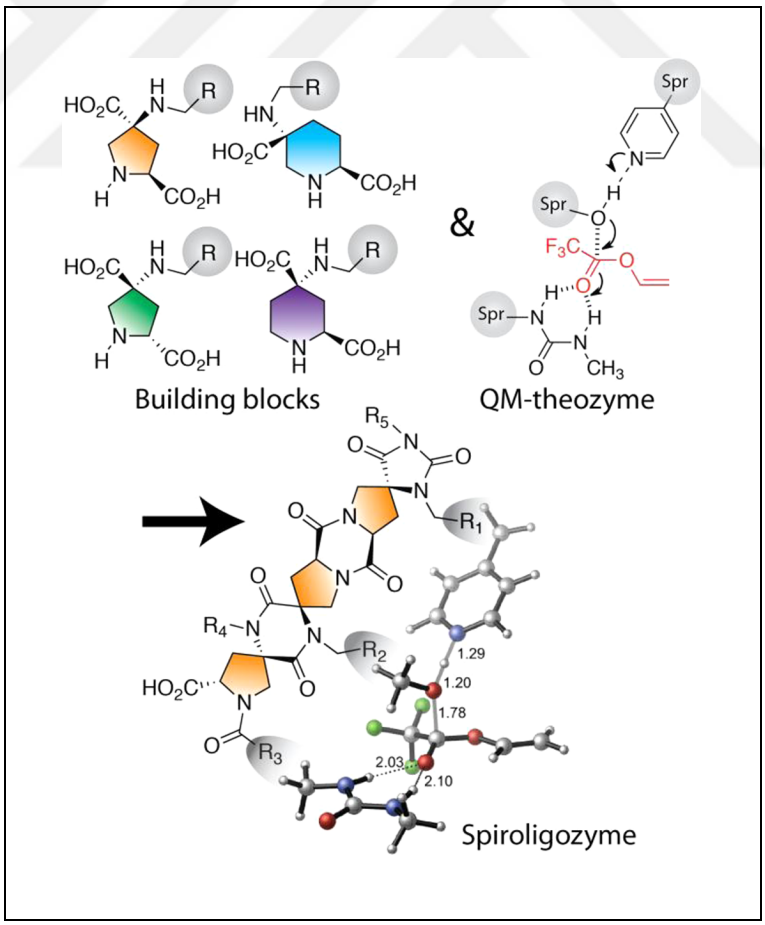

Figure 1.14. Inside-out approach of spiroligozymes [10]

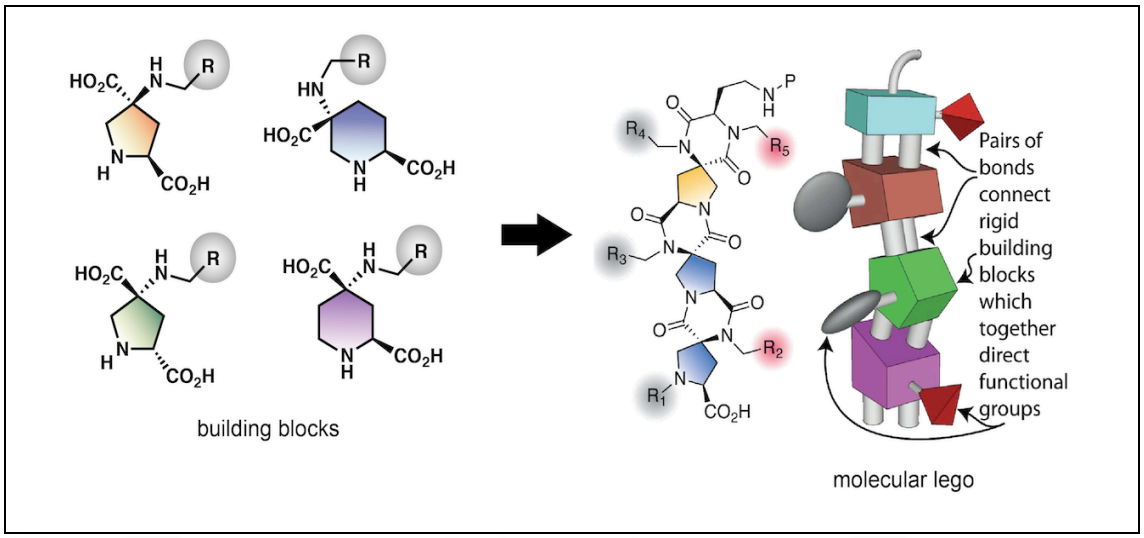

Figure 1.15. Molecular lego for design of spiroligozyme [10]

Bifunctional (pyridine–alcohol) and trifunctional (pyridine-alcohol-urea) spiroligozymes designed using this approach catalyzed the transesterification reaction of carboxyl esters. The bifunctional spiroligozyme BF3 accelerated the reaction between vinyl trifluoroacetate and methanol 2700 fold compared to the background reaction with a benzyl alcohol. However, product formation was slow. For faster product formation, urea was attached to BF3 spiroligozyme as an oxyanion hole motif and a trifunctional spiroligozyme TF3 was obtained [10]. Trifunctional catalysts are known to perform in a more complex catalytic environment [51].

This trifunctional spiroligozyme accelerated first step of the reaction 2200-fold than the background reaction, and accelerated the second step of the reaction 130-fold than the background reaction. However, molecular dynamics simulations showed that, H-bond interaction between pyridine and alcohol was not maintained during the reaction unlike their naturally evolved counterparts [10].

Here we suggest a new computational protocol that will allow identification of structural changes in TF3 that will maintain the required preorganized H-bond network essential for catalysis.

2. METHODOLOGY

2.1. COMPUTATIONAL EVALUATION PROTOCOL

The computational protocol applied to identify structural modifications that will increase the occupancy of H-bond network in an organocatalytic framework is summarized in Figure 2.1. Details of each step are explained in the following subsections.

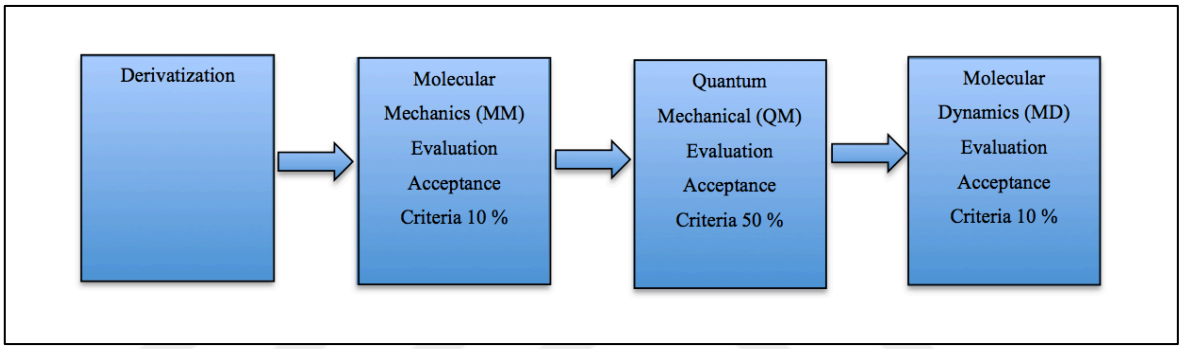

Figure 2.1. The computational protocol and selection criteria applied to TF3 spiroligozyme

2.1.1. Derivatization

Medchem Transformations is an approach that applies transformation rules to existing ligands to obtain new chemical structures. The transformations can switch functional groups or change just one or all parts of a ring while keeping remaining parts of ligand the same. These transformations can be applied iteratively, which results in cumulative changes in the initial structures. Individual transformations form minor modifications on the chemical structure of ligand. There are three types of transformation in the library. These are; atom transform, ring transform and ring creation. Transformation rules are applied by a match and replace algorithm [52];

- A substructure search is executed to pair the query of every transformation rule to the input molecule. Each resulting match is considered for further steps.
- The paired atoms are changed with those of the result.

- The remaining atoms of the ligand are connected again properly. Transformations, which end up with unconnected heavy-atoms, are eliminated. Duplicates are deleted once 3-D coordinates have been produced [52].

175 transformation reactions are defined in this tool. Figure 2.2 shows the Medchem transformation tool box [52].

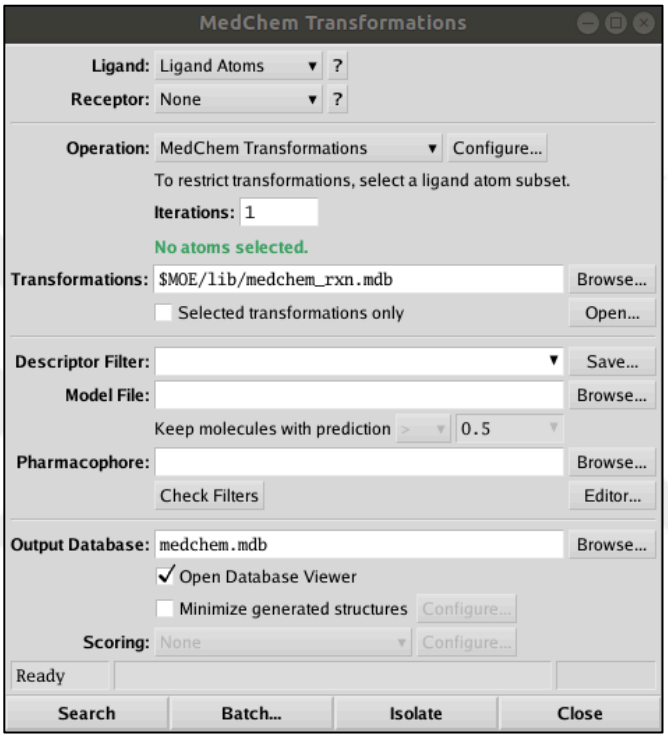

Figure 2.2. Medchem transformation tool [52]

In this study, Medchem transformation tool of MOE was used to generate derivatives of the parent molecule (TF3).

2.1.2. Molecular Mechanics (MM) Evaluation

Molecular mechanics (MM) depends on a basic model of the interactions in a system with the help of processes like opening and closing of angles and stretching or rotations of bonds. Some known functions, such as Hooke's law, are used to define these contributions, forming a satisfactory force field.

Molecular modelling force fields can be described by a four-component equation of the intramolecular and intermolecular interactions in a system as shown in equation 2.1 The equation includes the energetic penalties associated with the deviation of bonds/angles away from their "equilibrium" positions and rotation around bonds, and also describes the non-bonded interactions using the Lennard-Jones potential for Van-der-Waals forces and Coulomb potential for electrostatic forces.

$$PE(r^N) = \sum_{bonds} \frac{k_i}{2}\left(l_i - l_{i,0}\right)^2 + \sum_{angles} \frac{k_i}{2}\left(\theta_i - \theta_{i,0}\right)^2 + \sum_{torsions} \frac{V_n}{2}\left(1 + \cos\left(n\omega - \gamma\right)\right) + \sum_{i=1}^{N}\sum_{j=i+1}^{N}\left(4\varepsilon_{ij}\left[\left(\frac{\sigma_{ij}}{r_{ij}}\right)^{12} - \left(\frac{\sigma_{ij}}{r_{ij}}\right)^{6}\right] + \frac{q_i q_j}{4\pi\varepsilon_0 r_{ij}}\right) \quad (2.1)$$

$PE(r^N)$ represents the potential energy as a function of positions (r) of N particles (generally atoms) [53].

Conformational search generates a discrete sampling of the space limited to local minima of the potential energy function. It is a tool to produce energetically reasonable 3-D atomic configurations of molecular systems with or without geometric constraints [54]. Figure 2.3 shows conformational search tool box in MOE.

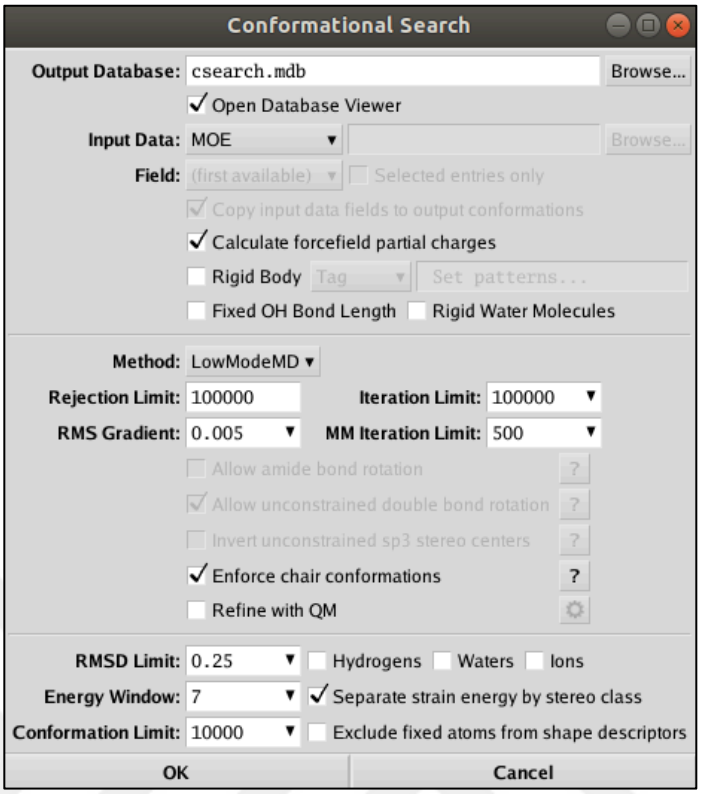

Figure 2.3. Conformational search tool [54]

The conformational search tool of MOE comprises three methods to produce conformers, the output of each exposed to energy minimization.

Systematic Search: This method creates molecular conformers by rotating non-ring bonds in a molecule with increasing discrete dihedral [54].

Stochastic Search: This method produces conformers by rotating all bonds includes ring bonds and inverting tetrahedral centers randomly followed by energy minimization of all atoms [55].

LowModeMD Search: This method produces conformers by a short ~ 1 ps run of Molecular Dynamics (MD) at constant temperature followed by energy minimization of all atoms. LowModeMD Search is very efficient in the analysis of small molecules [56], [57], [58].

Fine discrete conformational samples, of the rotatable bonds, are impractical and systematically generating such "coverage collections" for large complex systems is an unsolved problem. For many properties, a collection of low energy local minima is often a good representative of the entire conformation space [56], [57]. A conformational search was carried out for each derivative with the MMFF94x force field using lowmode MD sampling procedure as implemented in MOE. MMFF94x is specifically parametrized for small organic molecules [59], [60], [61].

2.1.3. Quantum Mechanical (QM) Evaluation

Schrödinger equation is the fundamental of quantum mechanics. Schrödinger equation can be solved exactly for only a few systems, such as the particle on a sphere and hydrogen atom.

Time-independent Schrödinger equation can be defined as;

$$\hat{H}\psi = E\psi \tag{2.2}$$

where $\hat{H}$ is Hamiltonian operator, including kinetic and potential energy, ψ is the wave function and E is the electronic energy.

For systems that do not have the exact solution of the Schrödinger equation several electronic structure methods were developed that depend on the approximate / alternative solutions (like ab-initio, semi-empirical and density functional theory). Among these, density functional theory has become a widely employed method to study complex systems with chemical accuracy [53].

In this thesis, all quantum mechanical calculations were done using Gaussian 16 [62]. In the quantum mechanical calculations, all geometry optimizations were accomplished at the M06-2X/ 6-31G (d) level of theory [63]. Chloroform was used as the solvent. Solvent and medium effects were taken into account in the optimizations using the integral-equation-formalism polarizable continuum model (IEF-PCM). In the QM evaluation of conformer libraries, energies were determined by single-point calculations with the M06-2X/6-31G(d) using IEF-PCM with radii and nonelectrostatic terms for the SMD solvation model as

implemented in Gaussian 16 [63], [64], [65], [66], [67].

Populations of conformers of each derivative for both MM and QM evaluations were determined using the Boltzmann distribution;

$$\text{Population} = \frac{e^{-\Delta E/RT}}{\sum\left(e^{-\Delta E/RT}\right)} \times 100 \tag{2.3}$$

2.1.4. Molecular Dynamics (MD) Simulations

Molecular dynamics is a method that can predict state of the system at any future from the current state of the system. Newton's equations of motion are applied to derive sets of atomic positions in sequence. As such, the real dynamics of the system is explored, from which time averages of properties can be obtained.

Nature of the realistic potentials requires continuous monitoring, therefore, the equations of motion is integrated in a series of short time steps. This time interval usually changes between 1 femtosecond (fs) to 10 fs. This corresponds to 10^{-15} s to 10^{-14} s. To produce new positions and velocities for a short time ahead, the forces on the atoms are calculated and combined with the current positions and velocities for each step. The force acting on each atom is considered as constant during the time interval. As such, MD simulation creates a trajectory, which defines the changes in dynamic variables with time. Thermodynamic averages are calculated as time averages using numerical integration of the following equation [53];

$$\langle A \rangle = \frac{1}{M}\sum_{i=1}^{M} A(p^N, r^N) \tag{2.4}$$

In the evaluation of preorganization of spiroligozymes, the MD simulation protocol, which successfully predicted the activities of the computationally designed enzymes, were used. MD simulations were carried out using AMBER 12 to assess whether the designed catalytic contacts were maintained in a dynamic environment in the presence of explicit solvent molecules [68]. TF3 spiroligozyme parameters were obtained with the

antechamber module of AMBER 12 by the general AMBER force field (GAFF), with partial charges set to fit the electrostatic potential generated at HF/6-31G(d) by RESP [68], [69]. Charges were determined using Gaussian 16 according to the Merz-Singh-Kollman scheme [70], [71]. The spiroligozymes were placed in a chloroform box taking care that there is at least 10 Å solvent layer around them [72]. A two-step minimization approach were applied. Firstly the positions of solvent molecules were minimized followed by unrestrained minimization of all atoms. The system was heated from 0 to 300 K by applying the constant volume periodic boundary conditions in six 50 K steps. A harmonic limit of 10 kcal/mol were applied to the spiroligozyme and the Langevin equilibration scheme was utilized to control and equalize the temperature. During heating 1 fs time step was applied. The heated system was brought to equilibrium at a fixed volume for 2 ns and then at a constant pressure of 1 atm for 2 ns using a 2 fs time step. The 20 ns production molecular dynamics simulation was performed using the isothermal-isobaric ensemble (NPT). Post-MD data analysis was done with the ptraj module of AMBER 12.

MD population is a term that is used to define cumulation of MD snapshots in the H-bond region ($1.2 < d < 3.2$; $90 < \theta < 180$) in the H-bond distance-angle plot. This region is indicated in the blue rectangle on the corresponding plots in the results and discussion section.

2.1.5. Selection Criteria

All derivatives except the ones, in which transformation has altered the catalytic functional groups are evaluated using MM calculations. All derivatives with an MM population above 10 percent are evaluated using QM calculations. All derivatives with a QM population above 50 percent are evaluated using MD simulations.

Figure 2.1 shows the flowchart of selection criteria that is applied to TF3 spiroligozyme.

3. RESULTS AND DISCUSSION

TF3 is a trifunctional spiroligozyme (Figure 3.1) developed using the "inside-out" design strategy. TF3 accelerated the rate of transesterification reaction between methanol and vinyl trifluoroacetate 2200 -fold for the acylation step and 130-fold for the deacylation step [10]. In Figure 3.1, the catalytic groups are highlighted within the square. The conformer with the hydrogen bond between pyridine-alcohol catalytic dyad is defined as the active conformer.

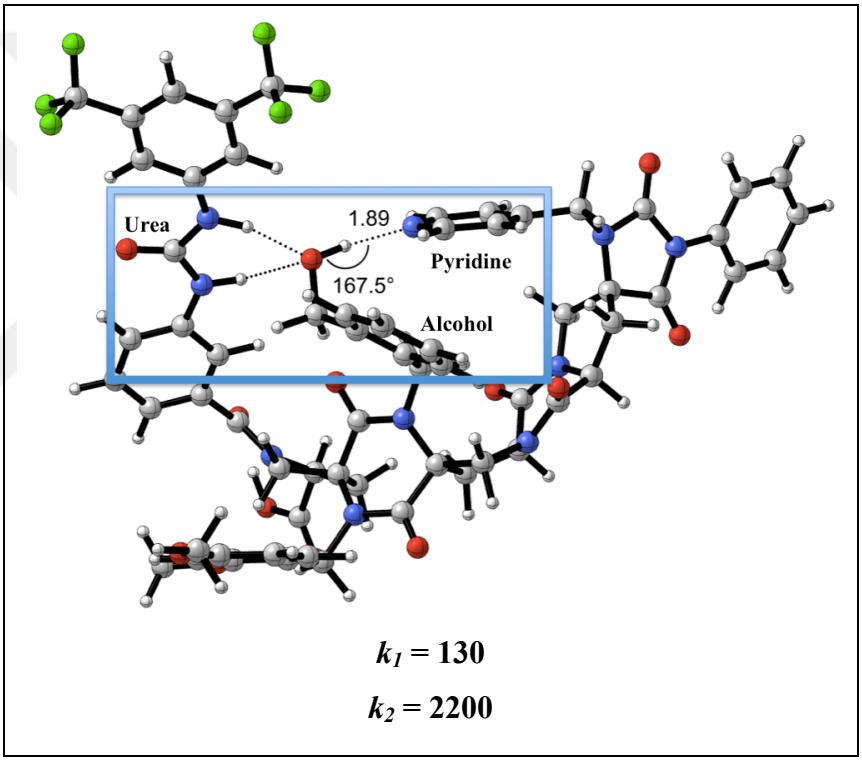

Figure 3.1. TF3 spiroligozyme [10]

The conformational search for TF3 spiroligozyme generated 44 conformers. Table 3.1 shows all conformers with MM population above 1 percent and all the active conformers regardless of their population. The lowest energy conformer shown in Figure 3.2 does not show a H-bond between the alcohol-pyridine catalytic dyad and has 82 percent MM population. The required H-bond interaction is displayed in conformers 12, 19, 24, 27 and 38. Yet, all these active conformers are at least 4.1 kcal/mol higher in energy than the lowest energy conformer and total MM population of the active conformers sum up to 0

percent. QM analysis showed similar results in terms of the total population of the active conformers and inactive conformers. The lowest energy conformer is found to be conformer 2, with 87 percent population. The lowest energy active conformer is conformer 24, which is 5 kcal/mol higher in energy with 0 percent population. Figure 3.2 shows conformer 24 of TF3 spiroligozyme.

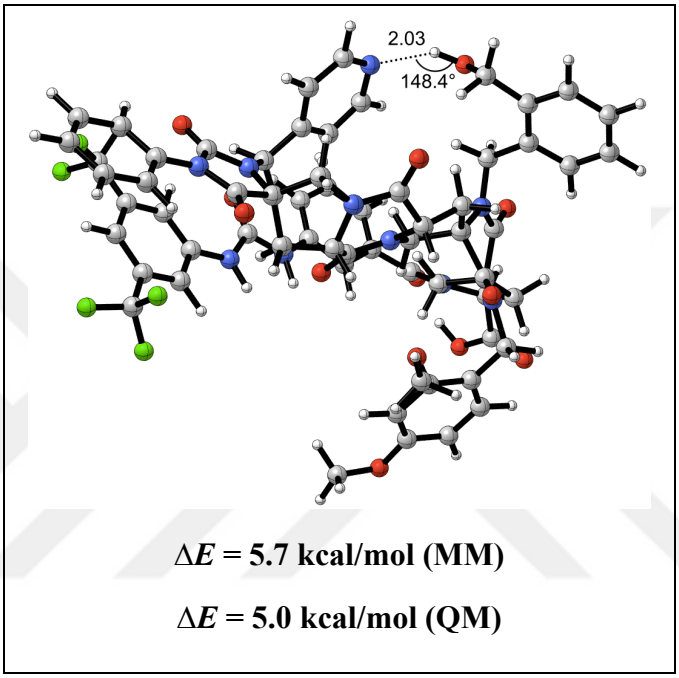

Figure 3.2. TF3 spiroligozyme - conformer 24

Table 3.1. MM and QM evaluation of TF3 spiroligozyme

TF3				
Conformer Number	**ΔE (kcal/mol) Molecular Mechanics (MM) MMFF94x**	**MM Population (%)**	**ΔE (kcal/mol) Quantum Mechanics (QM) M06-2X/6-31G(d)**	**QM Population (%)**
1	0.0	82	5.7	0
2	1.0	15	0.0	87
3	2.0	3	6.8	0
4	3.0	1	1.1	13
12 ACTIVE	4.1	0	8.8	0
19 ACTIVE	5.2	0	10.4	0
24 ACTIVE	5.7	0	5.0	0
27 ACTIVE	6.0	0	10.3	0
38 ACTIVE	6.7	0	9.0	0

Table 3.2 shows relative energies of active and inactive conformer clusters TF3 spiroligozyme. The relative energy of active conformers with respect to the conformers with no H-bond is 5.0 kcal/mol.

Table 3.2. Populations and relative energies of active and inactive conformer clusters of TF3

TF3	**QM Population (%)**	**Δ*E* (kcal/mol) Quantum Mechanics (QM) M062X-6-31G(d)**
Total Active Conformers	0	$\Delta E = 5.0$
Total Conformers with no H-bond	100	0.0

Figure 3.3 shows the MD results of TF3. The cumulation of snapshots with an of H-bond between the catalytic dyad is shown within the rectangle in Figure 3.3.(a). MD population of TF3 is calculated as 0 percent.

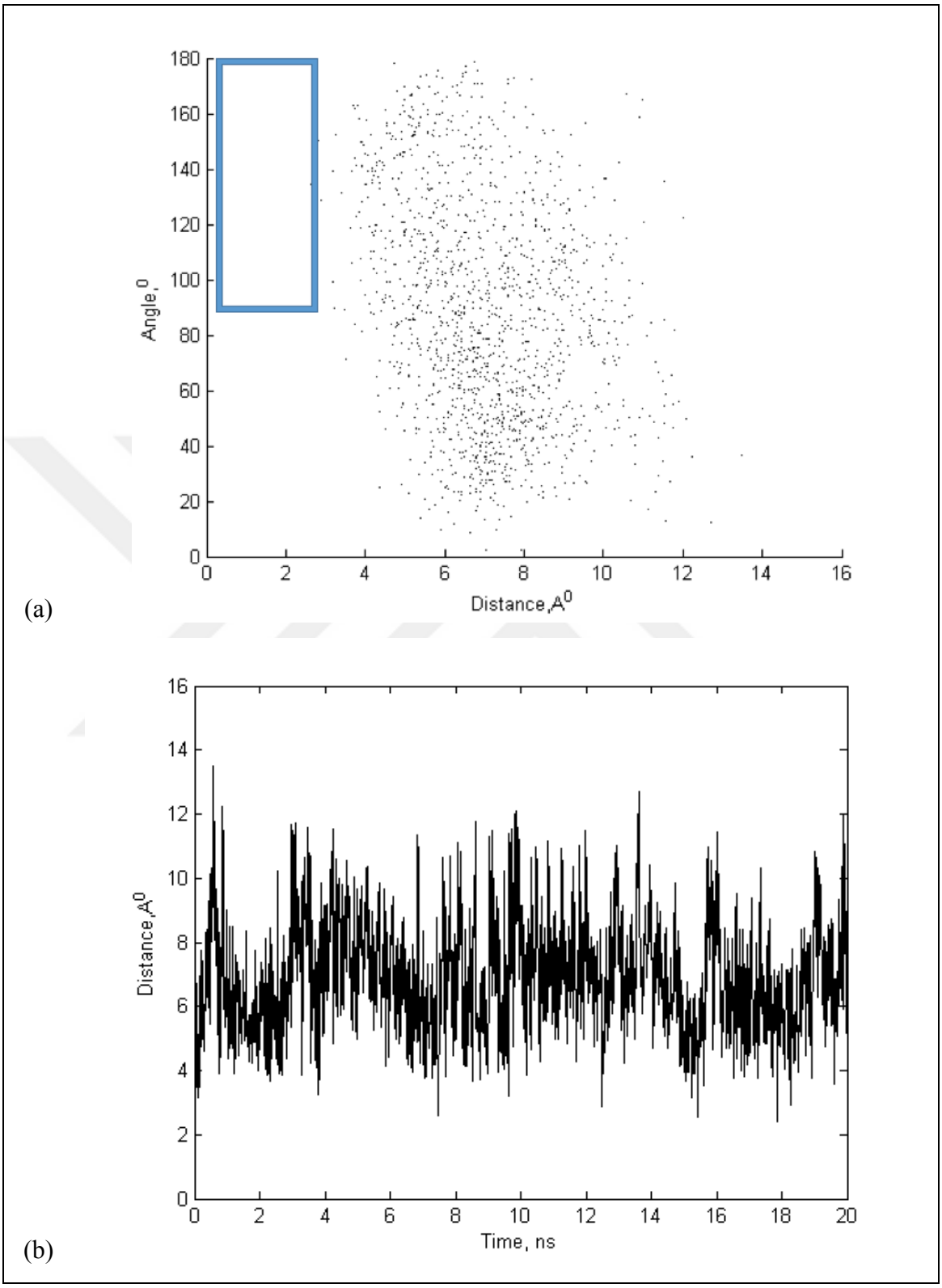

Figure 3.3. MD results of TF3 spiroligozyme (a) Pyridine-alcohol interaction - angle vs. distance, (b) Pyridine-alcohol interaction - distance vs. time

These results show that catalytic performance of TF3 can be improved by further stabilization of the H-bond network between the catalytic functional groups. For this purpose structural modifications were evaluated. TF3 spiroligozyme is taken as the parent catalyst and used in derivatization.

Derivatization: TF3 spiroligozyme was derivatized using Medchem transformation tool of MOE [52]. In the first iteration, 258 derivatives of TF3 spiroligozyme were obtained. Transformation and populations for all 258 derivatives are given in Appendix A. When the number of iterations for TF3 spiroligozyme was increased to 2, over eight thousand derivatives were obtained. However, increasing number of the iterations affects synthesizability of the derivatives in a negative way so, the derivatives of iteration 1 were evaluated in this thesis. If the transformation alters the catalytic groups, (alcohol, pyridine, urea) which are involved in catalysis, these derivatives were not taken into account. That is, 65 derivatives of 258 derivatives were not considered for further evaluation and 193 derivatives were analyzed.

Molecular Mechanics (MM) Evaluation: Conformational analysis of each derivative was performed, except for the derivatives, in which the transformation occurred in catalytic functional groups; alcohol, pyridine and urea.

After conformational search, conformers of these 193 derivatives were examined one-by-one to observe the preorganization of the catalytic groups. MM analysis showed that 23 out of 193 derivatives have MM population of active conformers above 10 percent. These derivatives were selected for QM evaluation.

Quantum Mechanical (QM) Evaluation: Selected 23 derivatives with MM population more than 10 percent were evaluated using single point energy calculations with density functional theory. For each selected derivative, single-point energies of all conformers with MM population higher than 1 percent and all active conformers regardless of their population were calculated using density functional theory at the M06-2X/6-31G(d) level.

The energy difference between the active conformer and the lowest energy conformer was examined. Derivatives with QM population above 50 percent were considered as potential active spiroligozymes. After QM calculations 11 derivatives, which have QM population greater than 50 percent were selected for MD evaluations.

Molecular Dynamics (MD) Evaluation: It is desired to observe a strong H-bond between alcohol-pyridine in a dynamic solvent environment such as in the example of Cathepsin K's MD results [26], [27]. None of derivatives had a populaion above the 10 percent selection criterion.

Figure 3.4 shows the computational protocol results applied to TF3 spiroligozyme. The results for these derivatives are discussed in the following sections.

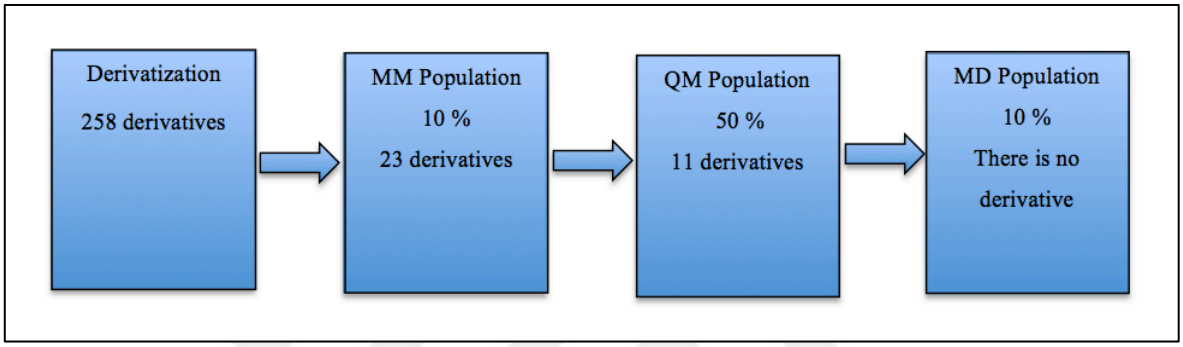

Figure 3.4. The computational protocol results applied to TF3 spiroligozyme

According to the computational protocol results, 11 of 258 derivatives will be discussed in the following sections of this thesis. These derivatives are; DER1, DER6, DER15, DER41, DER64, DER72, DER77, DER112, DER135, DER146 and DER162. These derivatives are summarized in Table 3.3.

Table 3.3 shows data about the derivatives consisting of transformation reactions, synthesizability score, number of conformers in library and where the modifications occurred in their structure. "Backbone" represents the structural changes in the backbone of the spiroligozme and "remote" corresponds to the structural changes away from the catalytic active functional groups.

Table 3.3. TF3 spiroligozyme derivatives satisfying the MM and QM selection criteria

Derivative Name	Transformation Reaction	Synthesizability Score	Number of Conformers	Modification	MM Population 10 %	QM Population 50 %	MD Population 10 %
DER1	C=O to C=S reaction	0.6774	53	Backbone	67	99	4
DER6	C=O to C=S reaction	0.6774	106	Backbone	10	97	1
DER15	C=O to SO_2 reaction	0.7447	91	Backbone	16	92	0
DER41	C[NOSFClBRI] to C(cyano) reaction	0.6702	88	Remote	27	99	0
DER64	Cyclo56 reaction	0.6596	94	Backbone	19	95	1
DER72	N14 substraction reaction	0.6667	83	Backbone	92	97	0
DER77	Amide to amine reaction	0.6739	97	Backbone	65	100	0
DER112	Benzene to pyridine reaction	0.6667	114	Remote	24	50	0
DER135	hom [NOS]CH_2 reaction	0.6702	89	Remote	83	94	0
DER146	Methylate [OS] inversion reaction	0.6630	65	Remote	12	100	2
DER162	Phenyl to indole reaction	0.5833	62	Remote	21	100	0

3.1. DER1

DER1 is formed by the transformation of C = O bond to C = S bond. Figure 3.5 shows this transformation. Figure 3.6 shows the transformed part of DER1 in the blue ring.

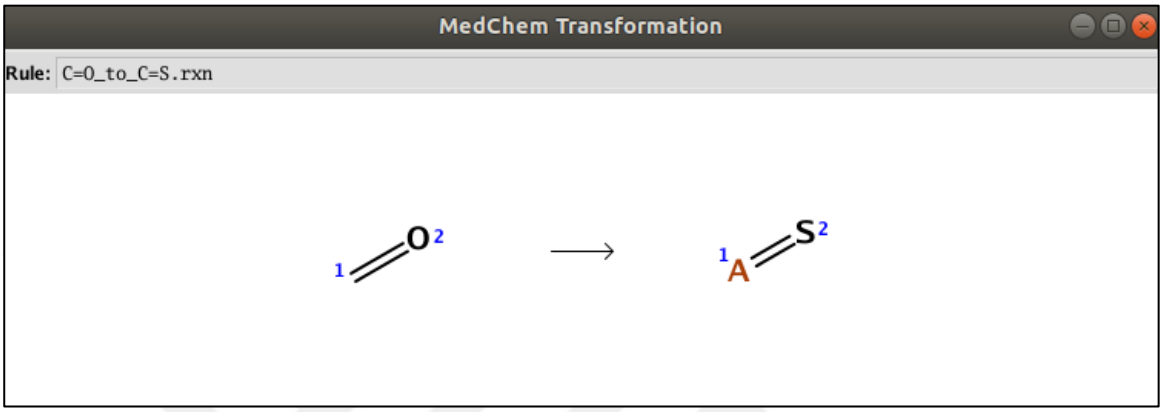

Figure 3.5. Transformation rule applied to DER1

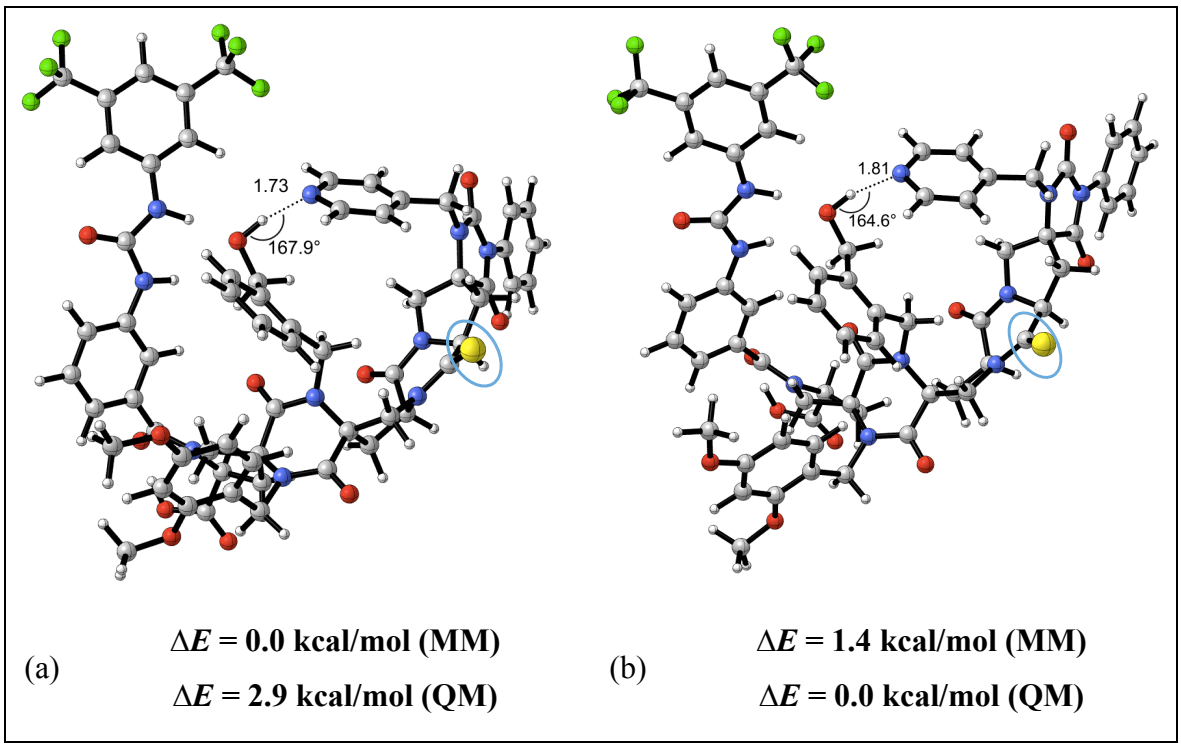

Figure 3.6. Lowest energy conformers of DER1 (a) Conformer 1 (b) Conformer 4

The conformational search for DER1 generated 53 conformers. Table 3.4 shows the results of DER1according to MM and QM evaluation. Conformers 1, 4, 9, 38, 40 and 50 show the required H-bond between alcohol and pyridine. So, these conformers are described as active conformers. Figure 3.6 shows conformers, 1 and 4.

According to the calculations based on MMFF94x force field for DER1, conformer 1 is the lowest energy active conformer. The results obtained by M06-2X / 6-31G (d), showed that conformer 4 is the lowest energy active conformer and conformer 1 is 2.9 kcal/mol higher in energy. For conformer 1, MM population is 60 percent whereas the QM population is 1 percent. However, conformer 4 has a QM population of 97 percent.

Table 3.4. MM and QM evaluation of DER1

DER1				
Conformer Number	**Δ*E* (kcal/mol) Molecular Mechanics (MM) MMFF94x**	**MM Population (%)**	**Δ*E* (kcal/mol) Quantum Mechanics (QM) M06-2X/6-31G(d)**	**QM Population (%)**
1 ACTIVE	0.0	60	2.9	1
2	0.8	14	5.3	0
3	1.0	11	4.0	0
4 ACTIVE	1.4	6	0.0	97
5	1.6	4	7.9	0
6	2.2	1	9.3	0
7	2.3	1	7.7	0
8	2.5	1	2.9	1
9 ACTIVE	2.6	1	2.6	1
10	2.6	1	9.9	0
11	3.5	0	7.3	0
38 ACTIVE	6.3	0	4.9	0
40 ACTIVE	6.4	0	6.5	0
50 ACTIVE	3.5	0	6.9	0

In order to test the agreement between MM and QM optimized geometries and the energetic trends, all conformers in Table 3.4 were subjected to geometry optimization at the M06-2X/6-31G(d) level of theory.

Figure 3.7 shows the MM and QM optimized geometry of conformer 4. Length of the H-bond between catalytic dyad is slightly increased after optimization. Also after QM optimization linearity of this bond is decreased. Even though it is very difficult to accurately quantify the strength of H-bonds, the linearity and shorter distance between the atoms, which comprises the H-bond, is known to be a good indicator of trends in H-bond

strength. That is, MM slightly overestimates the strength of the H-bond between the catalytic dyad. After optimization, the 2.9 kcal/mol energy difference between conformer 4 and conformer 1 has dropped to 0.8 kcal/mol. Despite lower energy differences, the conformer energies followed the same trend showing that the cost-effective single point energy calculations are safe to describe the energetic trends in QM evaluation of conformers rather than computational demanding geometry optimizations.

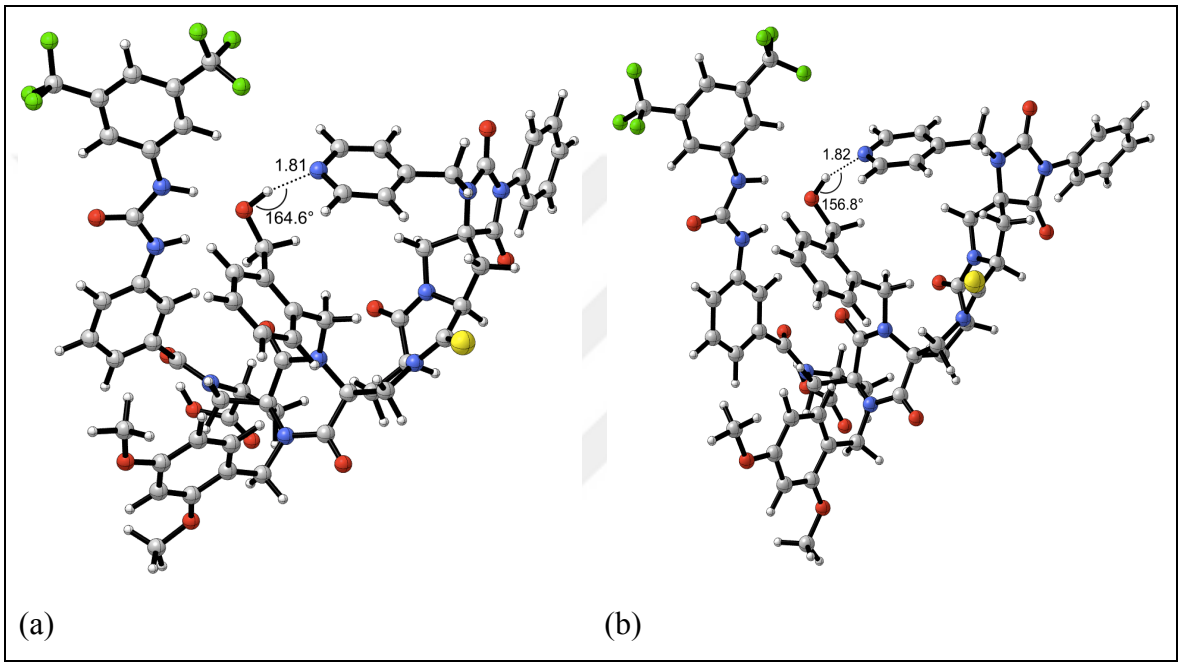

Figure 3.7. Optimization of DER1 - conformer 4 (a) MM optimization, (b) QM optimization

Cumulative QM population of 99 percent for active conformers versus 1 percent cumulative QM population for inactive conformers corresponds to an energy difference, ΔE, of 2.7 kcal/mol (Table 3.5).

Table 3.5. Populations and relative energies of active and inactive conformer clusters of DER1

DER1	**QM Population (%)**	**Δ*E* (kcal/mol) Quantum Mechanics (QM) M062X-6-31G(d)**
Total Active Conformers	99	0.0
Total Conformers with no H-bond	1	$\Delta E = 2.7$

With a total MM population of 67 percent and QM population of 99 percent active conformer, DER1 is subjected to MD evaluation. Figure 3.8.(a) shows, distance versus angle plot for the H-bond between pyridine and alcohol of DER1. Figure 3.8.(a) shows that distance and angle relationship of the H-bond between alcohol and pyridine are cumulated in the $6Å < d < 8Å$ and $60^0 < \theta < 120^0$ region rather than the H-bond region indicated with the blue box. MD population of DER1 is 4 percent. Fluctuation of distance between pyridine and alcohol shown in Figure 3.8.(b) indicates that the H-bond between the catalytic dyad formed from time to time, but was not maintained for long. Instead, an alternative strong H-bond between backbone oxygen and benzyl alcohol is established tightly (Figure 3.8 (c) and (d)). This interaction will be examined in detail section 3.12.

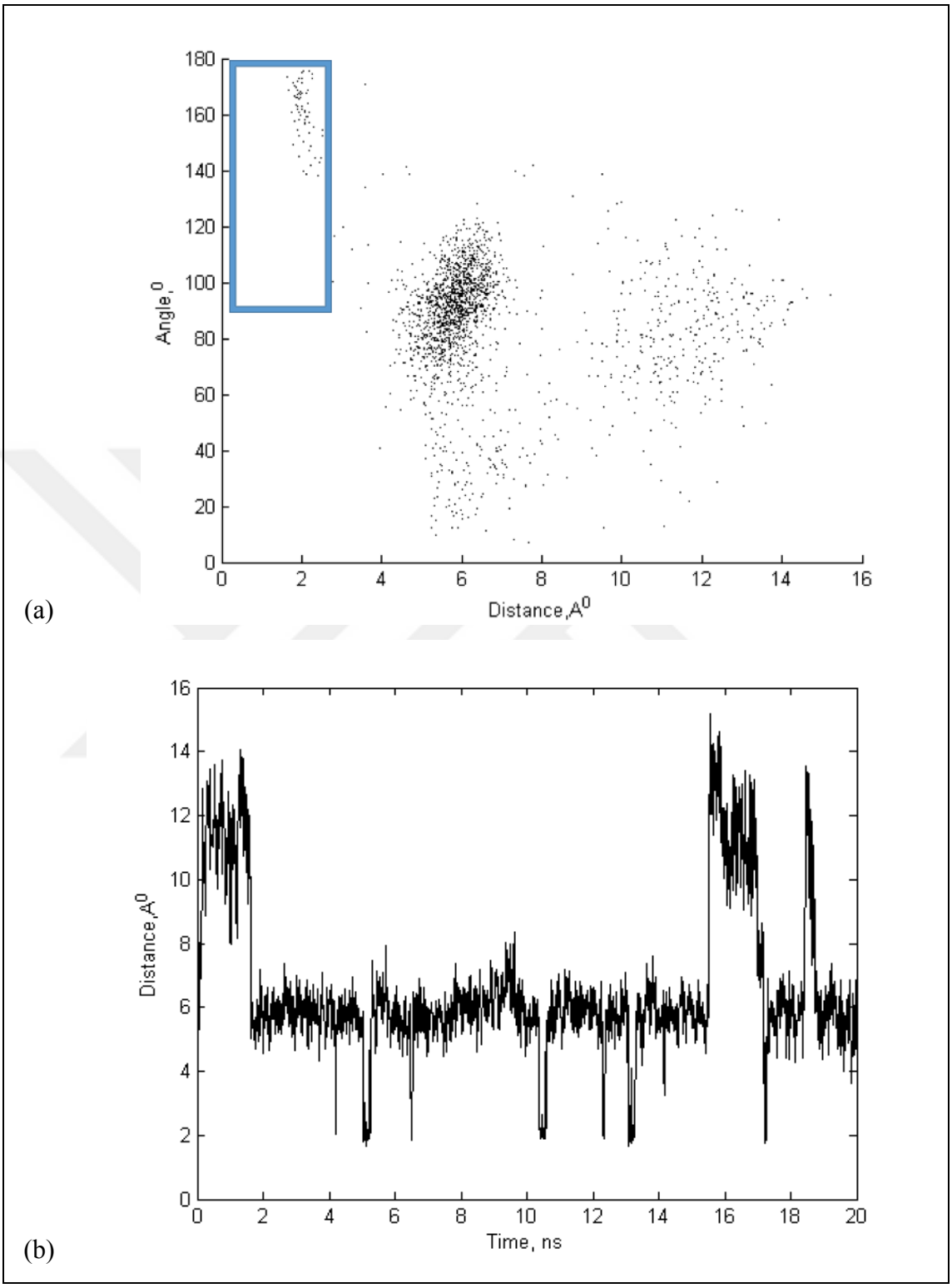

Figure 3.8. MD results of DER1 (a) Pyridine-alcohol H-bond interaction - angle vs. distance, (b) Pyridine-alcohol H-bond interaction - distance vs. time

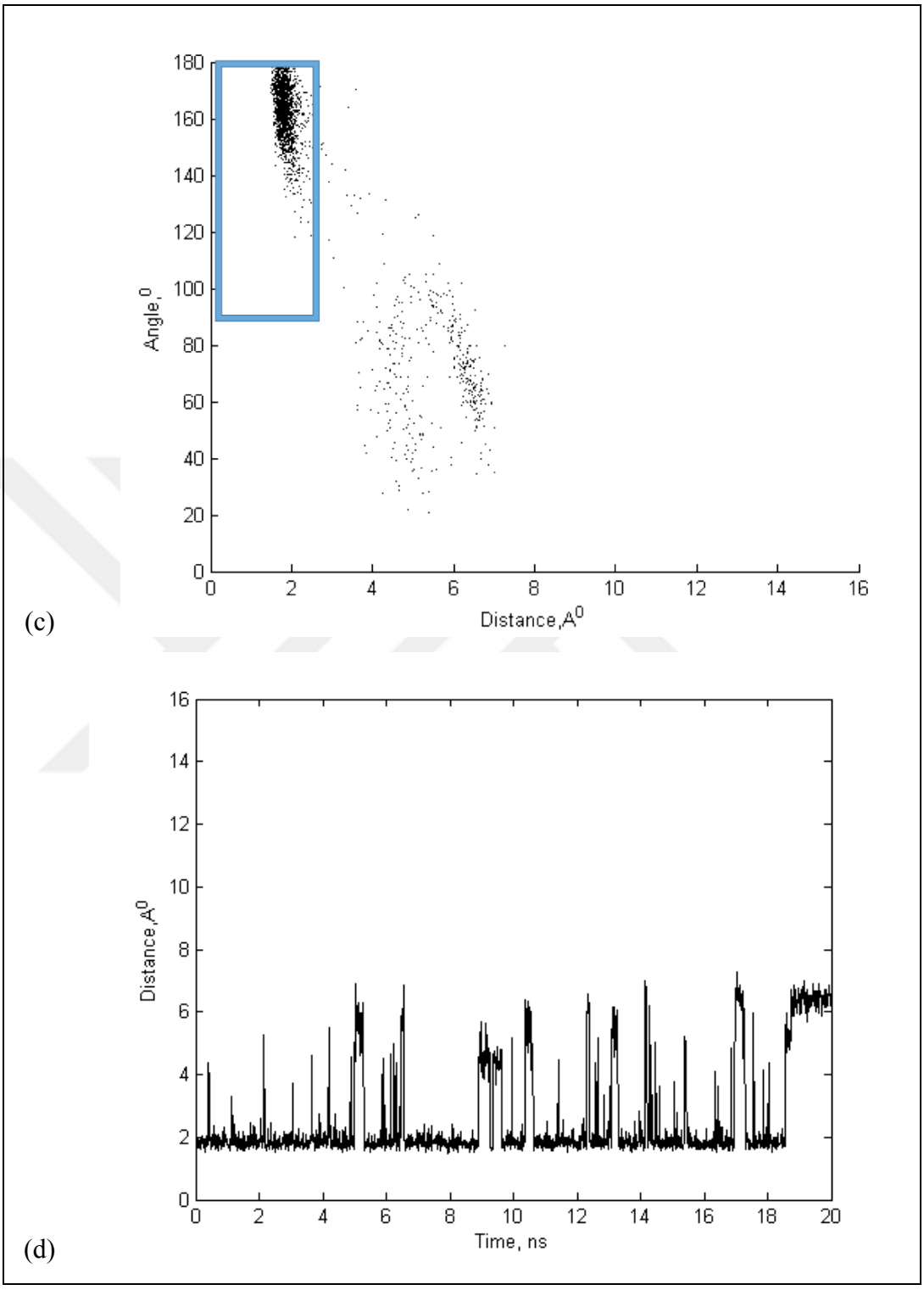

Figure 3.8. MD results of DER1 *(cont'd)* (c) Backbone oxygen-alcohol H-bond interaction - angle vs. distance, (d) Backbone oxygen-alcohol H-bond interaction - distance vs. time

3.2. DER6

DER6 is obtained by the same transformation shown in Figure 3.5. The conformers 1, 57 of DER6 and the transformed part in the blue ring are shown in Figure 3.9. The lowest energy conformer of MM evaluation is not active (Figure 3.9). Table 3.6 shows analysis of DER6.

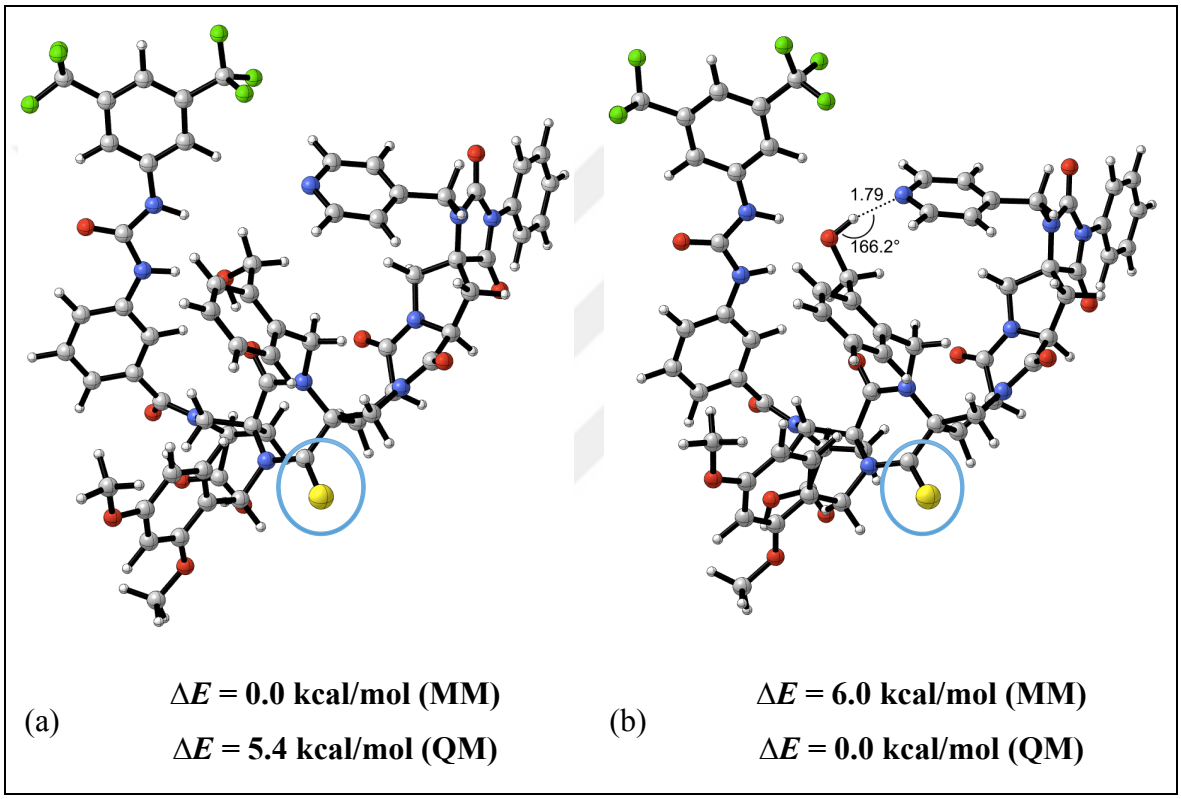

Figure 3.9. Lowest energy conformers of DER6 (a) Conformer 1 (b) Conformer 57

Table 3.6. MM and QM evaluation of DER6

DER6				
Conformer Number	**Δ*E* (kcal/mol) Molecular Mechanics (MM) MMFF94x**	**MM Population (%)**	**Δ*E* (kcal/mol) Quantum Mechanics (QM) M06-2X/6-31G(d)**	**QM Population (%)**
1	0.0	71	5.4	0
2 ACTIVE	1.2	10	2.19	2
3	1.4	6	2.23	2
4	1.6	5	5.0	0
5	1.7	4	5.8	0
6	2.0	2	5.4	0
7	2.2	2	6.1	0
8	3.2	0	5.3	0
9	3.4	0	3.1	1
10 ACTIVE	4.1	0	6.2	0
33 ACTIVE	5.1	0	12.1	0
36 ACTIVE	5.2	0	4.5	0
57 ACTIVE	6.0	0	0.0	95
61 ACTIVE	6.2	0	9.3	0
64 ACTIVE	6.3	0	3.8	0
66 ACTIVE	6.3	0	7.6	0
74 ACTIVE	6.5	0	8.1	0
77 ACTIVE	6.5	0	4.8	0
80 ACTIVE	6.6	0	13.4	0
102 ACTIVE	7.0	0	8.8	0

As shown in Table 3.7, the 94 percent difference in the cumulative QM populations between active conformers and inactive conformers indicates an energy difference of 2.1 kcal/mol between these two.

Table 3.7. Populations and relative energies of active and inactive conformer clusters of DER6

DER6	**QM Population (%)**	**Δ*E* (kcal/mol) Quantum Mechanics (QM) M062X-6-31G(d)**
Total Active Conformers	97	0.0
Total Conformers with no H-bond	3	$\Delta E = 2.1$

DER6 with a total MM population of 10 percent and QM population of 97 percent active conformer, is subjected to MD evaluation. Figure 3.10.(a) shows, distance versus angle plot for the H-bond between pyridine and alcohol of DER6. The distance and the angle between alcohol and pyridine is cumulated in the 6Å < d < 8Å and $0^0 < \theta < 120^0$ region rather than the H-bond region indicated with the blue box. MD population of DER6 was calculated as 1 percent. Figure 3.10.(b) shows the fluctuation of distance between pyridine and alcohol. H-bond between the catalytic dyad is disrupted at the beginning of the simulation and is not reformed throughout the simulated 20 ns.

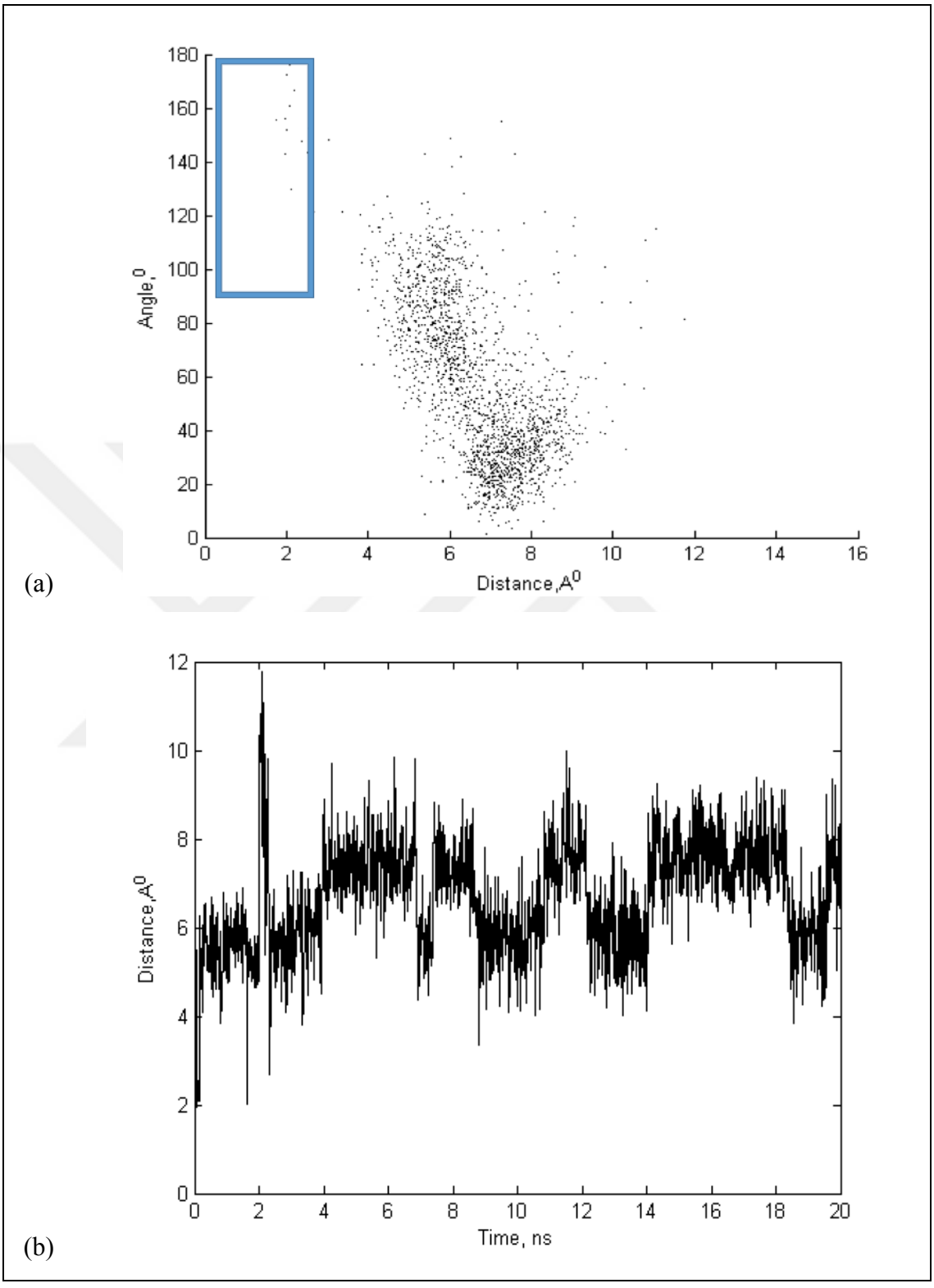

Figure 3.10. MD results of DER6 (a) Pyridine-alcohol H-bond interaction – angle vs. distance, (b) Pyridine-alcohol H-bond interaction - distance vs. time

3.3. DER15

DER15 is formed by the transformation of C=O to SO_2. Figure 3.11 shows the transformation used in the design of DER15. Figure 3.12 shows conformers 1 and 5 of DER15. The transformed part of DER15 in the blue ring can be seen from this figure.

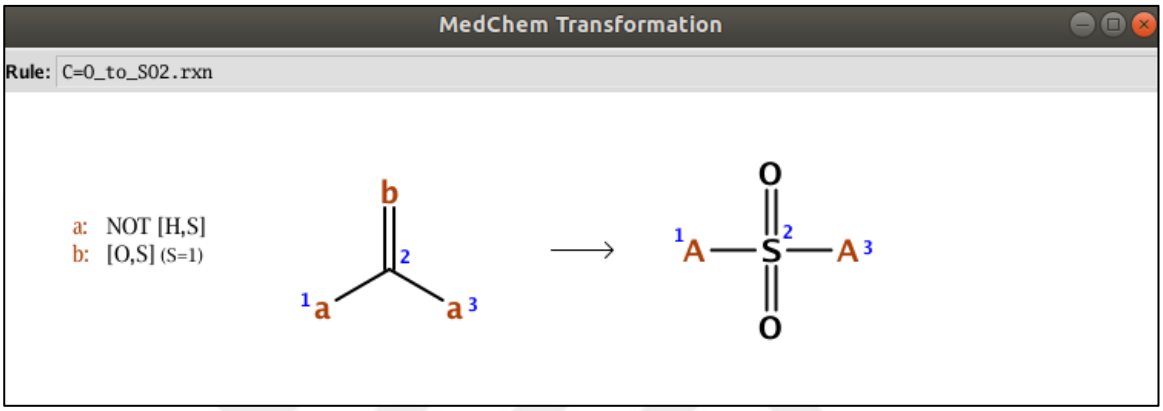

Figure 3.11. Transformation rule applied to DER15

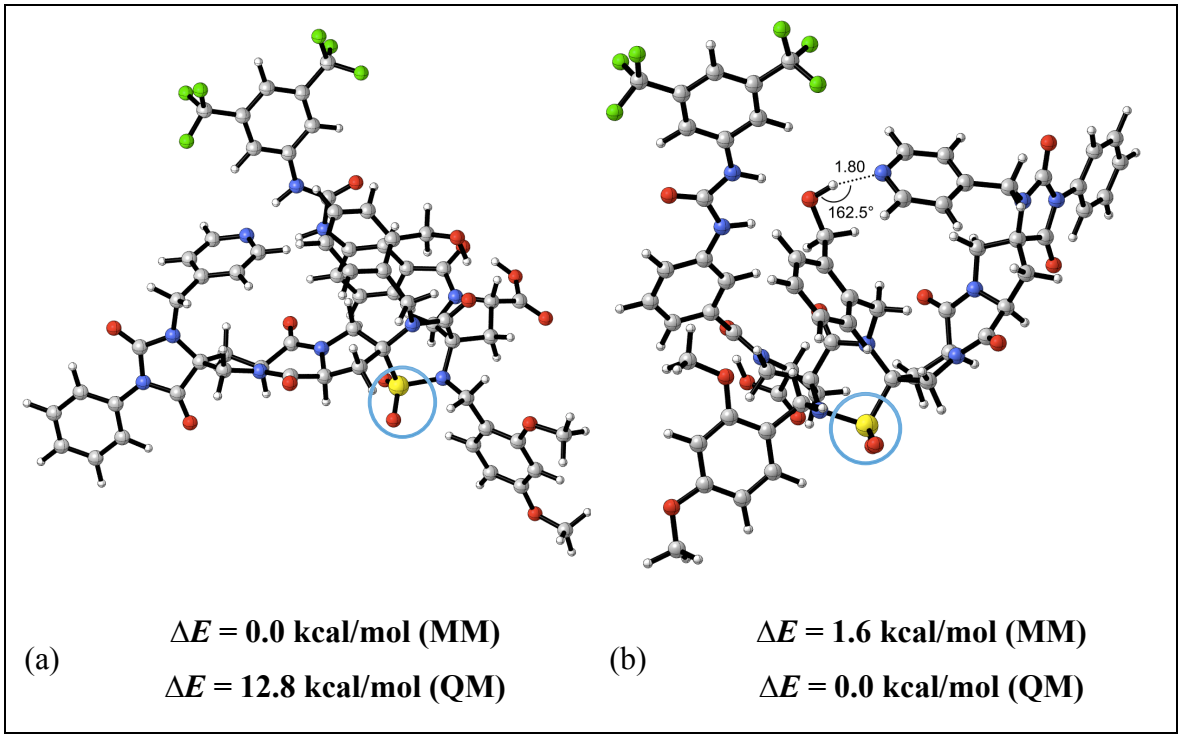

Figure 3.12. Lowest energy conformers of DER15 (a) Conformer 1, (b) Conformer 5

The conformational search for DER15 generated 91 conformers. Table 3.8 shows the results of DER15. Conformer 5 is the lowest energy active conformer according to the QM calculations. QM population of conformer 5 is 84 percent while it has 3 percent MM population. Conformer 1, which is the lowest energy conformer according to MM evaluation is not active. Although conformer 1 has 42 percent MM population, its QM population is 0 percent.

Table 3.8. MM and QM evaluation of DER15

DER15				
Conformer Number	**Δ*E* (kcal/mol) Molecular Mechanics (MM) MMFF94x**	**MM Population (%)**	**Δ*E* (kcal/mol) Quantum Mechanics (QM) M06-2X/6-31G(d)**	**QM Population (%)**
1	0.0	42	12.8	0
2	0.1	34	5.0	0
3 ACTIVE	0.7	13	5.7	0
4	1.2	5	2.5	1
5 ACTIVE	1.6	3	0.0	84
6	1.9	2	1.5	6
7	2.3	1	13.6	0
8	2.6	1	4.2	0
9 ACTIVE	3.0	0	1.4	8
10 ACTIVE	3.1	0	4.0	0
14 ACTIVE	3.7	0	6.3	0
27 ACTIVE	5.1	0	4.8	0
73 ACTIVE	6.1	0	9.7	0
75 ACTIVE	7.1	0	5.2	0
76 ACTIVE	8.1	0	12.3	0
87 ACTIVE	9.1	0	11.0	0

Table 3.9. Populations and relative energies of active and inactive conformer clusters of DER15

DER15	**QM Population (%)**	**Δ*E* (kcal/mol) Quantum Mechanics (QM) M062X-6-31G(d)**
Total Active Conformers	92	0.0
Total Conformers with no H-bond	8	$\Delta E = 1.5$

Table 3.9 shows the relative energy calculation of DER15. Cumulative active conformer population is 92 percent. These results showed that, inactive conformers are 1.5 kcal/mol higher in energy than the active conformers. DER15, which has total MM population of 16 percent and QM population of 92 percent active conformer is subjected to MD evaluation. However, MD simulations of DER15 showed that the H-bond between alcohol and pyridine was never formed.

3.4. DER41

DER41 is formed by transformation of a C-F bond in TF3 spiroligozymes to C-Cyano. Figure 3.13 shows this transformation. In Figure 3.14, the transformed part of the molecule can be observed in the blue ring.

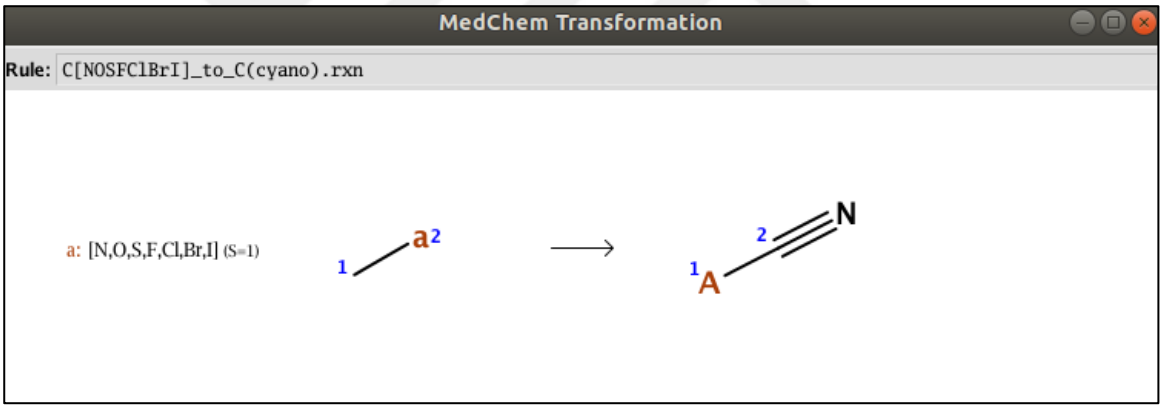

Figure 3.13. Transformation rule applied to DER41

Figure 3.14 shows the lowest energy conformers of DER41 for MM and QM evaluation, respectively. The conformational search for DER41 generated 88 conformers. The results in Table 3.10 show 12 conformers of DER41 are active. The calculations based on MMFF94x force field show that the lowest energy conformer is conformer 1 with no H-bond. QM calculations reveal the lowest energy conformer is active conformer 12 and its population is 97 percent.

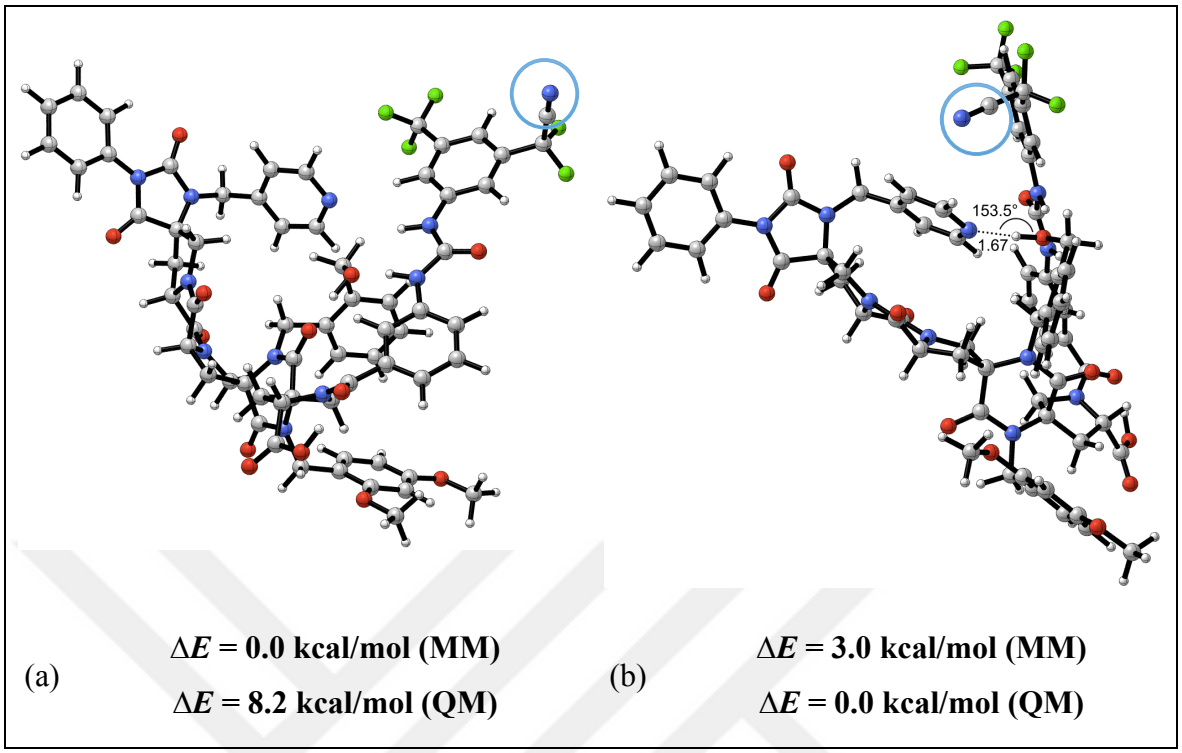

Figure 3.14. Lowest energy conformers of DER41 (a) Conformer 1, (b) Conformer 12

Table 3.10. MM and QM evaluation of DER41

DER41				
Conformer Number	**ΔE (kcal/mol) Molecular Mechanics (MM) MMFF94x**	**MM Population (%)**	**ΔE (kcal/mol) Quantum Mechanics (QM) M06-2X/6-31G(d)**	**QM Population (%)**
1	0.0	61	8.2	0
2 ACTIVE	0.9	13	3.7	0
3 ACTIVE	1.0	11	3.5	0
4 ACTIVE	1.8	3	7.9	0
5	1.9	2	3.3	0
6	2.0	2	12.8	0
7	2.0	2	4.5	0
8	2.0	2	6.0	0
9	2.1	2	4.0	0
10	2.4	1	16.6	0
11	2.6	1	14.4	0
12 ACTIVE	3.0	0	0.0	97
19 ACTIVE	4.2	0	11.9	0
23 ACTIVE	4.7	0	4.0	0
37 ACTIVE	5.6	0	4.7	0
46 ACTIVE	6.1	0	3.5	0
50 ACTIVE	6.2	0	5.9	0
63 ACTIVE	6.5	0	14.9	0
67 ACTIVE	6.6	0	2.4	2
79 ACTIVE	6.8	0	16.4	0

Table 3.11. Populations and relative energies of active and inactive conformer clusters of DER41

DER41	**QM Population (%)**	**Δ*E* (kcal/mol) Quantum Mechanics (QM) M062X-6-31G(d)**
Total Active Conformers	99	0.0
Total Conformers with no H-bond	1	Δ*E* = 2.7

Table 3.11 shows cumulative populations of DER41. The cumulative population difference between the active and inactive conformers is 98 percent. This difference corresponds to an energy difference, Δ*E,* of 2.7 kcal/mol.

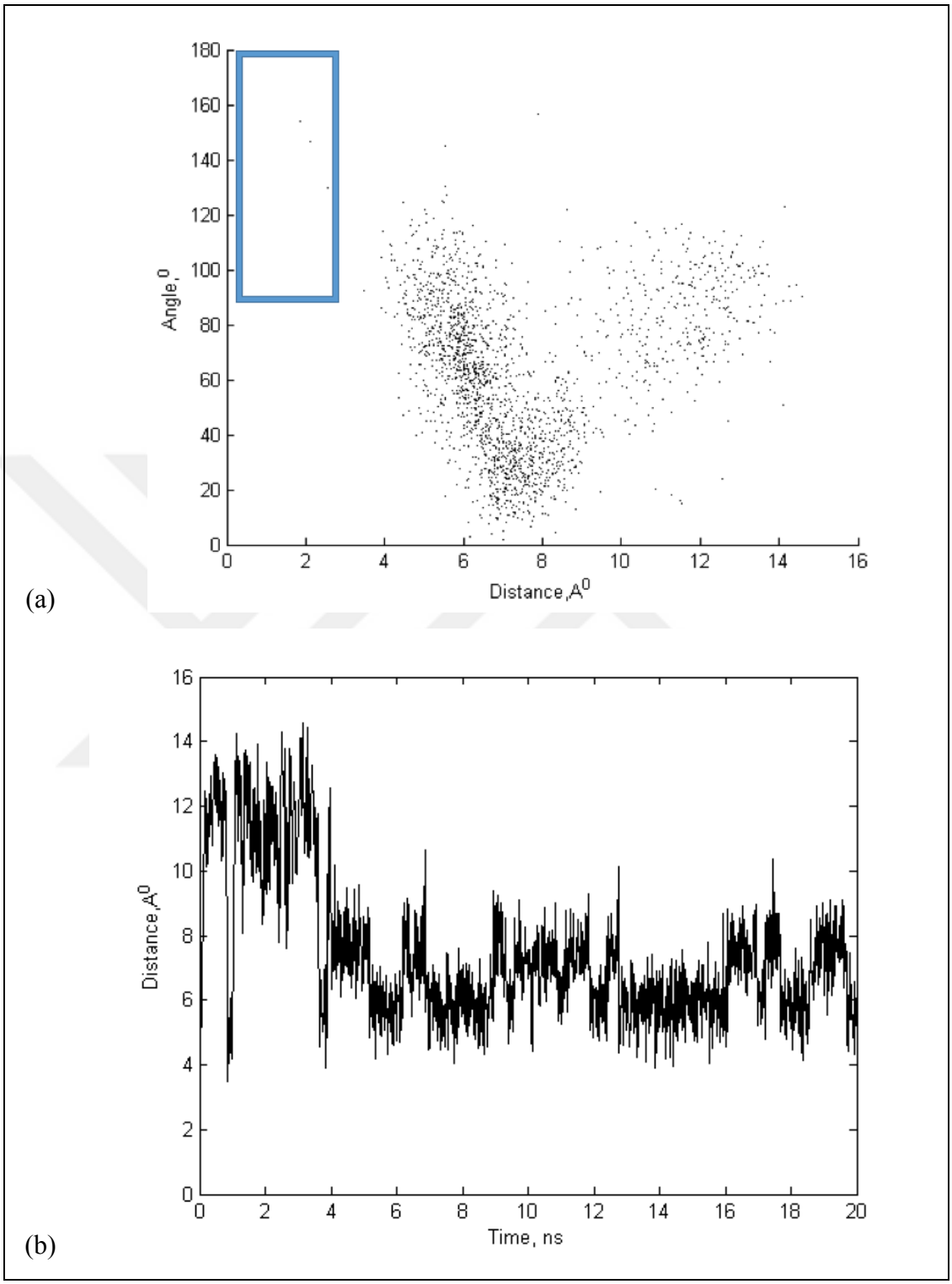

Figure 3.15. MD results of DER41 (a) Pyridine-alcohol H-bond interaction - angle vs. distance, (b) Pyridine-alcohol H-bond interaction - distance vs. time

DER41 with a total MM population of 27 percent and QM population of 99 percent active conformer, is subjected to MD evaluation. From Figure 3.15.(a) the distance and the angle between alcohol and pyridine is cumulated in the 6Å < d < 8Å and $0^0 < \theta < 120^0$ region rather than the H-bond region indicated with the blue box. MD population of DER41 was calculated as 0 percent, in accordance with the fluctuation of distance between pyridine and alcohol in Figure 3.15.(b).

3.5. DER64

DER64 is obtained by ring expansion in the backbone of TF3 spiroligozyme. Figure 3.16 shows the transformation rule. The transformed part in the blue ring and the lowest energy conformers of DER64 for both MM and QM evaluation can be seen from Figure 3.17.

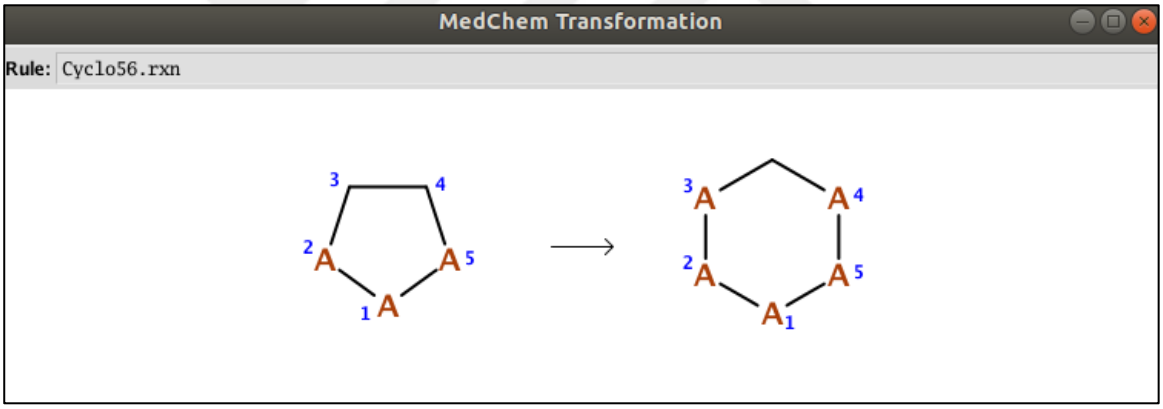

Figure 3.16. Transformation rule applied to DER64

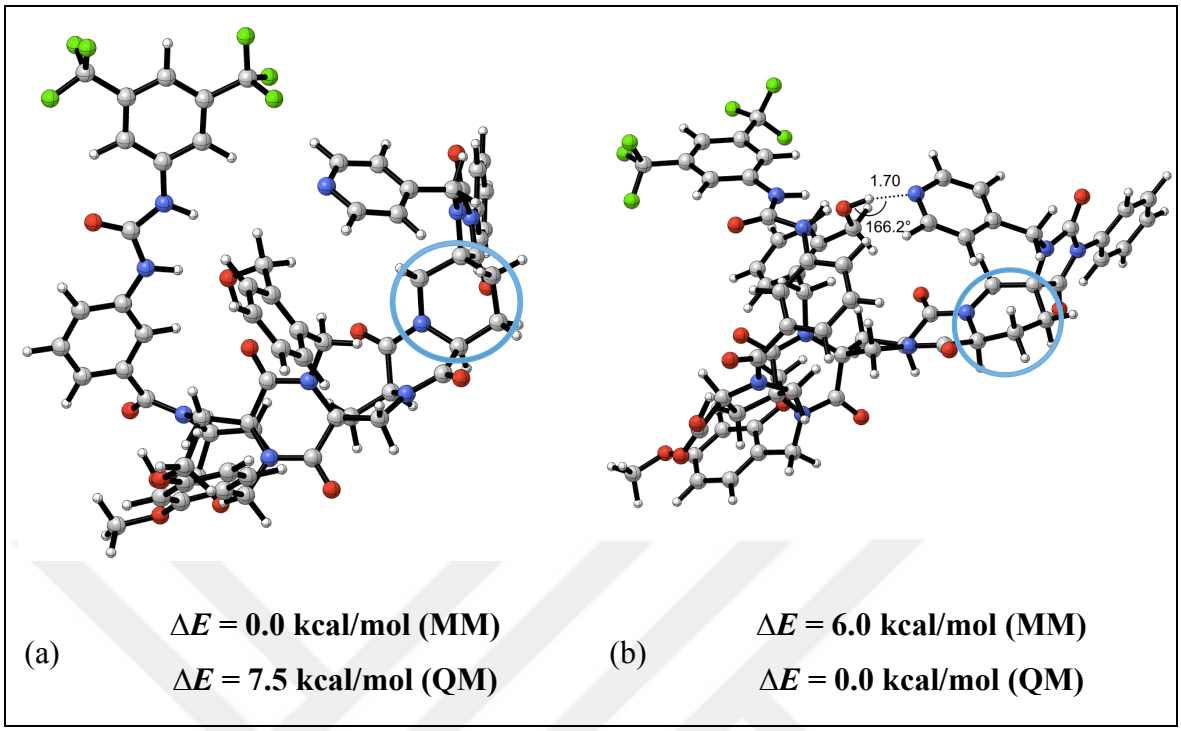

Figure 3.17. Lowest energy conformers of DER64 (a) Conformer 1, (b) Conformer 53

Table 3.12. MM and QM evaluation of DER64

DER64				
Conformer Number	**ΔE (kcal/mol) Molecular Mechanics (MM) MMFF94x**	**MM Population (%)**	**ΔE (kcal/mol) Quantum Mechanics (QM) M06-2X/6-31G(d)**	**QM Population (%)**
1	0.0	69	7.5	0
2 ACTIVE	0.8	19	5.8	0
3	1.4	6	4.1	0
4	2.1	2	0.8	19
5	2.3	1	7.2	0
6	2.4	1	2.2	2
7	2.5	1	4.2	0
8	2.7	1	7.5	0
9	2.9	0	12.2	0
10 ACTIVE	3.2	0	6.7	0
35 ACTIVE	4.7	0	0.8	20
53 ACTIVE	6.0	0	0.0	74
66 ACTIVE	6.4	0	2.1	1
68 ACTIVE	6.4	0	7.1	0
89 ACTIVE	6.9	0	6.5	0

The conformational search for DER64 generated 94 conformers. Lowest energy conformer of DER64 according to MM has a population of 69 percent while it has a population of 0 percent according to QM calculations (Table 3.12). The lowest energy active conformer according to QM evaluation is conformer 53. It has 74 percent QM population while has 0 percent MM population.

Table 3.13 shows relative energy calculations of DER64. Cumulative population of 95 percent for active conformers versus 5 percent cumulative population of inactive conformers corresponds to an energy difference, ΔE, of 1.7 kcal/mol.

Table 3.13. Populations and relative energies of active and inactive conformer clusters of DER64

DER64	**QM Population (%)**	**ΔE (kcal/mol) Quantum Mechanics (QM) M062X-6-31G(d)**
Total Active Conformers	95	0.0
Total Conformers with no H-bond	5	ΔE = 1.7

DER64 with a total MM population of 19 percent and QM population of 95 percent active conformer, is subjected to MD evaluation. Figure 3.18.(a) shows, distance versus angle plot for the H-bond between pyridine and alcohol of DER6. The distance and the angle between alcohol and pyridine is cumulated in the 3Å < d < 8Å and $0^0 < \theta < 180^0$ region rather than the H-bond region indicated with the blue box. Figure 3.18.(b) shows the fluctuation of distance between pyridine and alcohol. MD population of DER64 is calculated as 1 percent. MD results of DER64 showed that, H-bond between the catalytic dyad does not form.

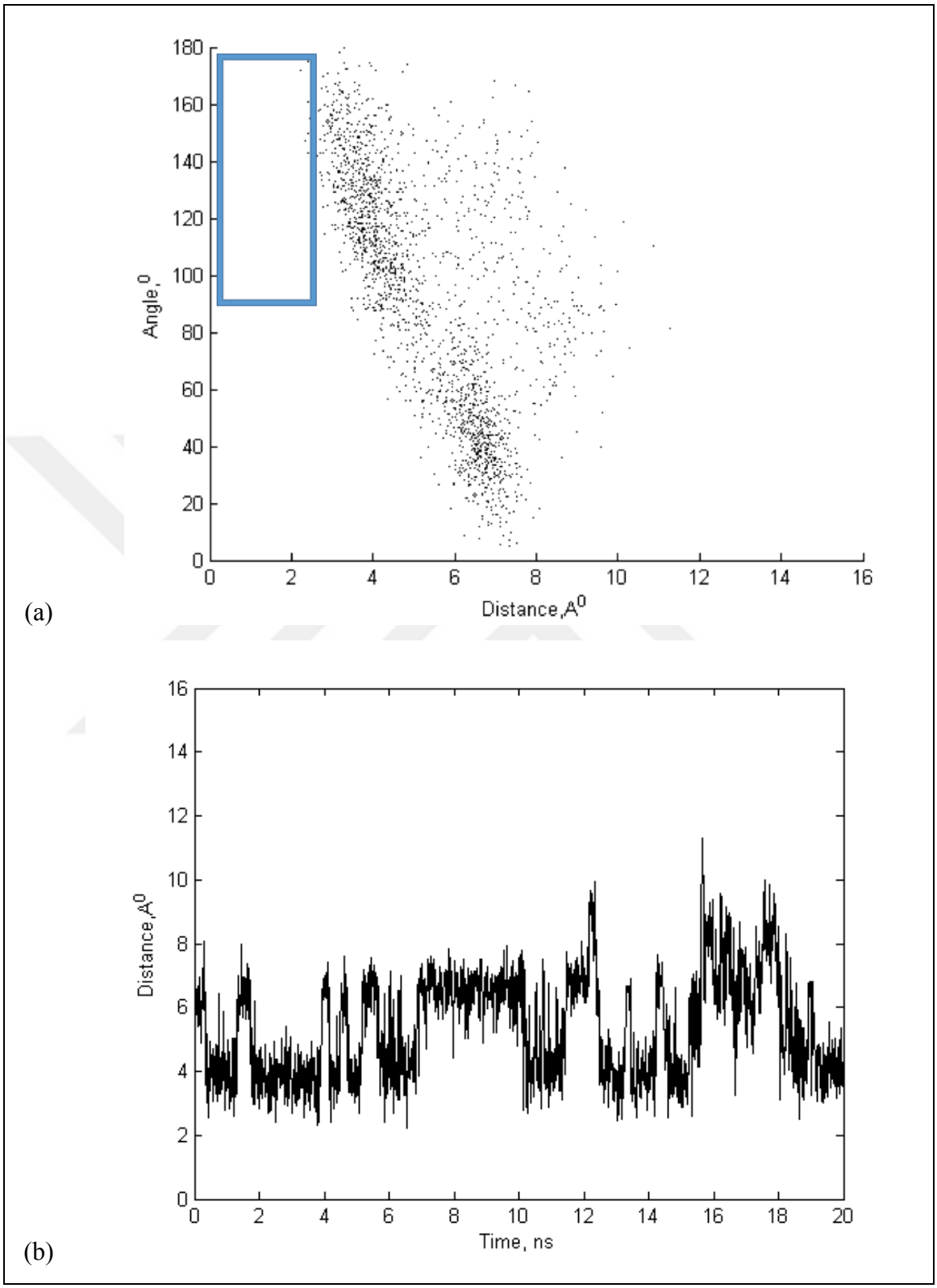

Figure 3.18. MD results of DER64 (a) Pyridine-alcohol H-bond interaction - angle vs. distance, (b) Pyridine-alcohol H-bond interaction - distance vs. time

3.6. DER72

DER72 has a ring transformation in the backbone. Figure 3.19 shows the transformation used in the design of DER72. Figure 3.20 shows the transformed part in the blue ring and the lowest energy conformers of DER72 for both MM and QM calculations (Table 3.14).

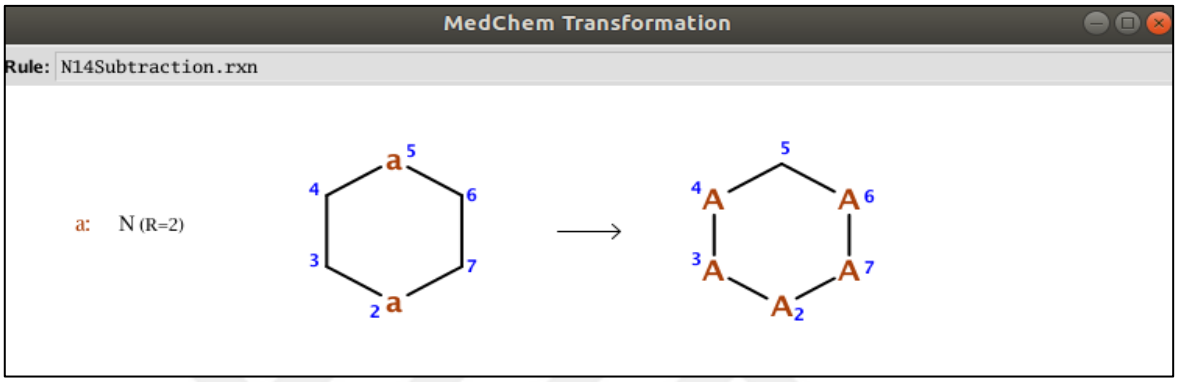

Figure 3.19. Transformation rule applied to DER72

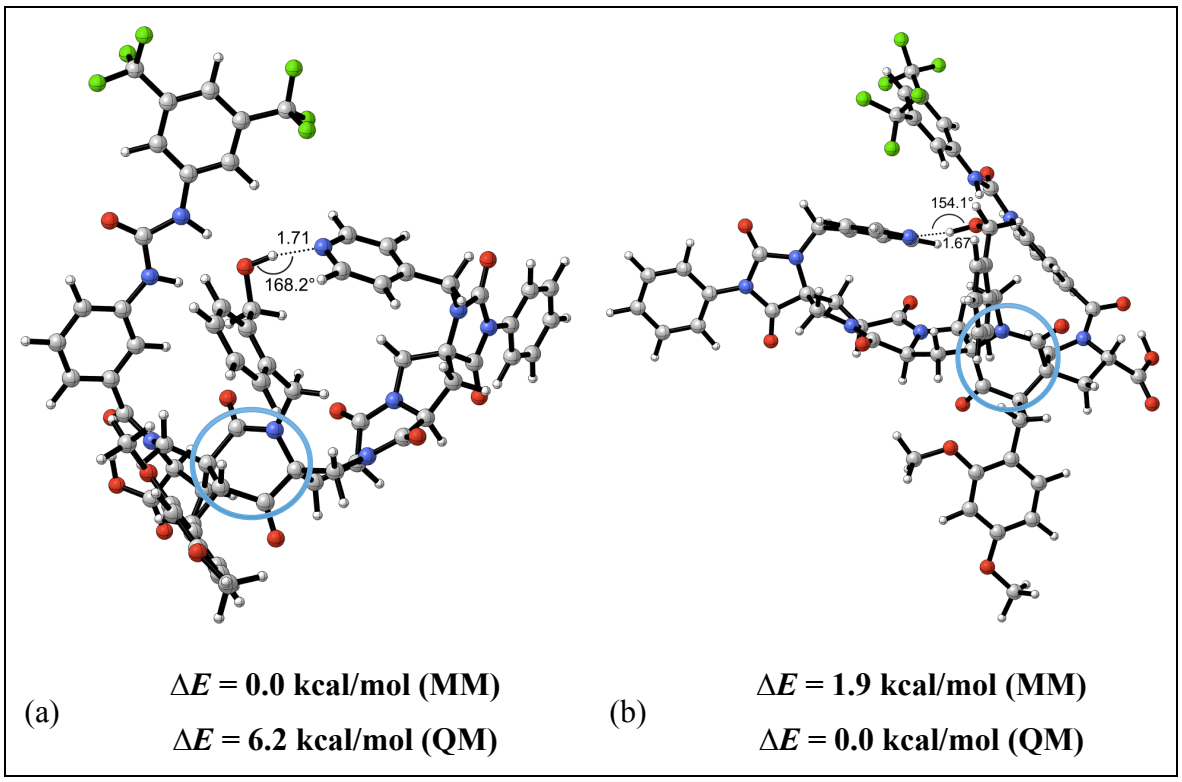

Figure 3.20. Lowest energy conformers of DER72 (a) Conformer 1, (b) Conformer 2

Table 3.14. MM and QM evaluation of DER72

DER72				
Conformer Number	**Δ*E* (kcal/mol) Molecular Mechanics (MM) MMFF94x**	**MM Population (%)**	**Δ*E* (kcal/mol) Quantum Mechanics (QM) M06-2X/6-31G(d)**	**QM Population (%)**
1 ACTIVE	0.0	88	6.2	0
2 ACTIVE	1.9	3	0.0	97
3	1.9	3	11.3	0
4	2.0	3	10.5	0
5	3.2	0	9.6	0
6	2.7	1	6.6	0
7	2.8	1	2.0	3
12 ACTIVE	3.8	0	16.2	0
13 ACTIVE	3.8	0	10.1	0
25 ACTIVE	4.9	0	9.3	0
26 ACTIVE	5.0	0	15.8	0
33 ACTIVE	5.3	0	14.6	0

Table 3.15. Populations and relative energies of active and inactive conformer clusters of DER72

DER72	**QM Population (%)**	**Δ*E* (kcal/mol) Quantum Mechanics (QM) M062X-6-31G(d)**
Total Active Conformers	97	0.0
Total Conformers with no H-bond	3	$\Delta E = 2.1$

DER72 has total MM population of 91 percent and QM population of 97 percent active conformers. Table 3.15 shows relative energy calculations of DER72. These results showed that, inactive conformers are 2.1 kcal/mol higher in energy than the active conformers. Figure 3.21.(a) shows distance versus angle plot for the H-bond between pyridine and alcohol of DER72. The distance and the angle between alcohol and pyridine is cumulated in the 10Å < d < 12Å and $40^0 < \theta < 100^0$ region rather than the H-bond region indicated with the blue box. Figure 3.21.(b) shows the fluctuation of distance between pyridine and alcohol. The H-bond between the catalytic dyad is not formed. MD population of DER72 was calculated as 0 percent.

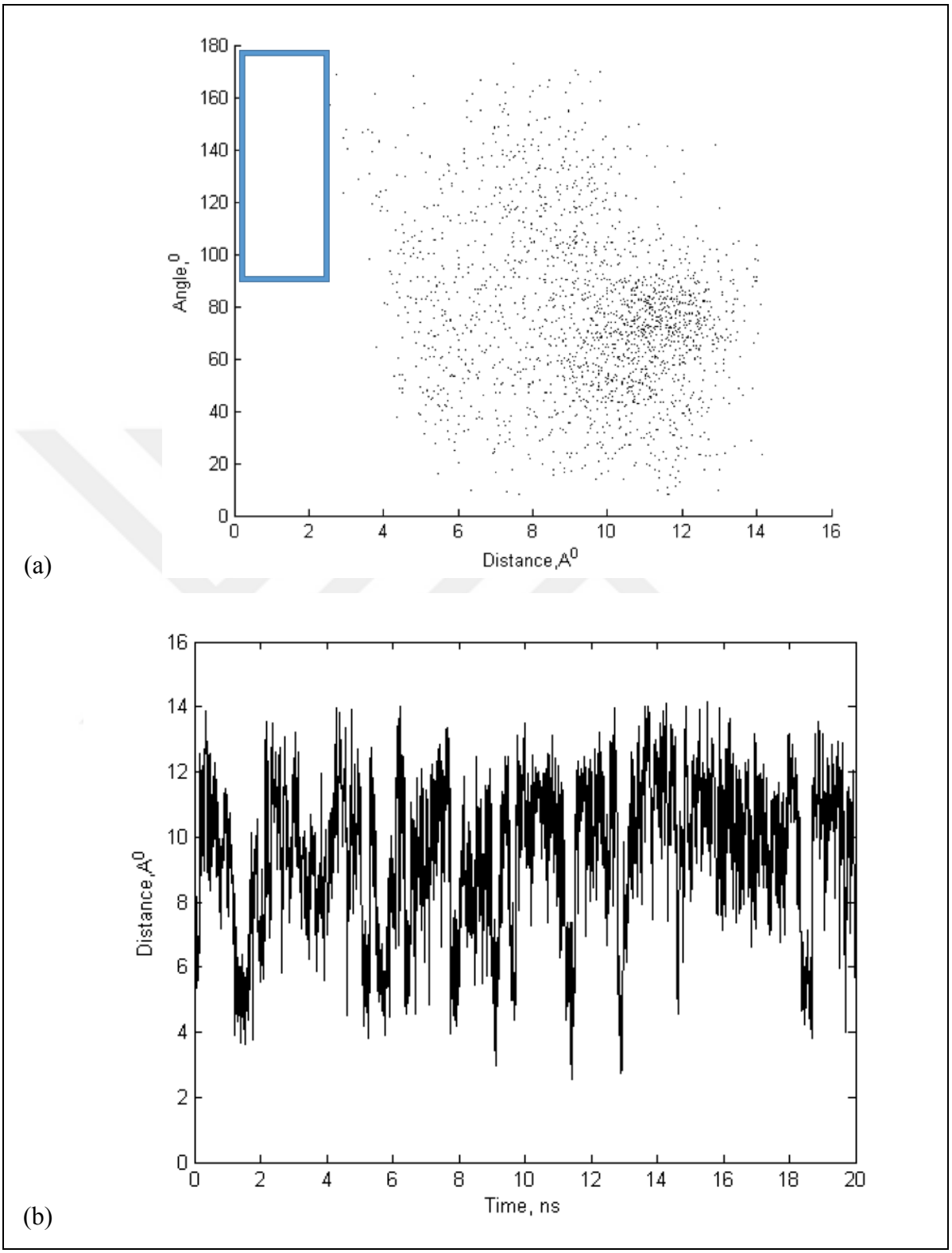

Figure 3.21. MD results of DER72 (a) Pyridine-alcohol H-bond interaction - angle vs. distance, (b) Pyridine-alcohol H-bond interaction - distance vs. time

3.7. DER77

This derivative is formed by amide to amine reaction. Figure 3.22 shows the transformation. The transformed part of DER77 is shown in Figure 3.23 in the blue ring.

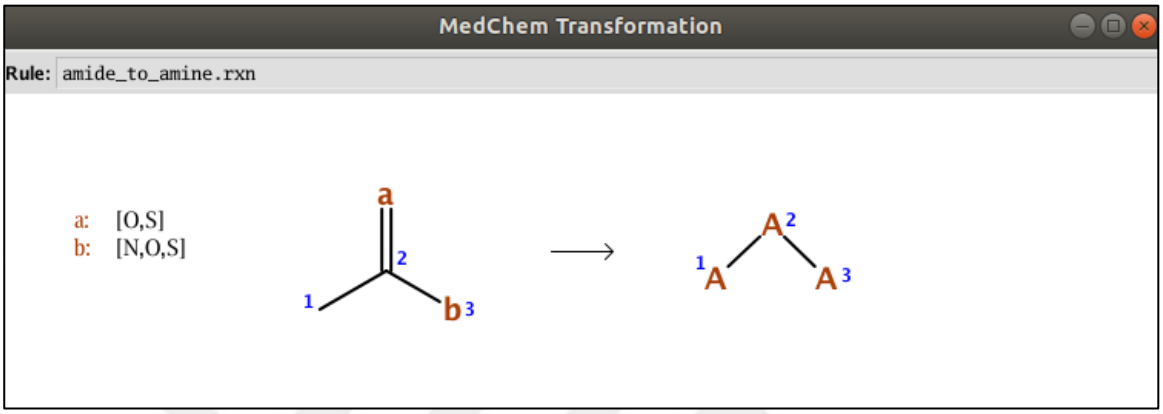

Figure 3.22. Transformation rule applied to DER77

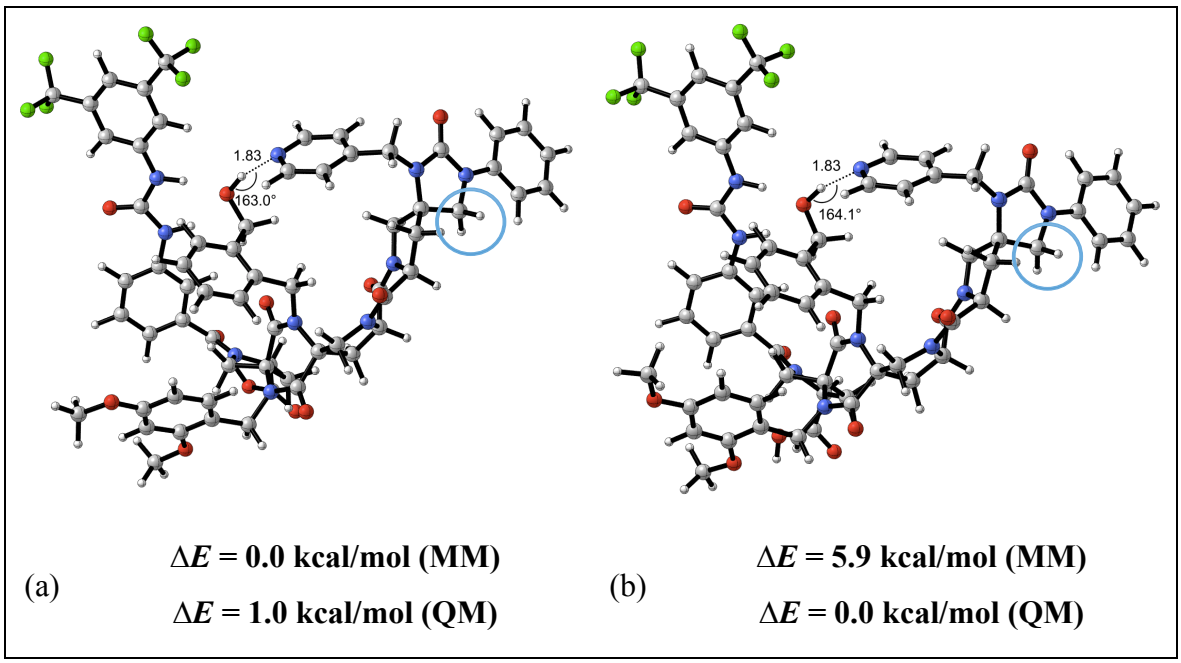

Figure 3.23. Lowest energy conformers of DER77 (a) Conformer 1, (b) Conformer 59

The conformational search for DER77 generated 97 conformers. Table 3.16 shows evaluation of DER77 for both MM and QM calculations. According to these results, 7 conformers of DER77 are active. Conformer 1 and 59 are the lowest energy active conformers of DER77 according to MM and QM evaluation, respectively (Figure 3.23).

QM evaluation shows that, conformer 1, which is the lowest energy conformer according to MM is 1 kcal/mol higher in energy than conformer 59, which is the lowest energy conformer according to QM calculation. Conformer 1 has 42 percent MM and 14 percent QM population while conformer 59 has 0 percent MM and 76 percent QM population.

Table 3.16. MM and QM evaluation of DER77

DER77				
Conformer Number	**Δ*E* (kcal/mol) Molecular Mechanics (MM) MMFF94x**	**MM Population (%)**	**Δ*E* (kcal/mol) Quantum Mechanics (QM) M06-2X/6-31G(d)**	**QM Population (%)**
1 ACTIVE	0.0	42	1.0	14
2 ACTIVE	0.4	21	1.3	9
3	0.7	12	3.7	0
4	0.8	11	3.6	0
5	1.5	3	7.5	0
6	1.7	3	8.6	0
7 ACTIVE	1.7	2	2.7	1
8	1.8	2	14.4	0
9	1.9	2	12.0	0
10	2.4	1	5.3	0
11	2.6	1	11.2	0
12	2.9	0	10.5	0
14 ACTIVE	3.4	0	4.4	0
55 ACTIVE	5.8	0	9.1	0
59 ACTIVE	5.9	0	0.0	76
75 ACTIVE	5.4	0	9.3	0

Table 3.17 shows relative energy calculation of DER77. Cumulative population of 100 percent for active conformers versus 0 percent cumulative population of inactive conformers corresponds to an energy difference, Δ*E,* of 4.0 kcal/mol.

Table 3.17. Populations and relative energies of active and inactive conformer clusters of DER77

DER77	**QM Population (%)**	**Δ*E* (kcal/mol) Quantum Mechanics (QM) M062X-6-31G(d)**
Total Active Conformers	100	0.0
Total Conformers with no H-bond	0	$\Delta E = 4.0$

The distance and the angle between alcohol and pyridine is cumulated in the 6Å < d < 8Å and $0^0 < \theta < 60^0$ region rather than the H-bond region indicated with the blue box. MD population of DER77 was calculated as 0 percent. Figure 3.24.(b) shows the fluctuation of distance between pyridine and alcohol. H-bond between the catalytic dyad is disrupted at the beginning of the simulation and it is not reformed.

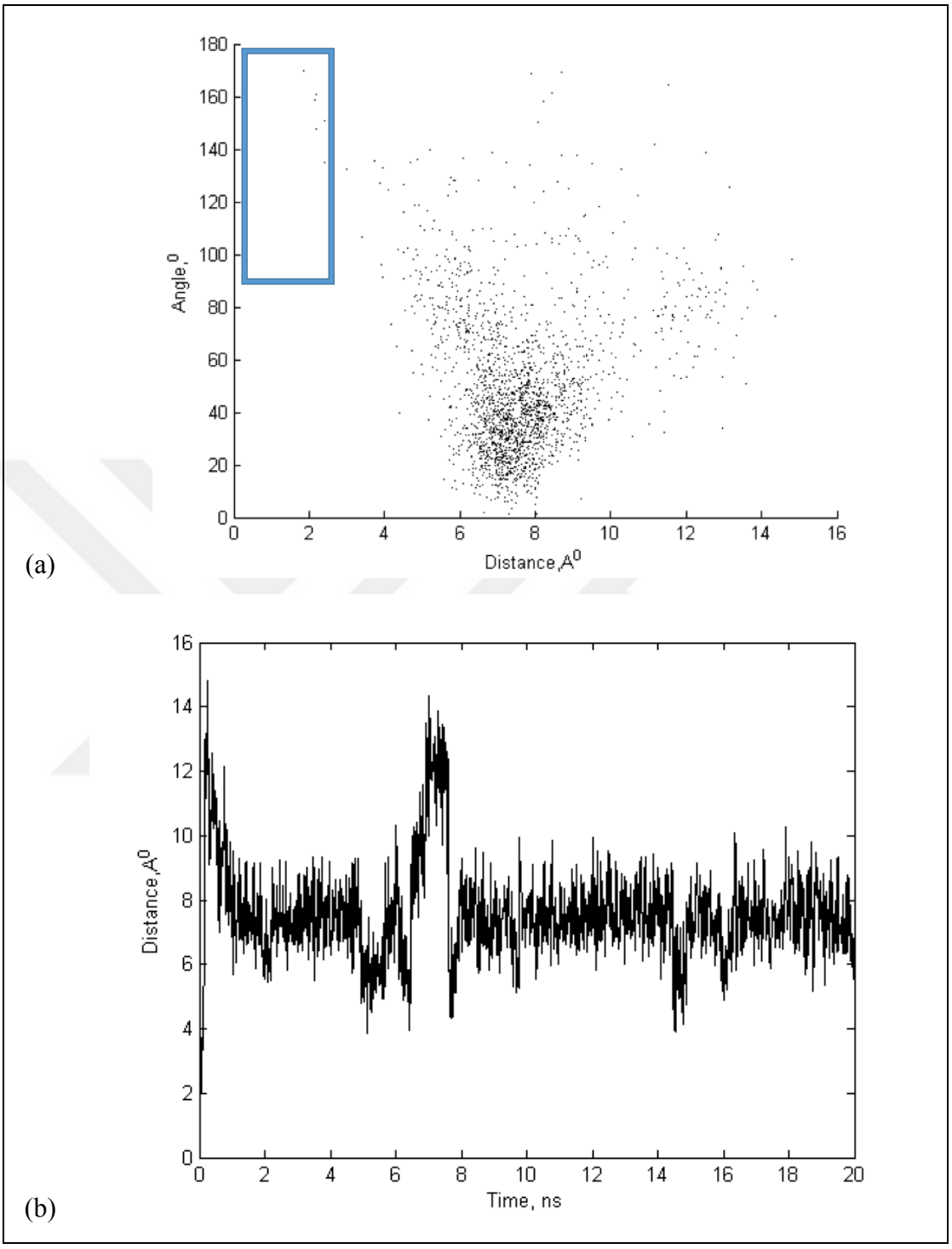

Figure 3.24. MD Results of DER77 (a) Pyridine-alcohol H-bond interaction - angle vs. distance (b) Pyridine-alcohol H-bond interaction - distance vs. time

3.8. DER112

DER112 is formed by the conversion of a benzene ring to pyridine. Figure 3.25 shows the transformation used in the design of DER112. The transformed part of DER112 in the blue ring is shown in Figure 3.26.

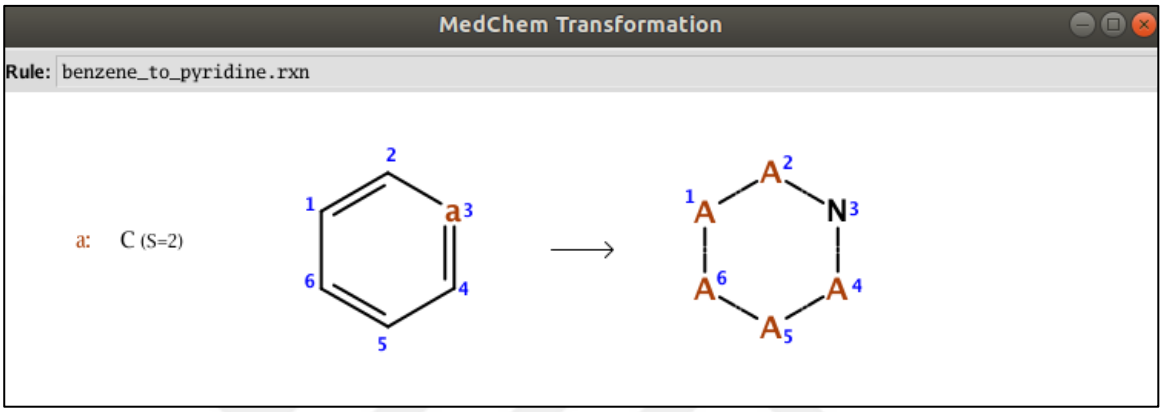

Figure 3.25. Transformation rule applied to DER112

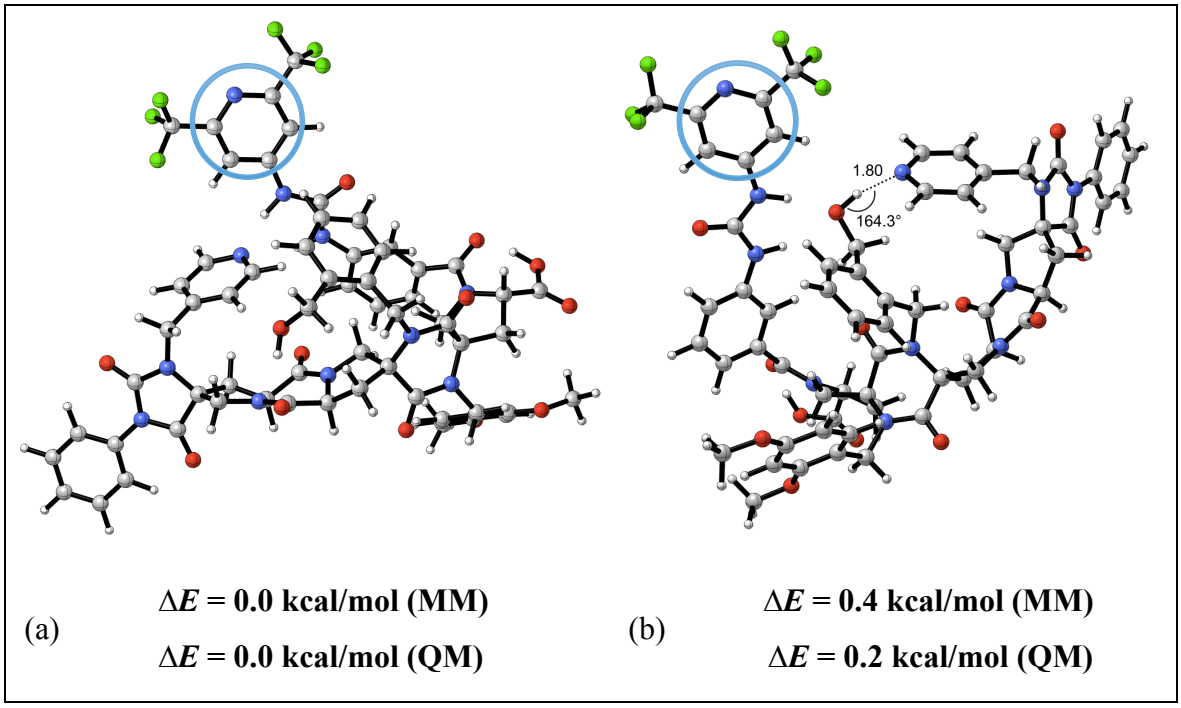

Figure 3.26. Lowest energy conformers of DER112 (a) Conformer 1, (b) Conformer 2

The conformational search for DER112 generated 114 conformers. The results obtained from the conformational analysis of DER112 are shown in Table 3.18. The inactive conformer 1 is the lowest energy conformer for both MM and QM evaluation. Conformer 2 is the lowest energy conformer between the active conformers. However, conformer 2 is only 0.2 kcal/mol higher in energy than the lowest energy conformer 1. Conformer 1 has 45 percent MM population and 42 percent QM population while conformer 2 has 24 percent MM population and 30 percent QM population.

Table 3.18. MM and QM evaluation of DER112

DER112				
Conformer Number	**Δ*E* (kcal/mol) Molecular Mechanics (MM) MMFF94x**	**MM Population (%)**	**Δ*E* (kcal/mol) Quantum Mechanics (QM) M06-2X/6-31G(d)**	**QM Population (%)**
1	0.0	45	0.0	42
2 ACTIVE	0.4	24	0.2	30
3	0.6	17	3.7	0
4	1.6	3	3.9	0
5	1.6	3	2.7	0
6	2.0	2	6.4	0
7	2.0	2	8.6	0
8	2.1	1	11.8	0
9	2.4	1	3.9	0
10	2.5	1	8.5	0
11	2.6	1	1.0	7
12	2.7	1	13.5	0
13	2.8	0	7.6	0
14	2.9	0	6.4	0
15	2.9	0	6.3	0
30 ACTIVE	4.3	0	10.6	0
32 ACTIVE	4.4	0	6.4	0
50 ACTIVE	5.3	0	9.5	0
75 ACTIVE	6.1	0	0.5	17
86 ACTIVE	6.3	0	1.7	2
89 ACTIVE	6.3	0	6.3	0
101 ACTIVE	6.6	0	7.8	0

Table 3.19 shows that DER112 consists of 50 percent active and 50 percent inactive cumulative conformer population indicating no energetic preference.

Table 3.19. Populations and relative energies of active and inactive conformer clusters of DER112

DER112	**QM Population (%)**	**Δ*E* (kcal/mol) Quantum Mechanics (QM) M062X-6-31G(d)**
Total Active Conformers	50	0.0
Total Conformers with no H-bond	50	0.0

DER112 with a total MM population of 24 percent and QM population of 50 percent active conformer, is subjected to MD evaluation. Figure 3.27 shows the MD results of DER112. The distance and the angle between alcohol and pyridine is cumulated in the 6Å < d < 8Å and $0^0 < \theta < 100^0$ region rather than the H-bond region indicated with the blue box. MD population of DER112 was calculated as 0 percent. These results show that H-bond between the catalytic dyad is not formed during the simulation.

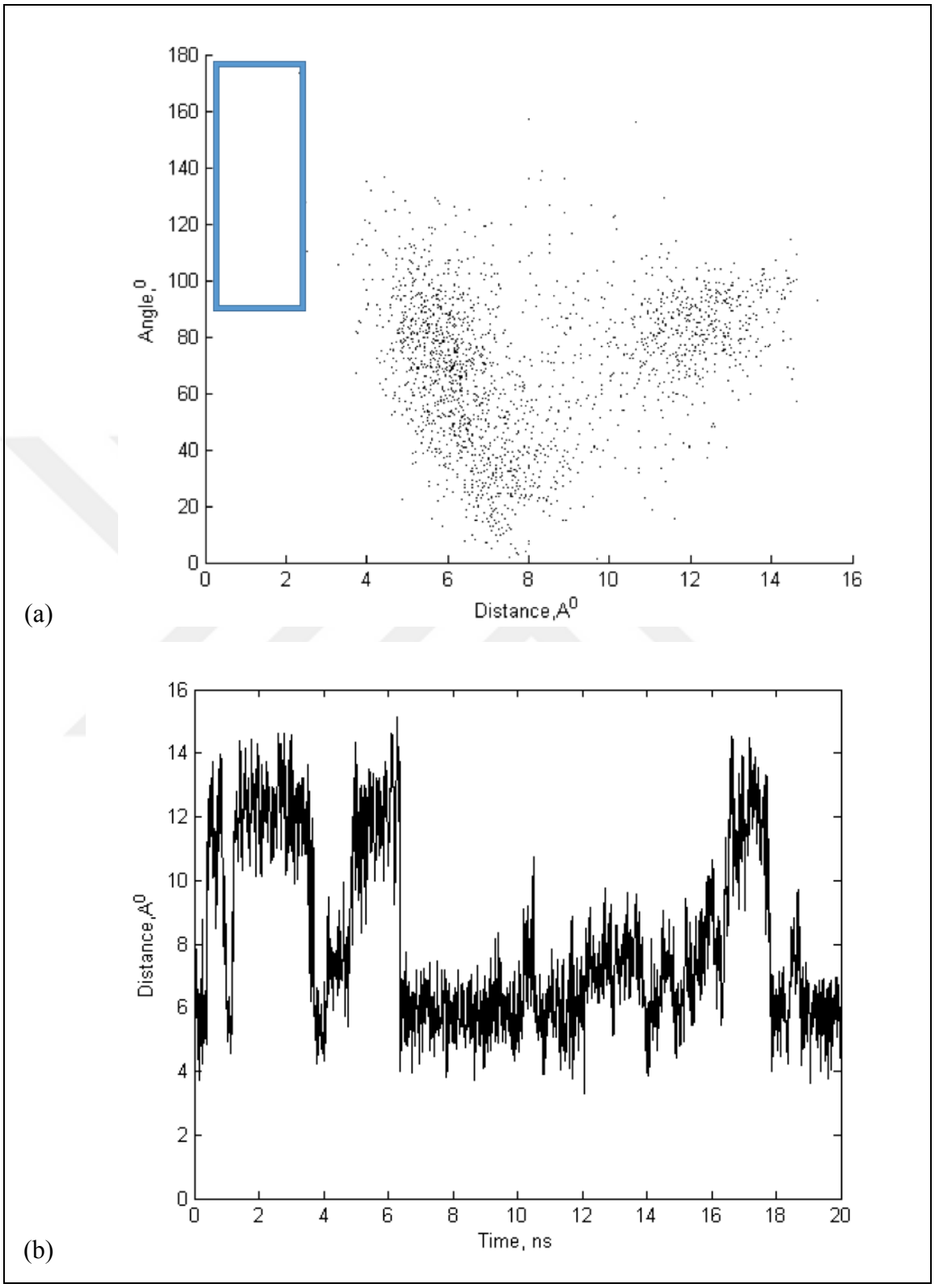

Figure 3.27. MD results of DER112 (a) Pyridine-alcohol H-bond interaction - angle vs. distance, (b) Pyridine-alcohol H-bond interaction - distance vs. time

3.9. DER135

DER135 is obtained by placing O-CH-CH_3 chain instead of O-CH_3, which is linked to one of the benzene rings in the TF3 spiroligozyme. Figure 3.28 shows the transformation used in the design of DER135. The transformed part is shown in Figure 3.29 in the blue ring.

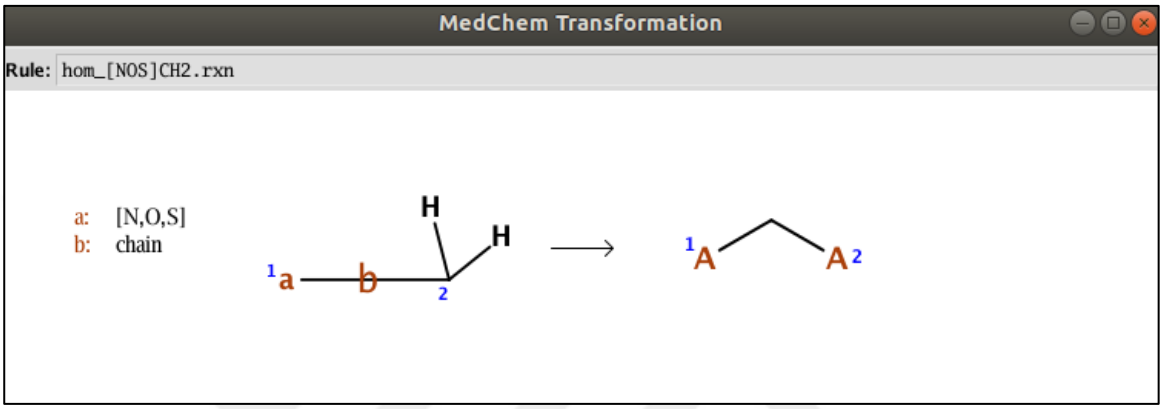

Figure 3.28. Transformation rule applied to DER135

Table 3.20. MM and QM evaluation of DER135

DER135				
Conformer Number	**Δ*E* (kcal/mol) Molecular Mechanics (MM) MMFF94x**	**MM Population (%)**	**Δ*E* (kcal/mol) Quantum Mechanics (QM) M06-2X/6-31G(d)**	**QM Population (%)**
1 ACTIVE	0.0	40	4.2	0
2 ACTIVE	0.3	26	3.7	0
3 ACTIVE	0.6	14	3.1	0
4	0.8	11	5.8	0
5 ACTIVE	1.5	3	1.3	9
6	1.7	2	3.5	0
7	1.9	2	3.8	0
8	2.1	1	8.5	0
9	2.5	1	2.4	1
10	2.9	0	1.7	5
11	3.0	0	7.1	0
26 ACTIVE	4.0	0	2.9	1
28 ACTIVE	4.2	0	6.5	0
36 ACTIVE	5.1	0	10.7	0
39 ACTIVE	5.2	0	0.0	83
43 ACTIVE	5.3	0	5.8	0
44 ACTIVE	5.5	0	11.2	0
48 ACTIVE	5.7	0	10.6	0
52 ACTIVE	5.8	0	5.3	0

The conformational search for DER135 generated 89 conformers. Table 3.20 shows the results obtained from the conformational analysis of DER135. Figure 3.29 shows conformers 1 and 39 of DER135. Conformer 1 is the lowest energy active conformer according to MM evaluation and conformer 39 is the lowest energy active conformer according to QM evaluation. However, conformer 1 is 4.2 kcal/mol higher in energy than conformer 39 according to QM calculations. Moreover, conformer 39 is 5.2 kcal/mol higher in energy than conformer 1 according to MM calculations. Although, conformer 39 has 83 percent QM population, it has 0 percent MM population.

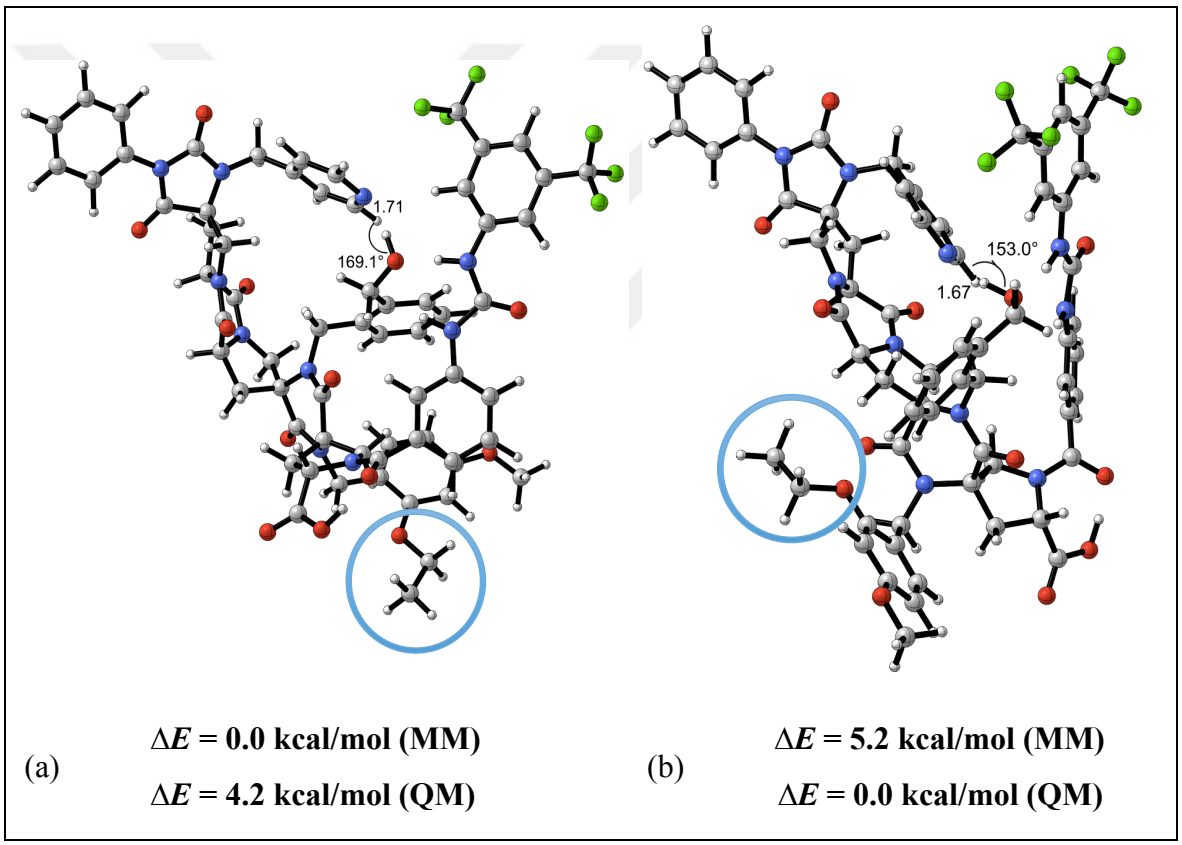

Figure 3.29. Lowest energy conformers of DER135 (a) Conformer 1, (b) Conformer 39

Table 3.21 shows the relative energy calculation of DER135. The 88 percent difference in the cumulative QM populations between active and inactive conformers indicates an energy difference of 1.6 kcal/mol between these two.

Table 3.21. Populations and relative energies of active and inactive conformer clusters of DER135

DER135	**QM Population (%)**	**Δ*E* (kcal/mol) Quantum Mechanics (QM) M062X-6-31G(d)**
Total Active Conformers	94	0.0
Total Conformers with no H-bond	6	$\Delta E = 1.6$

DER135 with a total MM population of 83 percent and QM population of 94 percent active conformer, is subjected to MD evaluation. The distance and the angle between alcohol and pyridine is cumulated in the 6Å < d < 8Å and $20^0 < \theta < 120^0$ region rather than the H-bond region indicated with the blue box (Figure 3.30(a)). Figure 3.30.(b) shows the fluctuation of distance between pyridine and alcohol. MD population of DER135 was calculated as 0 percent.

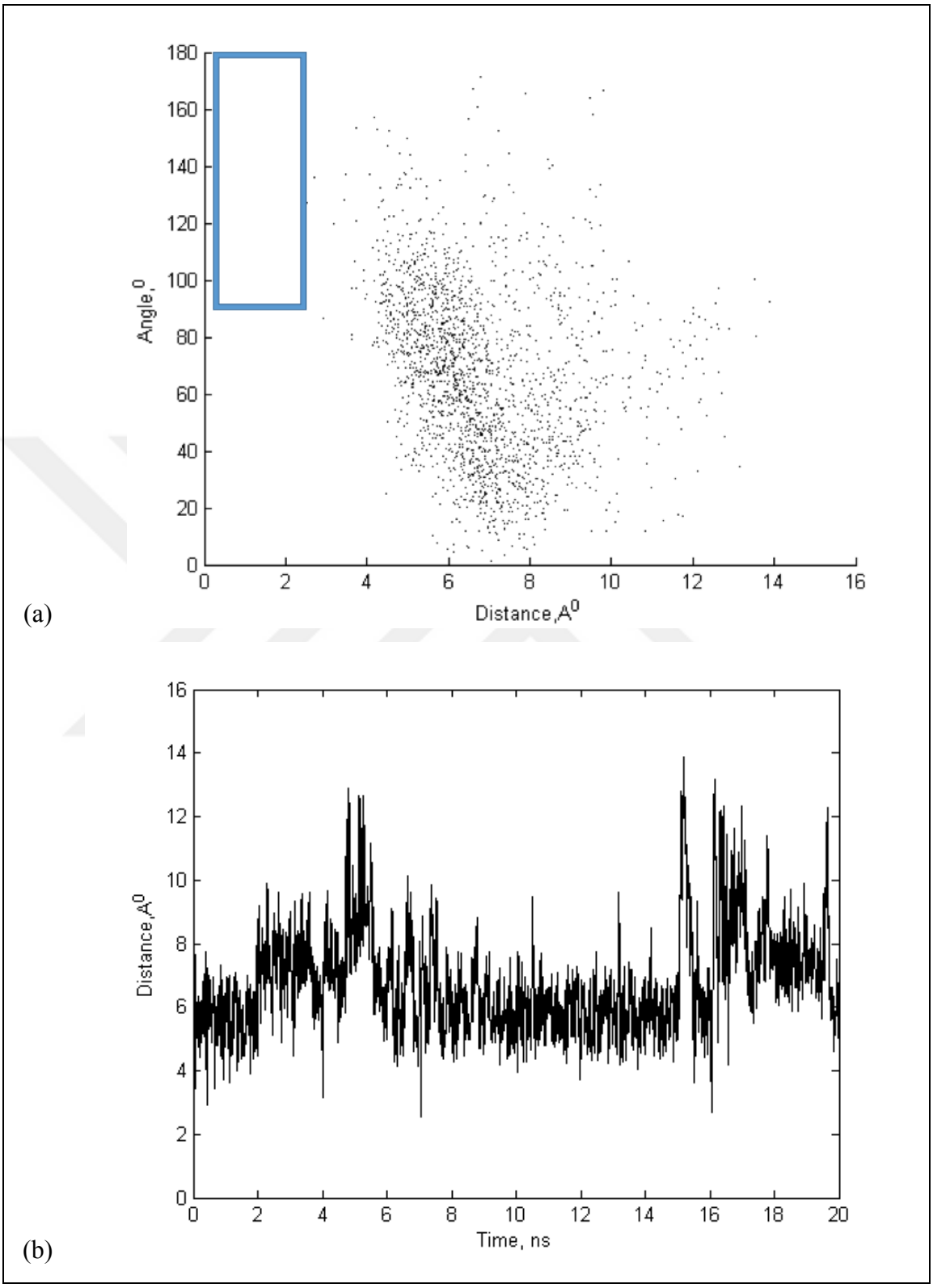

Figure 3.30. MD results of DER135 (a) Pyridine-alcohol H-bond interaction - angle vs. distance, (b) Pyridine-alcohol H-bond interaction - distance vs. time

3.10. DER146

DER146 is created by methylate inversion reaction. Figure 3.31 shows the transformation used in the design of DER146. The transformed part and the lowest energy conformers of DER146 can be seen from Figure 3.32.

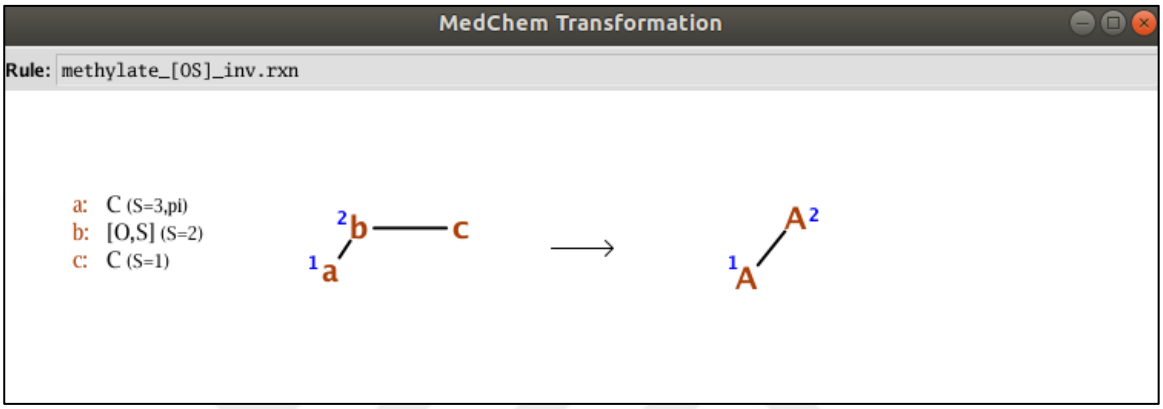

Figure 3.31. Transformation rule applied to DER146

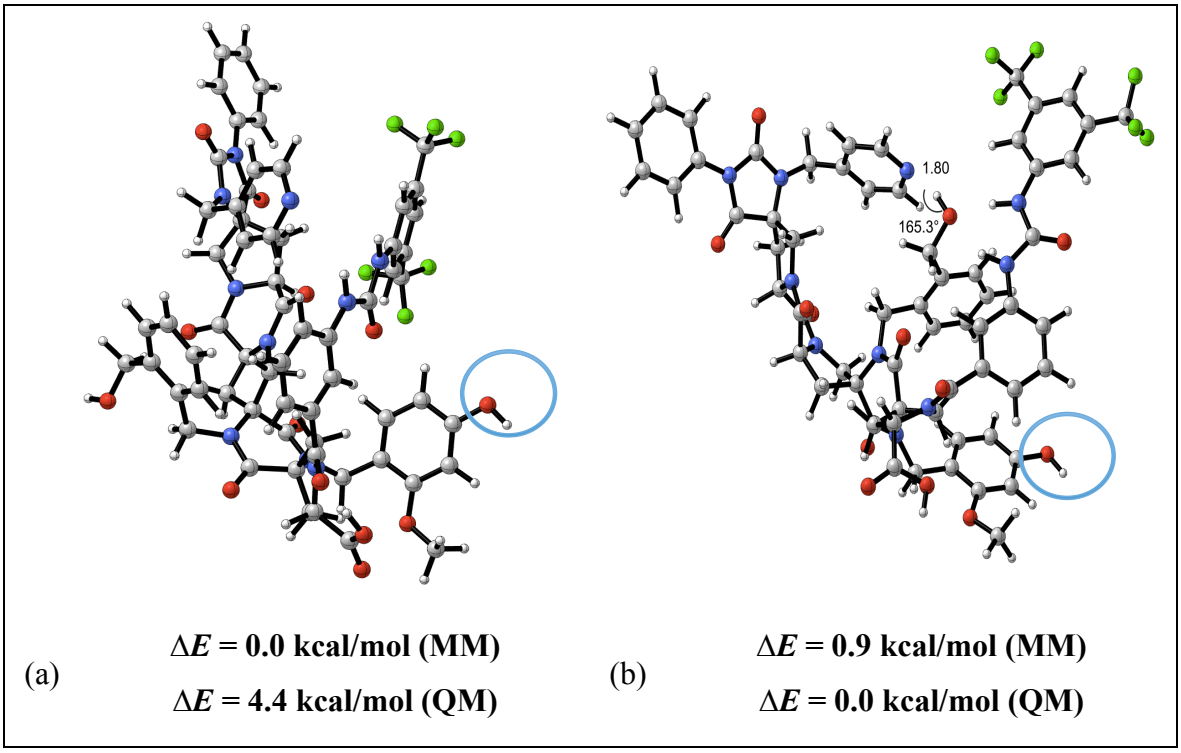

Figure 3.32. Lowest energy conformers of DER146 (a) Conformer 1, (b) Conformer 3

Table 3.22. MM and QM evaluation of DER146

DER146				
Conformer Number	**Δ*E* (kcal/mol) Molecular Mechanics (MM) MMFF94x**	**MM Population (%)**	**Δ*E* (kcal/mol) Quantum Mechanics (QM) M06-2X/6-31G(d)**	**QM Population (%)**
1	0.0	39	4.4	0
2	0.5	17	5.7	0
3 ACTIVE	0.9	9	0.0	100
4	1.0	8	9.9	0
5	1.0	8	8.6	0
6	1.1	6	11.6	0
7	1.2	5	9.3	0
8 ACTIVE	1.8	2	9.9	0
9	1.9	2	9.7	0
10 ACTIVE	1.9	1	9.3	0
11	2.0	1	13.9	0
12	2.3	1	10.7	0
13	2.7	0	5.3	0
14	2.8	0	11.6	0
15	3.3	0	4.8	0
58 ACTIVE	13.8	0	8.8	0

The conformational search for DER146 generated 65 conformers. Table 3.22 shows conformational analysis of DER146. The results showed that, active conformer 3 is the lowest energy conformer of DER146 obtained by QM calculations with 100 percent population. The lowest energy conformer based on MM evaluation (conformer 1) is 4.4 kcal/mol higher in energy than conformer 3 according to QM calculations.

Table 3.23. Populations and relative energies of active and inactive conformer clusters of DER146

DER146	**QM Population (%)**	**Δ*E* (kcal/mol) Quantum Mechanics (QM) M062X-6-31G(d)**
Total Active Conformers	100	0.0
Total Conformers with no H-bond	0	$\Delta E = 4.0$

QM population of 100 percent for active conformer corresponds to an energy difference of 4.0 kcal/mol between active and inactive conformers (Table 3.23).

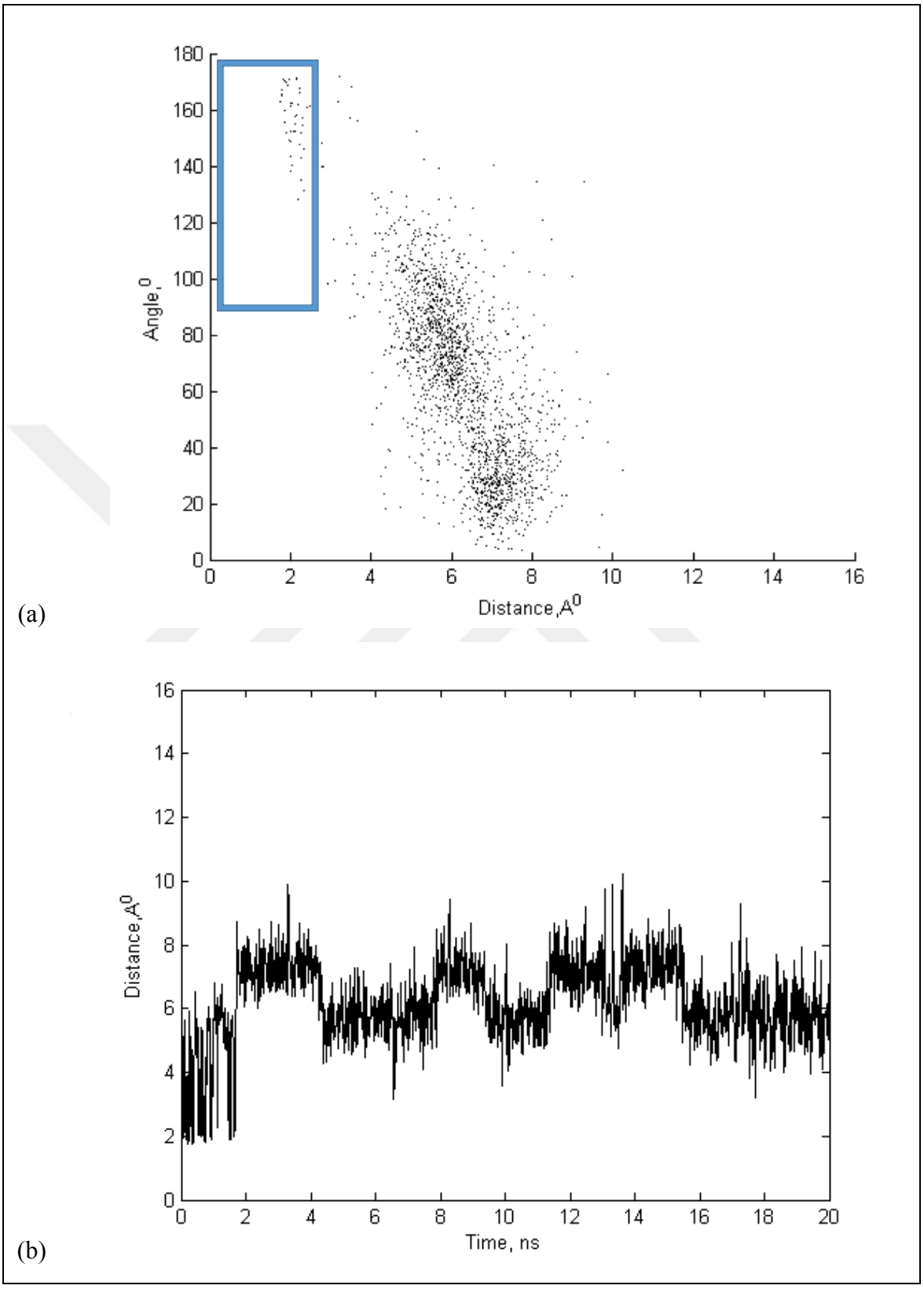

Figure 3.33. MD results of DER146 (a) Pyridine-alcohol H-bond interaction - angle vs. distance, (b) Pyridine-alcohol H-bond interaction - distance vs. time

DER146 with a total MM population of 12 percent and QM population of 100 percent active conformer, is subjected to MD evaluation. Figure 3.33 shows MD simulation results of DER146. The distance and the angle between alcohol and pyridine is cumulated in the 6Å < d < 8Å and $0^0 < \theta < 100^0$ region rather than the H-bond region indicated with the blue box. Figure 3.33.(b) shows the fluctuation of distance between pyridine and alcohol. H-bond between the catalytic dyad is disrupted after 2 ns of the simulation and is not reformed. MD population of DER146 was calculated as 2 percent.

3.11. DER162

DER162 is obtained by the transformation of phenyl to indole as shown in Figure 3.34. The transformed part and conformers of DER162 can be seen from Figure 3.35.

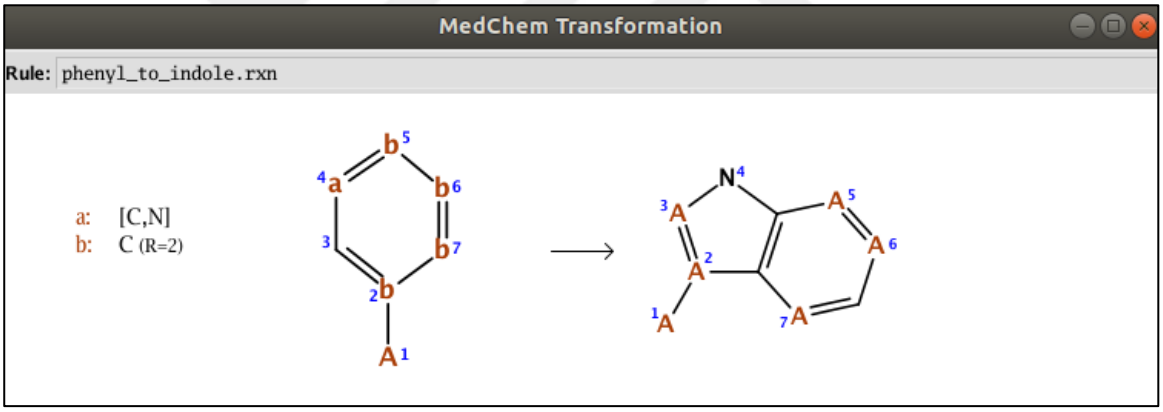

Figure 3.34. Transformation rule applied to DER162

The conformational search for DER162 generated 62 conformers. Table 3.24 shows conformational analysis of DER162. The active conformer 9 is the lowest energy active conformer of DER162 by DFT calculations with 100 percent population. The lowest energy conformer according to MM evaluation is not active (Figure 3.35).

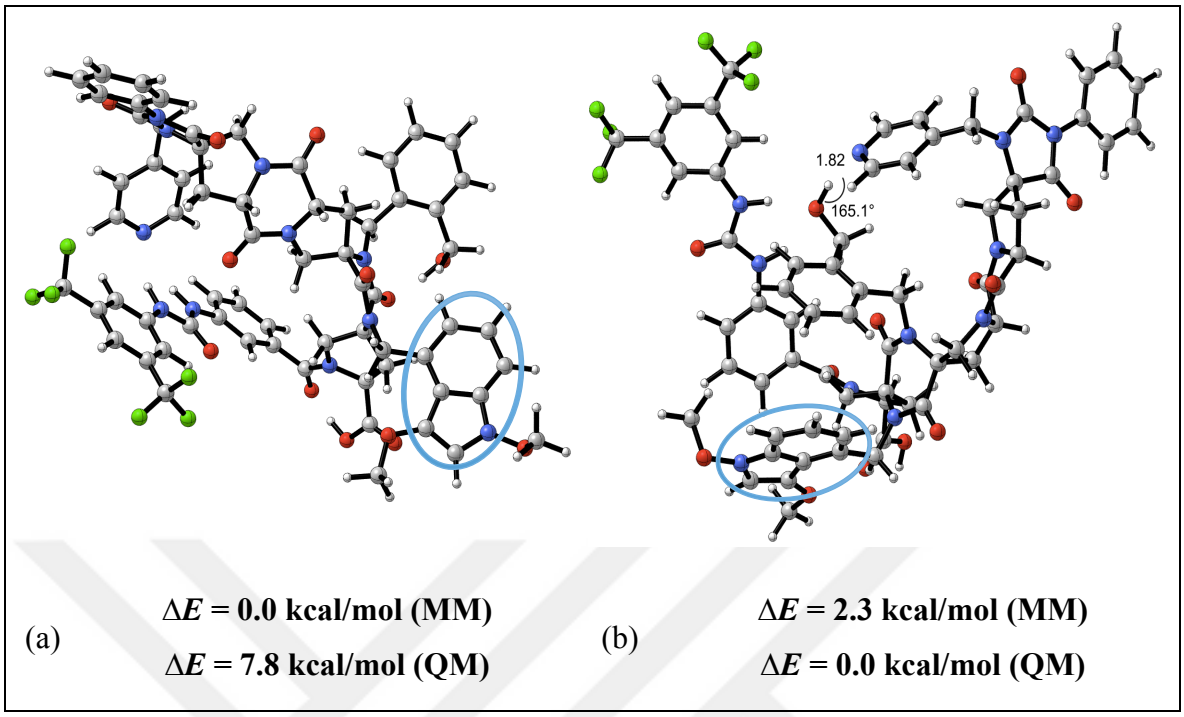

Figure 3.35. Lowest energy conformers of DER162 (a) Conformer 1, (b) Conformer 9

Table 3.24. MM and QM evaluation of DER162

DER162				
Conformer Number	**ΔE (kcal/mol) Molecular Mechanics (MM) MMFF94x**	**MM Population (%)**	**ΔE (kcal/mol) Quantum Mechanics (QM) M06-2X/6-31G(d)**	**QM Population (%)**
1	0.0	58	7.8	0
2 ACTIVE	0.6	20	4.8	0
3	1.3	7	11.2	0
4	1.6	4	9.8	0
5	1.7	3	13.7	0
6	1.8	3	8.3	0
7	1.9	2	5.2	0
8	2.0	2	6.6	0
9 ACTIVE	2.3	1	0.0	100
10	2.8	0	9.1	0
11	2.9	0	8.0	0
40 ACTIVE	5.6	0	10.4	0
42 ACTIVE	5.2	0	7.7	0

Table 3.25. Populations and relative energies of active and inactive conformer clusters of DER162

DER162	QM Population (%)	Δ*E* (kcal/mol) Quantum Mechanics (QM) M062X-6-31G(d)
Total Active Conformers	100	0.0
Total Conformers with no H-bond	0	Δ*E* = 5.0

Table 3.25 shows the relative energy calculations of DER162. Inactive conformers of DER162 are 5.0 kcal/mol higher in energy than the active conformers.

With a total MM population of 21 percent and QM population of 100 percent active conformer, DER162 is subjected to MD evaluation. MD simulations of DER162 shows that the H-bond between alcohol and pyridine could not maintained and MD population of DER162 was calculated as 0 percent.

3.12. DER5

MD results of DER1 showed that benzyl alcohol of the catalytic dyad mostly established a strong alternative H-bond with one of the backbone oxygens instead of pyridine (Figure 3.8.(c)). In order to investigate the possibility of eliminating this alternative interaction, DER5 is selected for further evaluation by MD simulations even though its QM and MM populations are below the selection criteria. DER5 is obtained by the same C=O to C=S transformation applied towards DER1, but the transformation occurred on the oxygen that alternatively interacts with the benzyl alcohol of the catalytic dyad. Figure 3.36 shows lowest energy conformers of DER5. The blue ring shows the transformed part of DER5.

DER5 was analyzed by MM and QM calculations (Table 3.26). The conformational search for DER5 generated 77 conformers. The lowest energy conformer of DER5 according to QM evaluation is the inactive conformer 5 (Figure 3.36.(b)).

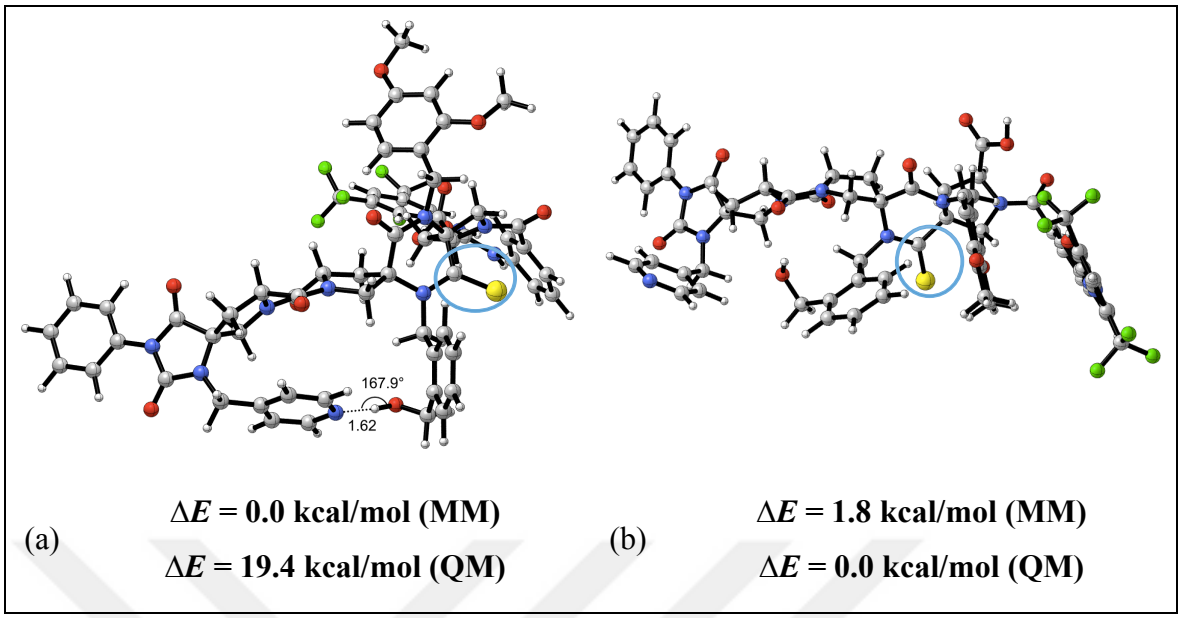

Figure 3.36. Lowest energy conformers of DER5 (a) Conformer 1, (b) Conformer 5

Table 3.26. MM and QM evaluation of DER5

DER5				
Conformer Number	**ΔE (kcal/mol) Molecular Mechanics (MM) MMFF94x**	**MM Population (%)**	**ΔE (kcal/mol) Quantum Mechanics (QM) M06-2X/6-31G(d)**	**QM Population (%)**
1 ACTIVE	0.0	72	19.4	0
2	1.1	11	6.9	0
3	1.6	5	10.1	0
4	1.6	5	8.4	0
5	1.8	3	0.0	100
6	2.4	1	6.3	0
7	2.7	1	10.7	0
8	2.8	1	9.2	0
9	2.8	1	12.1	0
10	2.9	1	8.6	0
11 ACTIVE	2.9	1	9.6	0
15 ACTIVE	3.4	0	3.8	0
20 ACTIVE	4.0	0	9.1	0
51 ACTIVE	5.7	0	11.2	0

Total of 100 percent inactive conformer population is indicative of 4.0 kcal/mol energy difference disfavoring the active conformer population (Table 3.27).

Table 3.27. Populations and relative energies of active and inactive conformer clusters of DER5

DER5	**QM Population (%)**	**Δ*E* (kcal/mol) Quantum Mechanics (QM) M062X-6-31G(d)**
Total Active Conformers	0	$\Delta E = 4.0$
Total Conformers with no H-bond	100	0.0

Figure 3.37 shows the results of MD simulations for DER5. From Figure 3.37.(a) the distance and the angle between alcohol and pyridine is cumulated in the 4Å < d < 8Å and $40^0 < \theta < 120^0$ region rather than the H-bond region indicated with the blue box. MD population of Figure 3.37.(b) shows the fluctuation of distance between pyridine and alcohol. DER5 was calculated as 1 percent lower than the MD population for DER1.

Interestingly, benzyl alcohol in DER5 mostly interacted with the backbone oxygen, which was transformed in DER1 (Figure 3.37.(c),(d), Figure 3.38 (b)). All of these results showed that, DER5 cannot be an alternative to DER1.

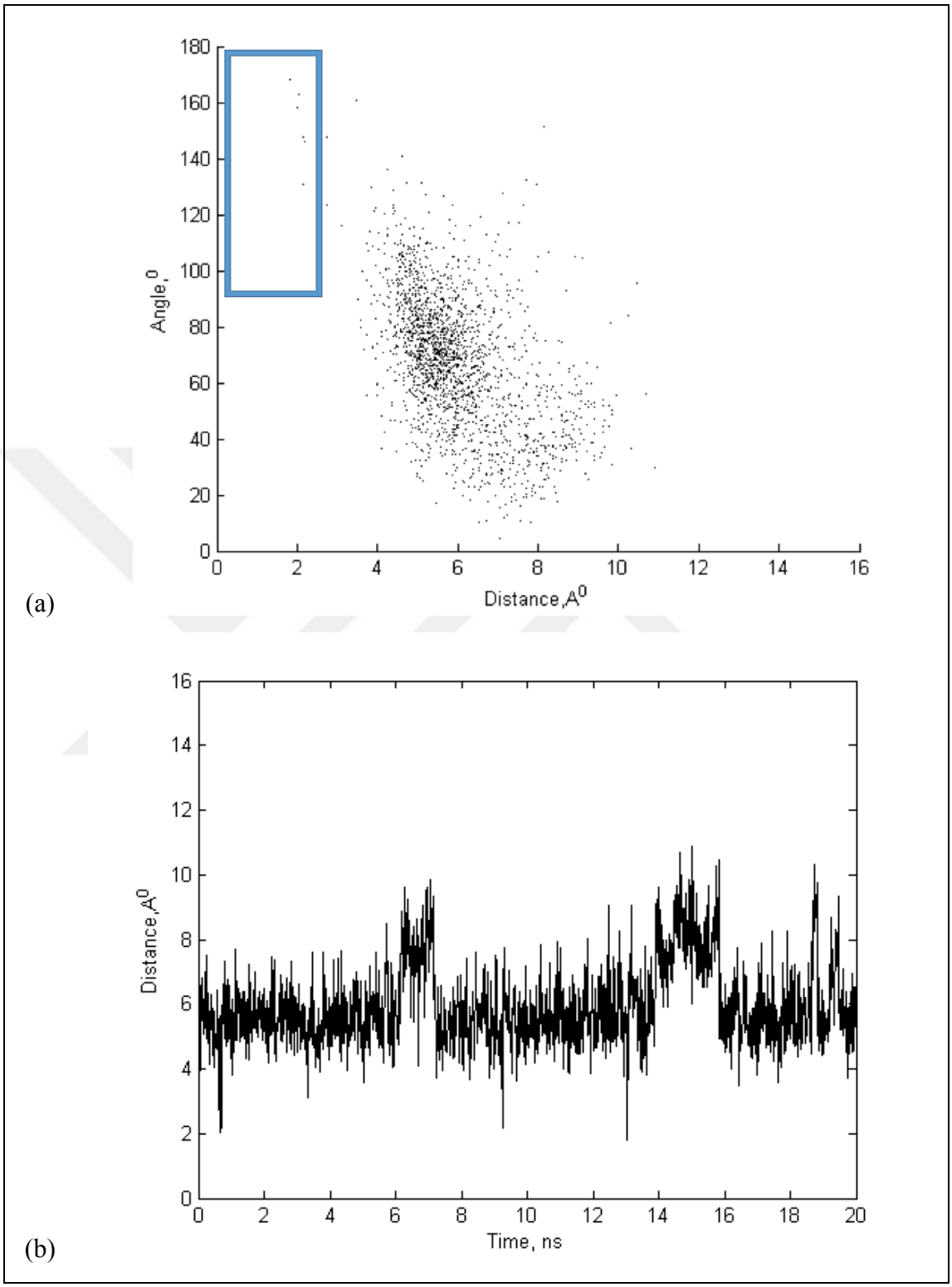

Figure 3.37. MD results of DER5 (a) Pyridine-alcohol H-bond interaction - angle vs. distance, (b) Pyridine-alcohol H-bond interaction - distance vs. time

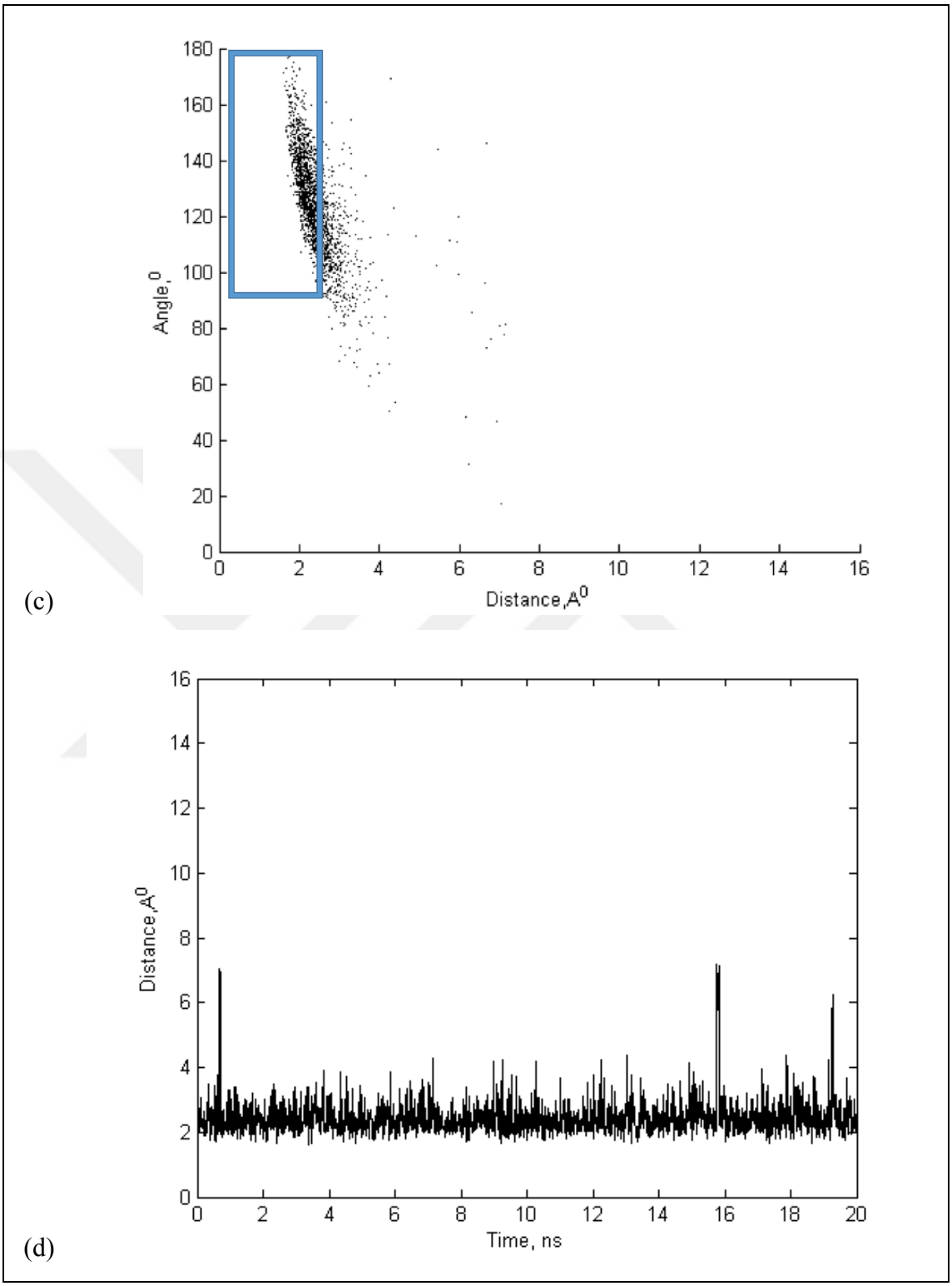

Figure 3.37. MD results of DER5 *(cont'd)* (c) Backbone oxygen-alcohol H-bond interaction - angle vs. distance, (d) Backbone oxygen-alcohol H-bond interaction - distance vs. time

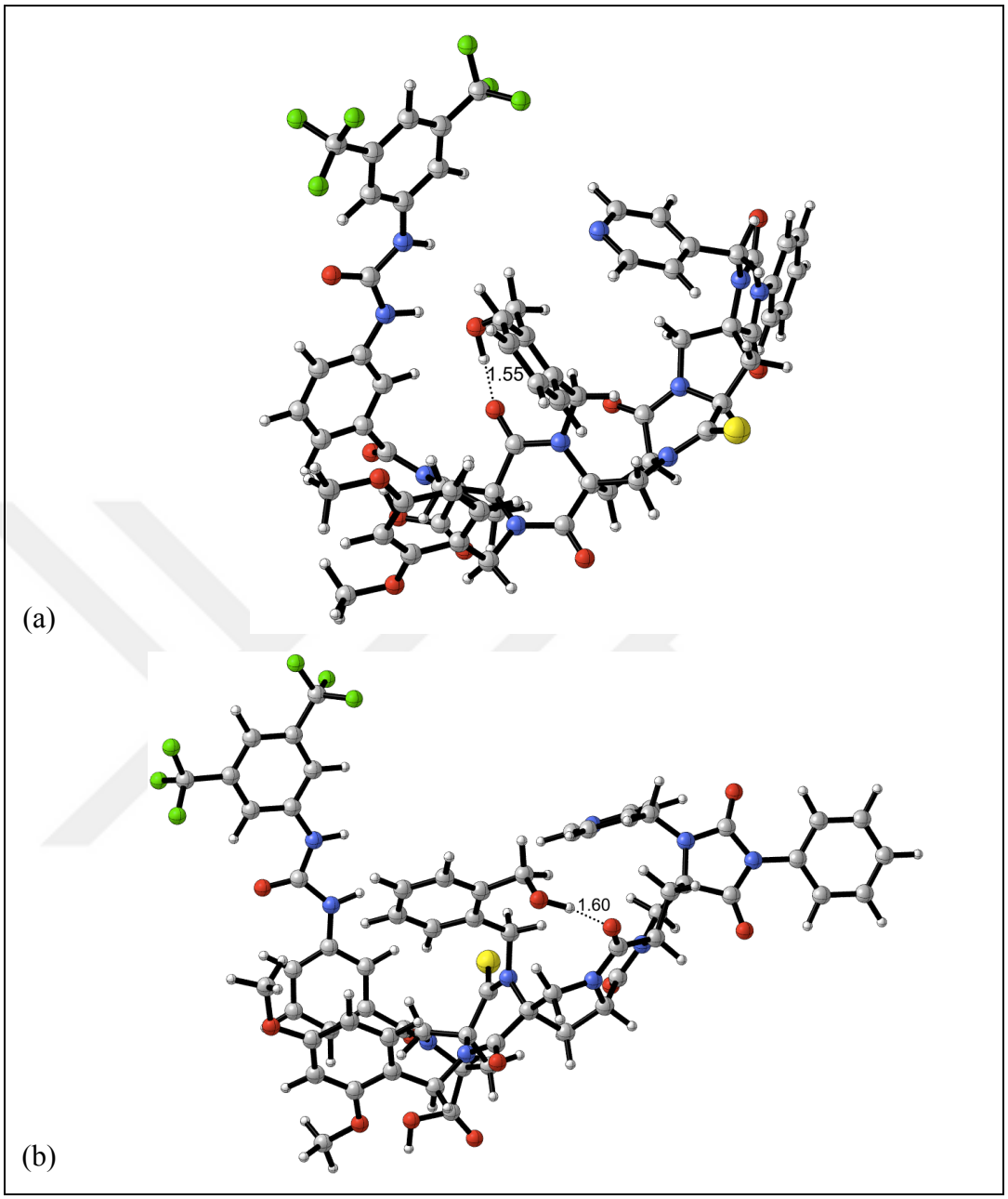

Figure 3.38. Alternative H-bond interactions in (a) DER1 (b) DER5

4. CONCLUSION

TF3 spiroligozyme was derivatized to obtain a catalyst with preorganized catalytic active site. 258 derivatives of TF3 were obtained by first iteration. 65 derivatives have transformation in their catalytic site. Conformation libraries were created for 193 derivatives of TF3.

Table 4.1. Comparison of populations

MOLECULE	MM POPULATION (10 %)	QM POPULATION (50 %)	MD POPULATION (10 %)
TF3	0 %	0 %	0 %
DER1	67 %	99 %	4 %
DER5	0 %	0 %	1 %
DER6	10 %	97 %	1 %
DER15	16 %	92 %	0 %
DER41	27 %	99 %	0 %
DER64	19 %	95 %	1 %
DER72	92 %	97 %	0 %
DER77	65 %	100 %	0 %
DER112	24 %	50 %	0 %
DER135	83 %	94 %	0 %
DER146	12 %	100 %	2 %
DER162	21 %	100 %	0 %

MM calculations were applied to derivatives, which contains active conformers in their libraries. According to MM calculations, 23 derivatives have active conformer population above 10 percent. QM calculations were applied to these 23 derivatives. 11 of these derivatives have at least 50 percent active conformer population. DER5 was also evaluated to compare with DER1. These 11 derivatives, TF3 and DER5 were evaluated with MD simulations.

Table 4.1 summarizes the populations of 11 derivatives, TF3 and DER5. According to the results shown in Table 4.1, DER72 has the highest active conformer population by MM evaluation. DER77, DER146 and DER162 have 100 percent active conformer population according to DFT calculations. It was expected to obtain a derivative has MD population above 10 percent. Although the satisfactory results of both MM and QM calculations, MD simulations showed that the evaluated derivatives cannot maintain the H-bond between pyridine and alcohol.

DER72 and DER77 are the most promising derivatives according to the both MM and QM calculations results. However, they have 0 percent MD populations. When MD populations of all these derivatives compared, DER1 has better results than the others. DER1 has 4 percent MD population. In the further work, energy profile of the derivatives is going to be evaluated. The promising derivatives will be examined experimentally. This study is going to be beneficial in the development of preorganization in the catalytic active site of organocatalysts.

REFERENCES

1. Ghaly A, Dave D, Brooks M, Budge S. Production of biodiesel by enzymatic transesterification: review. *American Journal of Biochemistry and Biotechnology*. 2010;6: 54-76.

2. Kuah E, Toh S, Yee J, Ma Q, Gao Z. Enzyme mimics: advances and applications, *Chemistry: A European Journal*. 2016;22: 8404-8430.

3. Shaikh I. Organocatalysis: key trends in green synthetic chemistry, challenges, scope towards heterogenization, and importance from research and industrial point of view. *Journal of Catalyst.* 2014;2014: 1-35.

4. Sebastian J, Muraleedharan C, Santhiagu A. A comparative study between chemical and enzymatic transesterification of high free fatty acid contained rubber seed oil for biodiesel production. *Cogent Engineering.* 2016;3: 1-12.

5. Mishra V, Goswami R. A review of production, properties and advantages of biodiesel. *Biofuels.* 2017;9: 273-289.

6. Norjannah B, Ong H, Masjuki H, Juan J, Chong W. Enzymatic transesterification for biodiesel production: a comprehensive review. *RSC Advances.* 2016;6: 60034-60055.

7. Breslow R. Biomimetic chemistry and artificial enzymes: catalysis by design. *American Chemical Society.* 1995;28: 146-153.

8. Lam M, Lee K, Mohamed A. Homogeneous, heterogeneous and enzymatic catalysis for transesterification of high free fatty acid oil (waste cooking oil) to biodiesel: A review. *Biotechnology Advances.* 2010;28: 500-518.

9. Nothling M, Xiao Z, Bhaskaran A, Blyth M, Bennett C, Coote M, Connal L. Synthetic

catalysts inspired by hydrolytic enzymes. *ACS Catalysis.* 2019;9: 168-187.

10. Kheirabadi M, Çelebi-Ölçüm N, Parker M, Zhao Q, Kiss G, Houk K, Schafmeister C. Spiroligozymes for transesterifications: design and relationship of structure to activity. *Journal of the American Chemical Society.* 2012;134: 18345-18353.

11. Carter P, Wells J. Dissecting the catalytic triad of a serine protease. *Nature.* 1998;332: 564-568.

12. Polgar L. The catalytic triad of serine peptidases. *Cellular and Molecular Life Sciences.* 2005;62: 2161-2172.

13. Fojan P. Jonson P, Petersen M, Petersen S. What distinguishes an esterase from a lipase: A novel structural approach. *Biochimie.* 2000;82: 1033−1041.

14. Shah S, Sharma S, Gupta M. Enzymatic transesterification for biodiesel production. *Indian Journal of Biochemistry & Biophysics.* 2003;40: 392-399.

15. Ishaka Z, Sairia N, Alias Y, Aroua M, Yusoffc R. A review of ionic liquids as catalysts for transesterification reactions of biodiesel and glycerol carbonate production. *Catalysis Reviews.* 2017;59: 44-93.

16. Svendsen A. Lipase protein engineering. *Biochimica et Biophysica Acta.* 2000;1543: 223-238.

17. Neitzel J. Enzyme catalysis: the serine proteases. *Nature Education.* 2010;3: 1-21.

18. Tantillo D, Chen J, Houk K. Theozymes and compuzymes: theoretical models for biological catalysis. *Current Opinion in Chemical Biology.* 1998;2: 743-750.

19. Cera E. Serine proteases. *IUBMB Life.* 2009;61: 510-515.

20. Hedstrom L. Serine protease mechanism and specifity. *Chemical Reviews.* 2002;102: 4501-4523.

21. Smith A, Müller R, Toscano M, Kast P, Hellinga H, Hilvert D, Houk K. Structural reorganization and preorganization in enzyme active sites: comparisons of experimental and theoretically ideal active site geometries in the multistep serine esterase reaction cycle. *Journal of American Chemical Society.* 2008;130: 15361-15373.

22. Yang H, Wong M. Oxyanion hole stabilization by C-H···O interaction in a transition state--a three-point interaction model for Cinchona alkaloid-catalyzed asymmetric methanolysis of meso-cyclic anhydrides. *Journal Of The American Chemical Society.* 2013;135: 5808-5818.

23. Mathew D, Thomas B, Devaky K. Design, synthesis and characterization of enzyme analogue built polymer catalysts as artificial hydrolases. *Artificial Cells, Nanomedicine and Biotechnology.* 2019;47: 1149-1172.

24. Kiser CN, Richards JH. Manipulating protein structure. *Exploring genetic algorithms.* 1997:552-553.

25. Kirby A. Enzyme mechanisms, models, and mimics. *Angewandte Chemie International.* 1996;35: 706-724.

26. Kiss G, Röthlisberger D, Baker D, Houk K. Evaluation and ranking of enzyme designs. *Protein Science.* 2010;19: 1760-1773.

27. Belding L, Taimoory S, Dudding T. Mirroring enzymes: the role of hydrogen bonding in an asymmetric organocatalyzed aza-henry reaction a dft study. *ACS Catalysis.* 2015;5: 343-349.

28. Kirby A. Enzyme mimics. *Angewandte Chemie International Edition.* 1994;33: 551-553.

29. Marchetti L, Levine M. Biomimetic catalysis. *ACS Catalysis.* 2011;1: 1090-1118.

30. Breslow R. Biomimetic chemistry: a frontier at the chemistry/biology interface. *Chemistry & Biology.* 1998;5: R27-R28.

31. Breslow R. Biomimetic chemistry: biology as an inspiration. *Journal of Biological Chemistry.* 2009;284: 1337-1342.

32. Breslow R. Biomimetic control of chemical selectivity. *Accounts of Chemical Research.* 1980;13: 170-177.

33. MacMillan D. The advent and development of organocatalysis. *Nature.* 2008;455: 304-308.

34. Miller S. In search of peptide-based catalysts for asymmetric organic synthesis. *Accounts of Chemical Research.* 2004;37: 601-610.

35. Ema T, Tanida D, Matsukawa T, Sakai T. Biomimetic trifunctional organocatalyst showing a great acceleration for the transesterification between vinyl ester and alcohol. *Chemical Communication.* 2008;8: 957-959.

36. Matsumoto M, Lee S, Waters M, Gagne M. A catalyst selection protocol that identifies biomimetic motifs from β-hairpin libraries. *Journal of American Chemical Society.* 2014;136: 15817-15820.

37. Maeda Y, Fang J, Ikezoe Y, Pike D, Nanda V, Matsui H. Molecular self-assembly strategy for generating catalytic hybrid polypeptides. *Plos One.* 2016;11: 1-10.

38. Goyal B, Patel K, Srivastava K, Durani S. *De novo* design of stereochemically-bent sixteen-residue β-hairpin as a hydrolase mimic. *RSC Advances.* 2015;5: 105400-105408.

39. Goyal B, Srivastava K, Patel K, Durani S. Modulation of β-hairpin peptide self-assembly: a twenty-residue poly-L β-hairpin modified rationally as a mixed-L,D hydrolase. *ChemistrySelect.* 2016;1: 2050-2057.

40. Hung P, Chen Y, Huang K, Yu C, Horng J. Design of polyproline-based catalysts for ester hydrolysis. *ACS Omega.* 2017;2: 5574-5581.

41. Nothling M, Ganesan A, Condic-Jurkic K, O'Mara M, Coote M, Connal L. Simple design of an enzyme-inspired supported catalyst based on a catalytic triad. *Chem.* 2017;2: 732-745.

42. Zhang C, Xue X, Luo Q, Li Y, Yang K, Zhuang X, Jiang Y, Zhang J, Liu J, Zou G, Liang X. Self-assembled peptide nanofibers designed as biological enzymes for catalyzing ester hydrolysis. *ACS Nano.* 2014;8: 11715-11723.

43. Zhang Q, He X, Han A, Tu Q, Fang G, Liu J, Wang S, Li H. Artificial hydrolase based on carbon nanotubes conjugated with peptides. *Nanoscale.* 2016;8: 16851-16856.

44. Meeuwissen J, Reek J. Supramolecular catalysis beyond enzyme mimics. *Nature.* 2010;2: 615-621.

45. Houk K, Cheong P. Computational prediction of small-molecule catalyst. *Nature.* 2008;455: 309-313.

46. Röthlisberger D, Khersonsky O, Wollacott A, Jiang L, DeChancie J, Betker J, Gallaher J, Althoff E, Zanghellini A, Dym O, Albeck S, Houk K, Tawfik D, Baker D. Kemp elimination catalysts by computational enzyme design. *Nature.* 2008;453: 190-

195.

47. Jiang L, Althoff E, Clemente F, Doyle L, Röthlisberger D, Zanghellini A, Gallaher J, Betker J, Fujie Tanaka F, Barbas C, Hilvert D, Houk K, Stoddard B, Baker D. De Novo Computational Design of Retro-Aldol Enzymes. *Science.* 2008;319: 1387-1391.

48. Siegel J, Zanghellini A, Lovick H, Kiss G, Lambert A, St.Clair J, Gallaher J, Hilvert D, Gelb M, Stoddard B, Houk K, Michael F, Baker D. Computational design of an enzyme catalyst for a stereoselective bimolecular diels-alder reaction. *Science.* 2010;329: 309-313.

49. Richter F, Blomberg R Khare S, Kiss G, Kuzin A, Smith A, Gallaher J, Pianowski Z, Helgeson R, Grjasnow A, Xiao R, Seetharaman J, Su M, Vorobiev S, Lew S, Forouhar F, Kornhaber G, Hunt J, Montelione G, Tong L, Houk K, Hilvert D, Baker D. Computational design of catalytic dyads and oxyanion holes for ester hydrolysis. *Journal of American Chemical Society.* 2012;134: 16197-16206.

50. Zhang X, DeChancie J, Gunaydin H, Chowdry A, Clemente F, Smith A, Handel T, Houk K. Quantum mechanical design of enzyme active sites. *The Journal of Organic Chemistry.* 2008;73: 889-899.

51. Liu F. The upside of downsizing: asymmetric trifunctional organocatalysts as small enzyme mimics for cooperative enhancement of both rate and enantioselectivity with regulation. *Chirality.* 2013;25: 675-683.

52. Chemical Computing Group. MedChem transformations; *MOE 2018.01,* 2019.

53. Leach A. *Molecular modelling principles and applications*, Harlow: Pearson; 2001.

54. Chemical Computing Group. Generating and analyzing conformations; *MOE2012.10*, 2012.

55. Ferguson D, Raber D. A new approach to probing conformational space with molecular mechanics: random incremental pulse search. *Journal of American Chemical Society.* 1989;111: 4371-4378.

56. Allen M, and Tildesley J. *Computer simulation of liquids.* Oxford: Oxford University Press; 1987.

57. Labute P. LowModeMD-implicit low-mode velocity filtering applied to conformational search of macrocycles and protein loops. *Journal of Chemical Information and Modeling.* 2010;50: 792-800.

58. Kolossvary I, Guida W. Low mode search. an efficient, automated computational method for conformational analysis: application to cyclic and acyclic alkanes and cyclic peptides. *Journal of American Chemical Society.* 1996;118: 5011-5019.

59. Halgren T. Merck molecular force field. I. basis, form, scope, parameterization, and performance of MMFF94. *Journal of Computational Chemistry.* 1996;17: 490-519.

60. González M. Force fields and molecular dynamics simulations. *Collection SFN.* 2011;12: 169-200.

61. Kessel A, Bental N. *Introduction to proteins, structure, function and motion.* Boca Raton: Taylor & Francis Group; 2010.

62. Lipparini F, Scalmani G, Mennucci B, Cances E, Caricato M, Frisch M. A variational formulation of the polarizable continuum model. *The Journal of Chemical Physics.* 2010;33: 1-12.

63. Zhao Y, Truhlar D. The M06 suite of density functionals for main group thermochemistry, thermochemical kinetics, noncovalent interactions, excited states, and transition elements: two new functionals and systematic testing of four M06-class

functionals and 12 other function. *Theoretical Chemistry Accounts.* 2008;120: 215-241.

64. Cossia M, Barone V. Solvent effect on vertical electronic transitions by the polarizable continuum model. *Journal Of Chemical Physics.* 2000;112: 2427-2435.

65. Cance E, Mennucci B, Tomasi J. A new integral equation formalism for the polarizable continuum model: Theoretical background and applications to isotropic and anisotropic dielectrics. *The Journal of Chemical Physics.* 1997;107: 3032-3041.

66. Tomasi J, Mennucci B, Cammi R. Quantum mechanical continuum solvation models. *Chemical Reviews.* 2005;105: 2999-3093.

67. Marenich A, Cramer C, Truhlar D. Universal solvation model based on solute electron density and on a continuum model of the solvent defined by the bulk dielectric constant and atomic surface tensions. *Journal of Physical Chemistry.* 2009;113: 6378-6396.

68. Case DA, Darden TA, Cheatham III TE, Simmerling CL, Wang J, Duke RE, Luo R, Walker RC, Zhang W, Merz KM, Roberts B, Hayik S, Roitberg A, Seabra G, Swails J, Götz AW, Kolossváry I, Wong KF, Paesani F, Vanicek J, Wolf RM, Liu J, Wu X, Brozell SR, Steinbrecher T, Gohlke H, Cai, Q, Ye X, Wang J, Hsieh M-J, Cui G, Roe DR, Mathews DH, Seetin MG, Salomon-Ferrer R, Sagui C, Babin V, Luchko T, Gusarov S, Kovalenko A, Kollman PA. *AMBER 12 reference manual*, University of California, San Francisco, 2012.

69. Wang J, Wolf R, Caldwell J, Kollman P, Case D. Development and testing of a general amber force field. *Journal of Computational Chemistry.* 2004;25: 1157-1174.

70. Singh U, Kollman P. An approach to computing electrostatic charges for molecules. *Journal of Computational Chemistry.* 1984;5: 129-145.

71. Besle B, Merz K, Kollman P. Atomic charges derived from semiempirical methods.

Journal of Computational Chemistry. 1990;11: 431-439.

72. Cieplak P, Caldwell J, Kollman P. Molecular mechanical models for organic and biological systems going beyond the atom centered two body additive approximation: aqueous solution free energies of methanol and n-methyl acetamide, nucleic acid base, and amide hydrogen bonding and chloroform. *Journal of Computational Chemistry.* 2001;22: 1048-1057.

APPENDIX A: DATABASE OF TF3 SPIROLIGOZYME

Table A.1. Transformation database of 258 derivatives of TF3 spiroligozyme by iteration (pages 89-140)

Number of Derivative	Transformation Reaction	Modification	MM population of active conformers	QM population of active conformers	MD population of active conformers	Number of Conformers
1	C=O to C=S	**Backbone** change of C to S at 4.ring of BB	67 %	99 %	4 %	53
2	C=O to C=S	**Backbone** change of C to S at 4.ring of BB	60 %	1 %	-	26
3	C=O to C=S	**Backbone** **Near Active Site (pyridine)** change of C to S at 6.ring of BB	2 %	16 %	0 %	73

4	C=O to C=S	**Backbone** **Near Active Site (pyridine)** change of C to S at 6.ring of BB	1 %	94 %	4 %	82
5	C=O to C=S	**Backbone** **Near Active Site (alcohol)** change of C to S at 2.ring of BB	0 %	0 %	1 %	77
6	C=O to C=S	**Backbone** **Near Active Site (alcohol)** change of C to S at 2.ring of BB	10 %	97 %	1 %	106
7	C=O to C=S	**Remote** change of C to S near 1.ring of BB	There is no active conformer	There is no active conformer	There is no active conformer	171
8	C=O to C=S	**UREA CHANGED**	**UREA CHANGED**	**UREA CHANGED**	**UREA CHANGED**	**UREA CHANGED**

9	C=O to C=S	**Remote** change of C to S near 1.ring of BB	0 %	0 %	-	80
10	C=O to SO2	**Backbone** change of C to S at 4.ring of BB	45 %	0 %	-	71
11	C=O to SO2	**Backbone** change of C to S at 4.ring of BB	0 %	0 %	-	64
12	C=O to SO2	**Backbone** **Near Active Site (pyridine)** change of CO to SO_2 at 6.ring of BB	0 %	93 %	0 %	105
13	C=O to SO2	**Backbone** **Near Active Site (pyridine)** change of CO to SO_2 at 6.ring of BB	There is no active conformer	There is no active conformer	There is no active conformer	172

14	C=O to SO2	**Backbone** **Near Active Site (alcohol)** change of CO to SO_2 at 2.ring of BB	There is no active conformer	There is no active conformer	There is no active conformer	174
15	C=O to SO2	**Backbone** **Near Active Site (alcohol)** change of CO to SO_2 at 2.ring of BB	16 %	92 %	0 %	91
16	C=O to SO2	**Remote** change of CO to SO_2 near 1.ring of BB	There is no active conformer	There is no active conformer	There is no active conformer	162
17	C=O to SO2	**UREA CHANGED**	**UREA CHANGED**	**UREA CHANGED**	**UREA CHANGED**	**UREA CHANGED**
18	C=O to SO_2	**Remote** change of CO to SO_2 near 1.ring of BB	6 %	0 %	-	68

19	CF_3 TO CARBOXYLATE	**Near Active Site** change of CF_3 to carboxylate	There is no active conformer	There is no active conformer	There is no active conformer	115
20	CF_3 TO CHLORINE	**Near Active Site** change of CF_3 to chlorine	There is no active conformer	There is no active conformer	There is no active conformer	153
21	CF_3 TO CYANO	**Near Active Site** change of CF_3 to cyano	0 %	-	-	41
22	CF_3 TO METHOXY	**Near Active Site** change of CF_3 to $O(CH_3)$	There is no active conformer	There is no active conformer	There is no active conformer	190
23	CF_3 TO METHOXY	**Near Active Site** change of CF_3 to $NH(CH_3)$	0 %	0 %	-	28

24	CF_3 TO METHOXY	**Near Active Site** change of CF_3 to $S(CH_3)$	0 %	1 %	-	178
25	C[NOSFClBr] to C(OMe)	**Near Active Site** change of F to $O(CH_3)$	0 %	-	-	27
26	C[NOSFClBr] to C(OMe)	**Near Active Site** change of F to $NH(CH_3)$	8 %	-	-	47
27	C[NOSFClBr] to C(OMe)	**Near Active Site** change of F to $S(CH_3)$	There is no active conformer	There is no active conformer	There is no active conformer	152
28	C[NOSFClBr] to C(OMe)	**Remote** change of OH to OCH_3 near 1.ring of BB	2%	-	-	27

29	C[NOSFClBr] to C(OMe)	**Remote** change of OH to $NH(CH_3)$ near 1.ring of BB	There is no active conformer	There is no active conformer	There is no active conformer	180
30	C[NOSFClBr] to C(OMe)	**Remote** change of OH to $S(CH_3)$ near 1.ring of BB	10 %	0 %	-	115
31	C[NOSFClBr] to C(OMe)	**ALCOHOL CHANGED**	**ALCOHOL CHANGED**	**ALCOHOL CHANGED**	**ALCOHOL CHANGED**	**ALCOHOL CHANGED**
32	C[NOSFClBr] to C(OMe)	**ALCOHOL CHANGED**	**ALCOHOL CHANGED**	**ALCOHOL CHANGED**	**ALCOHOL CHANGED**	**ALCOHOL CHANGED**
33	C[NOSFClBr] to C(OMe)	**ALCOHOL CHANGED**	**ALCOHOL CHANGED**	**ALCOHOL CHANGED**	**ALCOHOL CHANGED**	**ALCOHOL CHANGED**

34	C[CNSFClBrI] to C(O).rxn	**Near Active Site** change of F to OH	There is no active conformer	There is no active conformer	There is no active conformer	205
35	C[COSFClBRI] to C(N).rxn	**Near Active Site** change of F to NH_2	28 %	0 %	-	172
36	C[COSFClBRI] to C(N).rxn	**Remote** change of OH to NH_2 near 1.ring of BB	There is no active conformer	There is no active conformer	There is no active conformer	187
37	C[COSFClBRI] to C(N).rxn	**ALCOHOL CHANGED**	**ALCOHOL CHANGED**	**ALCOHOL CHANGED**	**ALCOHOL CHANGED**	**ALCOHOL CHANGED**
38	C[NOSFClBRI] to C(C).rxn	**Near Active Site** change of F to CH_3	There is no active conformer	There is no active conformer	There is no active conformer	174

39	C[NOSFClBRI] to C(C).rxn	**Remote** change of OH to CH_3 near 1.ring of BB	There is no active conformer	There is no active conformer	There is no active conformer	201
40	C[NOSFClBRI] to C(C).rxn	**ALCOHOL CHANGED**	**ALCOHOL CHANGED**	**ALCOHOL CHANGED**	**ALCOHOL CHANGED**	**ALCOHOL CHANGED**
41	C[NOSFClBRI] to C(cyano).rxn	**Near Active Site** change of F to cyano	27 %	99 %	0 %	88
42	C[NOSFClBRI] to C(cyano).rxn	**Remote** change of OH to Cyano near 1.ring of BB	There is no active conformer	There is no active conformer	There is no active conformer	195
43	C[NOSFClBRI] to C(cyano).rxn	**ALCOHOL CHANGED**	**ALCOHOL CHANGED**	**ALCOHOL CHANGED**	**ALCOHOL CHANGED**	**ALCOHOL CHANGED**

44	C[NOS]C to C(C=O)C.rxn	**UREA CHANGED**	**UREA CHANGED**	**UREA CHANGED**	**UREA CHANGED**	**UREA CHANGED**
45	C[NOS]C to C(C=O)C.rxn	**UREA CHANGED**	**UREA CHANGED**	**UREA CHANGED**	**UREA CHANGED**	**UREA CHANGED**
46	C[NOS]C to C(C=O)C.rxn	**Remote** near 2.ring of BB	0 %	97%	0 %	24
47	C[NOS]C to C(C=O)C.rxn	**Remote** near 2.ring of BB	There is no active conformer	There is no active conformer	There is no active conformer	162
48	C[NOS]C to C(S=O)C.rxn	**UREA CHANGED**	**UREA CHANGED**	**UREA CHANGED**	**UREA CHANGED**	**UREA CHANGED**

49	C[NOS]C to C(S=O)C.rxn	**UREA CHANGED**	**UREA CHANGED**	**UREA CHANGED**	**UREA CHANGED**	**UREA CHANGED**
50	C[NOS]C to C(S=O)C.rxn	**Remote** change of OCH_3 to $SO(CH_3)$ near 2.ring of BB	42 %	6 %	-	252
51	C[NOS]C to C(S=O)C.rxn	**Remote** change of OCH_3 to $SO(CH_3)$ near 2.ring of BB	0 %	30 %	-	271
52	C[NOS]C to C(SO2)C.rxn	**UREA CHANGED**	**UREA CHANGED**	**UREA CHANGED**	**UREA CHANGED**	**UREA CHANGED**
53	C[NOS]C to C(SO2)C.rxn	**UREA CHANGED**	**UREA CHANGED**	**UREA CHANGED**	**UREA CHANGED**	**UREA CHANGED**

54	C[NOS]C to C(SO2)C.rxn	**Remote** change of OCH_3 to $SO_2(CH_3)$ near 2.ring of BB	There is no active conformer	There is no active conformer	There is no active conformer	162
55	C[NOS]C to C(SO2)C.rxn	**Remote** change of OCH_3 to $SO_2(CH_3)$ near 2.ring of BB	There is no active conformer	There is no active conformer	There is no active conformer	57
56	C[NO]C to CSC.rxn	**UREA CHANGED**	**UREA CHANGED**	**UREA CHANGED**	**UREA CHANGED**	**UREA CHANGED**
57	C[NO]C to CSC.rxn	**UREA CHANGED**	**UREA CHANGED**	**UREA CHANGED**	**UREA CHANGED**	**UREA CHANGED**
58	C[NO]C to CSC.rxn	**UREA CHANGED**	**UREA CHANGED**	**UREA CHANGED**	**UREA CHANGED**	**UREA CHANGED**

59	C[NO]C to CSC.rxn	**UREA CHANGED**	**UREA CHANGED**	**UREA CHANGED**	**UREA CHANGED**	**UREA CHANGED**
60	C[NO]C to CSC.rxn	**Remote** change of OCH_3 to SCH_3 near 2.ring of BB	0 %	-	-	31
61	C[NO]C to CSC.rxn	**Remote** change of OCH_3 to $NHCH_3$ near 2.ring of BB	0 %	1 %	-	110
62	C[NO]C to CSC.rxn	**Remote** change of OCH_3 to SCH_3 near 2.ring of BB	0 %	-	-	31
63	C[NO]C to CSC.rxn	**Remote** change of OCH_3 to $NHCH_3$ near 2.ring of BB	There is no active conformer	There is no active conformer	There is no active conformer	148

64	Cyclo56.rxn	**Backbone** change of 5.ring of BB	19 %	95 %	1 %	94
65	Cyclo56.rxn	**Backbone** change of 3.ring of BB	There is no active conformer	There is no active conformer	There is no active conformer	22
66	Cyclo56.rxn	**Backbone** change of 5.ring of BB	There is no active conformer	There is no active conformer	There is no active conformer	137
67	Cyclo56.rxn	**Backbone** **Near Active Site (pyridine)** change of 6.ring of BB	There is no active conformer	There is no active conformer	There is no active conformer	154
68	Cyclo56.rxn	**Backbone** change of 3.ring of BB	There is no active conformer	There is no active conformer	There is no active conformer	48

69	Cyclo56.rxn	**Backbone** change of 1.ring of BB	There is no active conformer	There is no active conformer	There is no active conformer	67
70	Cyclo56.rxn	**Backbone** change of 1.ring of BB	0 %	100 %	0%	73
71	N14Substraction.rxn	**Backbone** **Near Active Site (alcohol)** 2.ring of BB	0 %	-	-	144
72	N14Substraction.rxn	**Backbone** **Near Active Site (alcohol)** 2.ring of BB	92%	97%	0 %	83
73	ace [NOS].rxn	**Remote** change of OH to $O(COCH_3)$ near 1.ring of BB	0 %	-	-	50

74	ace [NOS].rxn	**ALCOHOL CHANGED**	**ALCOHOL CHANGED**	**ALCOHOL CHANGED**	**ALCOHOL CHANGED**	**ALCOHOL CHANGED**
75	amide to amine.rxn	**Backbone** change of CO to CH_2 at 4. ring of BB	2 %	0 %	-	118
76	amide to amine.rxn	**Backbone** change of CO to CH_2 at 5. ring of BB	3 %	0 %	-	22
77	amide to amine.rxn	**Backbone** **Near Active Site (pyridine)** change of CO to CH_2 at 6.ring of BB	65 %	100 %	0 %	97
78	amide to amine.rxn	**Backbone** **Near Active Site (alcohol)** change of CO to CH_2 at 2.ring of BB	There is no active conformer	There is no active conformer	There is no active conformer	161

79	amide to amine.rxn	**Backbone** **Near Active Site (alcohol)** change of CO to CH_2 at 2.ring of BB	1 %	0 %	-	43
80	amide to amine.rxn	**Remote** O attached near 1.ring of BB	There is no active conformer	There is no active conformer	There is no active conformer	78
81	amide to amine.rxn	**Remote** change of CO to CH_2 near 1.ring of BB	There is no active conformer	There is no active conformer	There is no active conformer	157
82	amide to hydroxyethyl.rxn	**Backbone** change of N to C at 3. ring of BB	There is no active conformer	There is no active conformer	There is no active conformer	337
83	amide to hydroxyethyl.rxn	**Backbone** change of N to C at 5. ring of BB	There is no active conformer	There is no active conformer	There is no active conformer	246

84	amide to hydroxyethyl.rxn	**Backbone** **Near Active Site (pyridine)** change of N to C at 6.ring of BB	There is no active conformer	There is no active conformer	There is no active conformer	343
85	amide to hydroxyethyl.rxn	**Backbone** **Near Active Site (alcohol)** change of N to C at 2.ring of BB	0 %	0 %	0%	163
86	amide to hydroxyethyl.rxn	**Backbone** **Near Active Site (alcohol)** change of N to C at 2.ring of BB	There is no active conformer	There is no active conformer	There is no active conformer	342
87	amide to hydroxyethyl.rxn	**Backbone** change of N to C at 1. ring of BB	There is no active conformer	There is no active conformer	There is no active conformer	368
88	amide to ketone .rxn	**Backbone** change of N to C at 3. ring of BB	There is no active conformer	There is no active conformer	There is no active conformer	228

89	amide to ketone .rxn	**Backbone** change of N to C at 5. ring of BB	There is no active conformer	There is no active conformer	There is no active conformer	191
90	amide to ketone .rxn	**Backbone** **Near Active Site (pyridine)** change of N to C at 6.ring of BB	There is no active conformer	There is no active conformer	There is no active conformer	104
91	amide to ketone .rxn	**Backbone** **Near Active Site (pyridine)** change of N to C at 6.ring of BB	There is no active conformer	There is no active conformer	There is no active conformer	256
92	amide to ketone .rxn	**Backbone** change of N to C at 1. ring of BB	There is no active conformer	There is no active conformer	There is no active conformer	268
93	amide to ketone .rxn	**UREA CHANGED**	**UREA CHANGED**	**UREA CHANGED**	**UREA CHANGED**	**UREA CHANGED**

94	amide to ketone .rxn	**UREA CHANGED**	**UREA CHANGED**	**UREA CHANGED**	**UREA CHANGED**	**UREA CHANGED**
95	amine to amide.rxn	**Backbone** Oxygen attached to 3.ring of BB	There is no active conformer	There is no active conformer	There is no active conformer	157
96	amine to amide.rxn	**Backbone** oxygen attached to 5.ring of BB	There is no active conformer	There is no active conformer	There is no active conformer	193
97	amine to amide.rxn	**Near Active Site** oxygen attached between pyridine and 6.ring of BB	There is no active conformer	There is no active conformer	There is no active conformer	168
98	amine to amide.rxn	**Near Active Site** oxygen attached between alcohol and 2.ring of BB	There is no active conformer	There is no active conformer	There is no active conformer	177

99	amine to amide.rxn	**Remote** oxygen attached near 2.ring of BB	0 %	-	-	89
100	amine to amide.rxn	**Backbone** Oxygen attached to 1.ring of BB	5 %	90 %	0%	71
101	amine to amide.rxn	**ALCOHOL CHANGED**	**ALCOHOL CHANGED**	**ALCOHOL CHANGED**	**ALCOHOL CHANGED**	**ALCOHOL CHANGED**
102	aro6 N 12 switch.rxn	**PYRIDINE CHANGED**	**PYRIDINE CHANGED**	**PYRIDINE CHANGED**	**PYRIDINE CHANGED**	**PYRIDINE CHANGED**
103	aro6 N 13 switch.rxn	**PYRIDINE CHANGED**	**PYRIDINE CHANGED**	**PYRIDINE CHANGED**	**PYRIDINE CHANGED**	**PYRIDINE CHANGED**

104	benzene to pyridine.rxn	**Remote** change of the benzene near 6. ring of BB	100 %	11 %	-	40
105	benzene to pyridine.rxn	**Remote** change of the benzene near 6. ring of BB	There is no active conformer	There is no active conformer	There is no active conformer	94
106	benzene to pyridine.rxn	**Remote** change of the benzene near 6. ring of BB	0 %	2 %	0%	141
107	benzene to pyridine.rxn	**Near Active Site** Change of benzene near urea	0 %	-	-	106
108	benzene to pyridine.rxn	**Near Active Site** Change of benzene near urea	5 %	-	-	162

109	benzene to pyridine.rxn	**Near Active Site** Change of benzene near urea	73 %	0 %	0%	139
110	benzene to pyridine.rxn	**Near Active Site** Change of benzene near urea	3 %	0 %	-	250
111	benzene to pyridine.rxn	**Near Active Site** Change of the ring near urea	There is no active conformer	There is no active conformer	There is no active conformer	54
112	benzene to pyridine.rxn	**Near Active Site** Change of the ring near urea	24 %	50 %	0 %	114
113	benzene to pyridine.rxn	**Remote** change of the ring near 2. Ring of BB	There is no active conformer	There is no active conformer	There is no active conformer	184

114	benzene to pyridine.rxn	**Remote** change of the ring near 2. Ring of BB	0 %	-	-	26
115	benzene to pyridine.rxn	**Remote** change of the ring near 2. Ring of BB	100 %	39 %	0 %	97
116	benzene to pyridine.rxn	**ALCOHOL CHANGED**	**ALCOHOL CHANGED**	**ALCOHOL CHANGED**	**ALCOHOL CHANGED**	**ALCOHOL CHANGED**
117	benzene to pyridine.rxn	**ALCOHOL CHANGED**	**ALCOHOL CHANGED**	**ALCOHOL CHANGED**	**ALCOHOL CHANGED**	**ALCOHOL CHANGED**
118	benzene to pyridine.rxn	**ALCOHOL CHANGED**	**ALCOHOL CHANGED**	**ALCOHOL CHANGED**	**ALCOHOL CHANGED**	**ALCOHOL CHANGED**

119	benzene to pyridine.rxn	**ALCOHOL CHANGED**	**ALCOHOL CHANGED**	**ALCOHOL CHANGED**	**ALCOHOL CHANGED**	**ALCOHOL CHANGED**
120	carbonyl to cyclooxime.rxn	**Remote** ring attached to ring 1 of BB	4 %	-	-	47
121	carbonyl to cyclooxime.rxn	**Remote** ring attached to 1. ring of BB	3 %	10 %	0%	155
122	carbonyl to cyclooxime.rxn	**Remote** ring with S attached to 1. ring of BB	There is no active conformer	There is no active conformer	There is no active conformer	97
123	carbonyl to isooxazole3.rxn	**Remote** ring with O attached to 1. ring of BB	There is no active conformer	There is no active conformer	There is no active conformer	131

124	carbonyl to isooxazole3.rxn	**Remote** ring with O attached to 1. ring of BB	There is no active conformer	There is no active conformer	There is no active conformer	102
125	carboxylate to CF3.rxn	**Remote** CO(OH) changed to CF_3 near 1. ring of BB	There is no active conformer	There is no active conformer	There is no active conformer	193
126	carboxylate to acylsulfonamide. rxn	**Remote** CO(OH) changed to acylsufonamide near 1. ring of BB	1 %	-	-	165
127	carboxylate to sulfonamide.rxn	**Remote** change of CO(OH) near ring 1 of BB	1 %	0 %	0%	149
128	carboxylate to tetrazole.rxn	**Remote** ring attached to ring 1 of BB	There is no active conformer	There is no active conformer	There is no active conformer	168

129	ester to oxadiazole.rxn	**Backbone** ring attached to ring 1 of BB	There is no active conformer	There is no active conformer	There is no active conformer	171
130	ester to oxazole. rxn	**Backbone** ring attached to ring 1 of BB	There is no active conformer	There is no active conformer	There is no active conformer	180
131	hom [NOS]CH2.rxn	**Backbone** **Near Active Site (pyridine)** CH_2 attached between pyridine and 6. ring of BB	There is no active conformer	There is no active conformer	There is no active conformer	159
132	hom [NOS]CH2.rxn	**Backbone** **Near Active Site (alcohol)** CH_2 attached between alcohol and 2. ring of BB	There is no active conformer	There is no active conformer	There is no active conformer	171
133	hom [NOS]CH2.rxn	**Remote** CH_2 attached 2. ring of BB	0 %	49 %	0%	62

134	hom [NOS]CH2.rxn	**Remote** CH_2 attached to the ring near 2.ring of BB	0 %	100 %	-	60
135	hom [NOS]CH2.rxn	**Remote** CH_2 attached to the ring near 2.ring of BB	83 %	94 %	0 %	89
136	hom [NOS]CH2.rxn	**ALCOHOL CHANGED**	**ALCOHOL CHANGED**	**ALCOHOL CHANGED**	**ALCOHOL CHANGED**	**ALCOHOL CHANGED**
137	hydroxy to chlorine.rxn	**Remote** change of C(OH) to CCl near ring 1 of BB	There is no active conformer	There is no active conformer	There is no active conformer	196
138	methoxy to CF3.rxn	**Remote** change of OCH_3 to CF_3 at the ring near ring 2 of BB	There is no active conformer	There is no active conformer	There is no active conformer	23

139	methoxy to CF3.rxn	**Remote** change of OCH_3 to CF_3 at the ring near ring 2 of BB	There is no active conformer	There is no active conformer	There is no active conformer	182
140	methoxy to chlorine.rxn	**Remote** change of OCH_3 to Cl at the ring near ring 2 of BB	29 %	40 %	0 %	98
141	methoxy to chlorine.rxn	**Remote** change of OCH_3 to Cl at the ring near ring 2 of BB	There is no active conformer	There is no active conformer	There is no active conformer	176
142	methoxy to cyano.rxn	**Remote** change of OCH_3 to cyano at the ring near ring 2 of BB	78 %	27 %	0 %	145
143	methoxy to chlorine.rxn	**Remote** change of OCH_3 to cyano at the ring near ring 2 of BB	There is no active conformer	There is no active conformer	There is no active conformer	177

144	methylate N.rxn	**UREA CHANGED**	**UREA CHANGED**	**UREA CHANGED**	**UREA CHANGED**	**UREA CHANGED**
145	methylate N.rxn	**UREA CHANGED**	**UREA CHANGED**	**UREA CHANGED**	**UREA CHANGED**	**UREA CHANGED**
146	methylate [OS] inv.rxn	**Remote** change of OCH_3 to OH at the ring near ring 2 of BB	12 %	100 %	2 %	65
147	methylate [OS] inv.rxn	**Remote** change of OCH_3 to OH at the ring near ring 2 of BB	0 %	0 %	-	64
148	phenyl to indole.rxn	**Remote** a ring attached to the benzene near the ring 6 of BB	0 %	10 %	1%	92

149	phenyl to indole.rxn	**Remote** a ring attached to the benzene near the ring 6 of BB	There is no active conformer	There is no active conformer	There is no active conformer	203
150	phenyl to indole.rxn	**Remote** a ring with S attached to the benzene near the ring 6 of BB	There is no active conformer	There is no active conformer	There is no active conformer	178
151	phenyl to indole.rxn	**Near active site** a ring attached to the benzene near urea	There is no active conformer	There is no active conformer	There is no active conformer	43
152	phenyl to indole.rxn	**Near active site** a ring attached to the benzene near urea	There is no active conformer	There is no active conformer	There is no active conformer	167
153	phenyl to indole.rxn	**Near active site** a ring attached to the benzene near urea	There is no active conformer	There is no active conformer	There is no active conformer	160

154	phenyl to indole.rxn	**Near active site** a ring with O attached to the benzene near urea	There is no active conformer	There is no active conformer	There is no active conformer	179
155	phenyl to indole.rxn	**Near active site** a ring with S attached to the benzene near urea	There is no active conformer	There is no active conformer	There is no active conformer	175
156	phenyl to indole.rxn	**Near active site** a ring attached to the benzene near urea	There is no active conformer	There is no active conformer	There is no active conformer	172
157	phenyl to indole.rxn	**Near active site** a ring with O attached to the benzene near urea	There is no active conformer	There is no active conformer	There is no active conformer	167
158	phenyl to indole.rxn	**Near active site** a ring with S attached to the benzene near urea	There is no active conformer	There is no active conformer	There is no active conformer	182

159	phenyl to indole.rxn	**Near active site** a ring attached to the benzene near urea	There is no active conformer	There is no active conformer	There is no active conformer	54
160	phenyl to indole.rxn	**Near active site** a ring attached to the benzene near urea	There is no active conformer	There is no active conformer	There is no active conformer	36
161	phenyl to indole.rxn	**Near active site** a ring attached to the benzene near urea	There is no active conformer	There is no active conformer	There is no active conformer	43
162	phenyl to indole.rxn	**Remote** the ring changed near 2. ring of BB	21 %	100 %	0 %	62
163	phenyl to indole.rxn	**Remote** the ring changed near 2. ring of BB	0 %	0 %	-	41

164	phenyl to indole.rxn	**Remote** the ring changed near 2. ring of BB	There is no active conformer	There is no active conformer	There is no active conformer	172
165	phenyl to indole.rxn	**Remote** the ring changed near 2. ring of BB	60 %	0 %	0%	127
166	phenyl to indole.rxn	**Remote** the ring changed near 2. ring of BB	There is no active conformer	There is no active conformer	There is no active conformer	165
167	phenyl to indole.rxn	**Remote** the ring changed near 2. ring of BB	There is no active conformer	There is no active conformer	There is no active conformer	165
168	phenyl to indole.rxn	**Remote** the ring changed near 2. ring of BB	There is no active conformer	There is no active conformer	There is no active conformer	167

169	phenyl to indole.rxn	**Remote** the ring changed near 2. ring of BB	There is no active conformer	There is no active conformer	There is no active conformer	162
170	phenyl to indole.rxn	**Remote** the ring changed near 2. ring of BB	There is no active conformer	There is no active conformer	There is no active conformer	152
171	phenyl to indole.rxn	**Remote** the ring changed near 2. ring of BB	There is no active conformer	There is no active conformer	There is no active conformer	167
172	phenyl to indole.rxn	**Remote** the ring changed near 2. ring of BB	0 %	100 %	-	35
173	phenyl to indole.rxn	**Remote** the ring changed near 2. ring of BB	0 %	-	-	34

174	phenyl to indole.rxn	**Remote** the ring changed near 2. ring of BB	5 %	5 %	-	36
175	phenyl to indole.rxn	**Remote** the ring changed near 2. ring of BB	10 %	22 %	-	16
176	phenyl to indole.rxn	**ALCOHOL CHANGED**	**ALCOHOL CHANGED**	**ALCOHOL CHANGED**	**ALCOHOL CHANGED**	**ALCOHOL CHANGED**
177	phenyl to indole.rxn	**ALCOHOL CHANGED**	**ALCOHOL CHANGED**	**ALCOHOL CHANGED**	**ALCOHOL CHANGED**	**ALCOHOL CHANGED**
178	phenyl to indole.rxn	**ALCOHOL CHANGED**	**ALCOHOL CHANGED**	**ALCOHOL CHANGED**	**ALCOHOL CHANGED**	**ALCOHOL CHANGED**

179	phenyl to indole.rxn	**ALCOHOL CHANGED**	**ALCOHOL CHANGED**	**ALCOHOL CHANGED**	**ALCOHOL CHANGED**	**ALCOHOL CHANGED**
180	phenyl to indole.rxn	**ALCOHOL CHANGED**	**ALCOHOL CHANGED**	**ALCOHOL CHANGED**	**ALCOHOL CHANGED**	**ALCOHOL CHANGED**
181	phenyl to indole.rxn	**ALCOHOL CHANGED**	**ALCOHOL CHANGED**	**ALCOHOL CHANGED**	**ALCOHOL CHANGED**	**ALCOHOL CHANGED**
182	phenyl to indole.rxn	**ALCOHOL CHANGED**	**ALCOHOL CHANGED**	**ALCOHOL CHANGED**	**ALCOHOL CHANGED**	**ALCOHOL CHANGED**
183	phenyl to indole.rxn	**ALCOHOL CHANGED**	**ALCOHOL CHANGED**	**ALCOHOL CHANGED**	**ALCOHOL CHANGED**	**ALCOHOL CHANGED**

184	phenyl to indole.rxn	**ALCOHOL CHANGED**	**ALCOHOL CHANGED**	**ALCOHOL CHANGED**	**ALCOHOL CHANGED**	**ALCOHOL CHANGED**
185	phenyl to indole.rxn	**ALCOHOL CHANGED**	**ALCOHOL CHANGED**	**ALCOHOL CHANGED**	**ALCOHOL CHANGED**	**ALCOHOL CHANGED**
186	phenyl to indole.rxn	**ALCOHOL CHANGED**	**ALCOHOL CHANGED**	**ALCOHOL CHANGED**	**ALCOHOL CHANGED**	**ALCOHOL CHANGED**
187	phenyl to indole.rxn	**ALCOHOL CHANGED**	**ALCOHOL CHANGED**	**ALCOHOL CHANGED**	**ALCOHOL CHANGED**	**ALCOHOL CHANGED**
188	phenyl to oxime 1.rxn	**Near active site** benzene changed near urea	There is no active conformer	There is no active conformer	There is no active conformer	25

189	phenyl to oxime 1.rxn	**Near active site** benzene changed near urea	There is no active conformer	There is no active conformer	There is no active conformer	43
190	phenyl to oxime 1.rxn	**Near active site** benzene changed near urea	There is no active conformer	There is no active conformer	There is no active conformer	29
191	phenyl to thiophene 2.rxn	**Remote** benzene changed near 6. ring of BB	There is no active conformer	There is no active conformer	There is no active conformer	20
192	phenyl to oxime 2.rxn	**Remote** benzene changed near 6. ring of BB	1 %	100 %	0%	75
193	phenyl to oxime 2.rxn	**Remote** benzene changed near 6. ring of BB	0 %	-	-	34

194	phenyl to oxime 2.rxn	**Remote** benzene changed near 6. ring of BB	There is no active conformer	There is no active conformer	There is no active conformer	55
195	phenyl to oxime 2.rxn	**Remote** benzene changed near 6. ring of BB	There is no active conformer	There is no active conformer	There is no active conformer	27
196	phenyl to oxime 2.rxn	**Remote** benzene changed near 6. ring of BB	There is no active conformer	There is no active conformer	There is no active conformer	33
197	phenyl to oxime 2.rxn	**Near active site** benzene changed near urea	There is no active conformer	There is no active conformer	There is no active conformer	24
198	phenyl to oxime 2.rxn	**Near active site** benzene changed near urea	There is no active conformer	There is no active conformer	There is no active conformer	35

199	phenyl to oxime 2.rxn	**Near active site** benzene changed near urea	3 %	-	-	31
200	phenyl to oxime 2.rxn	**Near active site** benzene changed near urea	There is no active conformer	There is no active conformer	There is no active conformer	25
201	phenyl to oxime 2.rxn	**Near active site** benzene changed near urea	There is no active conformer	There is no active conformer	There is no active conformer	70
202	phenyl to oxime 2.rxn	**Near active site** benzene changed near urea	There is no active conformer	There is no active conformer	There is no active conformer	29
203	phenyl to oxime 2.rxn	**Remote** the ring changed near 2. ring of BB	0 %	-	-	45

204	phenyl to oxime 2.rxn	**Remote** the ring changed near 2. ring of BB	There is no active conformer	There is no active conformer	There is no active conformer	57
205	phenyl to oxime 2.rxn	**Remote** the ring changed near 2. ring of BB	There is no active conformer	There is no active conformer	There is no active conformer	24
206	phenyl to oxime 2.rxn	**ALCOHOL CHANGED**	**ALCOHOL CHANGED**	**ALCOHOL CHANGED**	**ALCOHOL CHANGED**	**ALCOHOL CHANGED**
207	phenyl to oxime 2.rxn	**ALCOHOL CHANGED**	**ALCOHOL CHANGED**	**ALCOHOL CHANGED**	**ALCOHOL CHANGED**	**ALCOHOL CHANGED**
208	phenyl to oxime 2.rxn	**ALCOHOL CHANGED**	**ALCOHOL CHANGED**	**ALCOHOL CHANGED**	**ALCOHOL CHANGED**	**ALCOHOL CHANGED**

209	phenyl to oxime 2.rxn	**ALCOHOL CHANGED**	**ALCOHOL CHANGED**	**ALCOHOL CHANGED**	**ALCOHOL CHANGED**	**ALCOHOL CHANGED**
210	phenyl to oxime 2.rxn	**ALCOHOL CHANGED**	**ALCOHOL CHANGED**	**ALCOHOL CHANGED**	**ALCOHOL CHANGED**	**ALCOHOL CHANGED**
211	phenyl to oxime 2.rxn	**ALCOHOL CHANGED**	**ALCOHOL CHANGED**	**ALCOHOL CHANGED**	**ALCOHOL CHANGED**	**ALCOHOL CHANGED**
212	phenyl to oxime 2.rxn	**ALCOHOL CHANGED**	**ALCOHOL CHANGED**	**ALCOHOL CHANGED**	**ALCOHOL CHANGED**	**ALCOHOL CHANGED**
213	phenyl to oxime 2.rxn	**ALCOHOL CHANGED**	**ALCOHOL CHANGED**	**ALCOHOL CHANGED**	**ALCOHOL CHANGED**	**ALCOHOL CHANGED**

214	phenyl to oxime 2.rxn	**ALCOHOL CHANGED**	**ALCOHOL CHANGED**	**ALCOHOL CHANGED**	**ALCOHOL CHANGED**	**ALCOHOL CHANGED**
215	phenyl to thiophene 3.rxn	**Near active site** benzene changed near urea	There is no active conformer	There is no active conformer	There is no active conformer	81
216	phenyl to thiophene 3.rxn	**Near active site** benzene changed near urea	0 %	1%	0%	165
217	phenyl to thiophene 3.rxn	**Near active site** benzene changed near urea	There is no active conformer	There is no active conformer	There is no active conformer	86
218	phenyl to thiophene 3.rxn	**Near active site** benzene changed near urea	There is no active conformer	There is no active conformer	There is no active conformer	103

219	phenyl to thiophene 3.rxn	**Near active site** benzene changed near urea	There is no active conformer	There is no active conformer	There is no active conformer	42
220	phenyl to thiophene 3.rxn	**Near active site** benzene changed near urea	4 %	5%	0%	69
221	phenyl to thiophene 3.rxn	**Near active site** benzene changed near urea	There is no active conformer	There is no active conformer	There is no active conformer	18
222	phenyl to thiophene 3.rxn	**Near active site** benzene changed near urea	There is no active conformer	There is no active conformer	There is no active conformer	74
223	phenyl to thiophene 3.rxn	**Near active site** benzene changed near urea	There is no active conformer	There is no active conformer	There is no active conformer	49

224	phenyl to thiophene 3.rxn	**Near active site** the ring changed near urea	There is no active conformer	There is no active conformer	There is no active conformer	16
225	phenyl to thiophene 3.rxn	**Near active site** the ring changed near urea	There is no active conformer	There is no active conformer	There is no active conformer	14
226	phenyl to thiophene 3.rxn	**Near active site** the ring changed near urea	There is no active conformer	There is no active conformer	There is no active conformer	41
227	phenyl to thiophene 3.rxn	**Near active site** the ring changed near urea	There is no active conformer	There is no active conformer	There is no active conformer	72
228	phenyl to thiophene 3.rxn	**Near active site** the ring changed near urea	There is no active conformer	There is no active conformer	There is no active conformer	31

229	phenyl to thiophene 3.rxn	**Near active site** the ring changed near urea	There is no active conformer	There is no active conformer	There is no active conformer	20
230	phenyl to thiophene 3.rxn	**Near active site** the ring changed near urea	There is no active conformer	There is no active conformer	There is no active conformer	107
231	phenyl to thiophene 3.rxn	**Near active site** the ring changed near urea	There is no active conformer	There is no active conformer	There is no active conformer	13
232	phenyl to thiophene 3.rxn	**Near active site** the ring changed near urea	There is no active conformer	There is no active conformer	There is no active conformer	16
233	phenyl to thiophene 3.rxn	**Remote** the ring changed near 2. ring of BB	There is no active conformer	There is no active conformer	There is no active conformer	17

234	phenyl to thiophene 3.rxn	**Remote** the ring changed near 2. ring of BB	There is no active conformer	There is no active conformer	There is no active conformer	19
235	phenyl to thiophene 3.rxn	**Remote** the ring changed near 2. ring of BB	There is no active conformer	There is no active conformer	There is no active conformer	167
236	phenyl to thiophene 3.rxn	**Remote** the ring changed near 2. ring of BB	There is no active conformer	There is no active conformer	There is no active conformer	17
237	phenyl to thiophene 3.rxn	**Remote** the ring changed near 2. ring of BB	There is no active conformer	There is no active conformer	There is no active conformer	177
238	phenyl to thiophene 3.rxn	**Remote** the ring changed near 2. ring of BB	There is no active conformer	There is no active conformer	There is no active conformer	52

239	phenyl to thiophene 4.rxn	**Near active site** benzene changed near urea	There is no active conformer	There is no active conformer	There is no active conformer	37
240	phenyl to thiophene 4.rxn	**Near active site** benzene changed near urea	There is no active conformer	There is no active conformer	There is no active conformer	20
241	phenyl to thiophene 4.rxn	**Near active site** benzene changed near urea	There is no active conformer	There is no active conformer	There is no active conformer	170
242	phenyl to thiophene 4.rxn	**Remote** the ring changed near 2. ring of BB	There is no active conformer	There is no active conformer	There is no active conformer	177
243	phenyl to thiophene 4.rxn	**Remote** the ring changed near 2. ring of BB	There is no active conformer	There is no active conformer	There is no active conformer	176

244	phenyl to thiophene 4.rxn	**Remote** the ring changed near 2. ring of BB	There is no active conformer	There is no active conformer	There is no active conformer	172
245	pyridine to benzene.rxn	**PYRIDINE CHANGED**	**PYRIDINE CHANGED**	**PYRIDINE CHANGED**	**PYRIDINE CHANGED**	**PYRIDINE CHANGED**
246	urea close 5.rxn	**PYRIDINE CHANGED**	**PYRIDINE CHANGED**	**PYRIDINE CHANGED**	**PYRIDINE CHANGED**	**PYRIDINE CHANGED**
247	urea to guanidine.rxn	**UREA CHANGED**	**UREA CHANGED**	**UREA CHANGED**	**UREA CHANGED**	**UREA CHANGED**
248	urea to guanidine.rxn	**UREA CHANGED**	**UREA CHANGED**	**UREA CHANGED**	**UREA CHANGED**	**UREA CHANGED**

249	urea to guanidine.rxn	**Backbone** **Near Active Site (pyridine)** change of CO to CNH at 6.ring of BB	There is no active conformer	There is no active conformer	There is no active conformer	43
250	urea to guanidine.rxn	**UREA CHANGED**	**UREA CHANGED**	**UREA CHANGED**	**UREA CHANGED**	**UREA CHANGED**
251	urea to guanidine.rxn	**UREA CHANGED**	**UREA CHANGED**	**UREA CHANGED**	**UREA CHANGED**	**UREA CHANGED**
252	urea to guanidine.rxn	**UREA CHANGED**	**UREA CHANGED**	**UREA CHANGED**	**UREA CHANGED**	**UREA CHANGED**
253	urea to guanidine.rxn	**UREA CHANGED**	**UREA CHANGED**	**UREA CHANGED**	**UREA CHANGED**	**UREA CHANGED**

254	urea to guanidine.rxn	**UREA CHANGED**	**UREA CHANGED**	**UREA CHANGED**	**UREA CHANGED**	**UREA CHANGED**
255	urea to guanidine.rxn	**UREA CHANGED**	**UREA CHANGED**	**UREA CHANGED**	**UREA CHANGED**	**UREA CHANGED**
256	urea to guanidine.rxn	**UREA CHANGED**	**UREA CHANGED**	**UREA CHANGED**	**UREA CHANGED**	**UREA CHANGED**
257	urea to guanidine.rxn	**UREA CHANGED**	**UREA CHANGED**	**UREA CHANGED**	**UREA CHANGED**	**UREA CHANGED**
258	urea to guanidine.rxn	**UREA CHANGED**	**UREA CHANGED**	**UREA CHANGED**	**UREA CHANGED**	**UREA CHANGED**

Table A.2. Database of 258 derivatives of TF3 spiroligozyme by iteration 1 (pages 141- 152)

Derivative Number	Transformation Reaction	RMSD	Synthesizability
1	C=O to C=S	0.2285	0.6774
2	C=O to C=S	0.2340	0.6774
3	C=O to C=S	0.2220	0.6774
4	C=O to C=S	0.2433	0.6667
5	C=O to C=S	0.2533	0.6774
6	C=O to C=S	0.2373	0.6774
7	C=O to C=S	0.2301	0.6667
8	C=O to C=S	0.2687	0.6667
9	C=O to C=S	0.2213	0.6774
10	C=O to SO2	0.2514	0.6702
11	C=O to SO2	0.2064	0.6702
12	C=O to SO2	0.2410	0.7766
13	C=O to SO2	0.2347	0.6702
14	C=O to SO2	0.2647	0.7553
15	C=O to SO2	0.2794	0.7447
16	C=O to SO2	0.2675	0.6702
17	C=O to SO2	0.2643	0.6702
18	C=O to SO2	0.2195	0.7128
19	CF3 TO CARBOXYL	0.2342	0.6630
20	CF3 TO CHLORINE	0.2323	0.6556

21	CF3 TO CYANO	0.2167	0.5275
22	CF3 TO METHOXY	0.2119	0.6593
23	CF3 TO METHOXY	0.2273	0.5385
24	CF3 TO METHOXY	0.2414	0.5385
25	C[NOSFClBr] to C(OMe)	0.2197	0.6702
26	C[NOSFClBr] to C(OMe)	0.2284	0.6702
27	C[NOSFClBr] to C(OMe)	0.2330	0.6702
28	C[NOSFClBr] to C(OMe)	0.2256	0.6809
29	C[NOSFClBr] to C(OMe)	0.2279	0.6809
30	C[NOSFClBr] to C(OMe)	0.2317	0.6809
31	C[NOSFClBr] to C(OMe)	0.2476	0.6702
32	C[NOSFClBr] to C(OMe)	0.2703	0.6702
33	C[NOSFClBr] to C(OMe)	0.2612	0.6702
34	C[CNSFClBrI] to C(O).rxn	0.2260	0.6667
35	C[COSFClBRI] to C(N).rxn	0.2196	0.6667
36	C[COSFClBRI] to C(N).rxn	0.2048	0.6774
37	C[COSFClBRI] to C(N).rxn	0.2456	0.6667
38	C[NOSFClBRI] to C(C).rxn	0.2113	0.6667
39	C[NOSFClBRI] to C(C).rxn	0.2039	0.6667
40	C[NOSFClBRI] to C(C).rxn	0.2736	0.6667
41	C[NOSFClBRI] to C(cyano).rxn	0.2124	0.6702
42	C[NOSFClBRI] to C(cyano).rxn	0.2020	0.6596
43	C[NOSFClBRI] to C(cyano).rxn	0.2632	0.6702

44	C[NOS]C to C(C=O)C.rxn	0.2112	0.6702
45	C[NOS]C to C(C=O)C.rxn	0.2409	0.6702
46	C[NOS]C to C(C=O)C.rxn	0.2137	0.6702
47	C[NOS]C to C(C=O)C.rxn	0.2400	0.5532
48	C[NOS]C to C(S=O)C.rxn	0.2817	0.6702
49	C[NOS]C to C(S=O)C.rxn	0.2712	0.6702
50	C[NOS]C to C(S=O)C.rxn	0.2389	0.6702
51	C[NOS]C to C(S=O)C.rxn	0.2682	0.6702
52	C[NOS]C to C(SO2)C.rxn	0.2950	0.6737
53	C[NOS]C to C(SO2)C.rxn	0.2742	0.6737
54	C[NOS]C to C(SO2)C.rxn	0.2446	0.5474
55	C[NOS]C to C(SO2)C.rxn	0.2673	0.5474
56	C[NO]C to CSC.rxn	0.2517	0.6667
57	C[NO]C to CSC.rxn	0.2199	0.6667
58	C[NO]C to CSC.rxn	0.2528	0.6667
59	C[NO]C to CSC.rxn	0.2495	0.6667
60	C[NO]C to CSC.rxn	0.2434	0.5699
61	C[NO]C to CSC.rxn	0.2244	0.6667
62	C[NO]C to CSC.rxn	0.2505	0.5699
63	C[NO]C to CSC.rxn	0.2256	0.5699
64	Cyclo56.rxn	0.2803	0.6596
65	Cyclo56.rxn	0.2715	0.6596
66	Cyclo56.rxn	0.2795	0.6596

67	Cyclo56.rxn	0.2897	0.7766
68	Cyclo56.rxn	0.3031	0.6596
69	Cyclo56.rxn	0.2936	0.6596
70	Cyclo56.rxn	0.2750	0.6596
71	N14Substraction.rxn	0.2211	0.5806
72	N14Substraction.rxn	0.2357	0.6667
73	ace [NOS].rxn	0.2331	0.6875
74	ace [NOS].rxn	0.2672	0.6771
75	amide to amine.rxn	0.2197	0.6739
76	amide to amine.rxn	0.2315	0.6739
77	amide to amine.rxn	0.2303	0.6739
78	amide to amine.rxn	0.1871	0.6739
79	amide to amine.rxn	0.2255	0.6739
80	amide to amine.rxn	0.2233	0.6630
81	amide to amine.rxn	0.2138	0.6848
82	amide to hydroxyethyl.rxn	0.2518	0.6774
83	amide to hydroxyethyl.rxn	0.2382	0.6774
84	amide to hydroxyethyl.rxn	0.2431	0.6667
85	amide to hydroxyethyl.rxn	0.2417	0.5806
86	amide to hydroxyethyl.rxn	0.2752	0.6559
87	amide to hydroxyethyl.rxn	0.2243	0.5914
88	amide to ketone .rxn	0.2209	0.6667
89	amide to ketone .rxn	0.2071	0.6667

90	amide to ketone .rxn	0.2518	0.6667
91	amide to ketone .rxn	0.2288	0.6237
92	amide to ketone .rxn	0.2036	0.5806
93	amide to ketone .rxn	0.2400	0.6667
94	amide to ketone .rxn	0.2417	0.6667
95	amine to amide.rxn	0.2124	0.7766
96	amine to amide.rxn	0.2280	0.7766
97	amine to amide.rxn	0.2319	0.6809
98	amine to amide.rxn	0.2459	0.6809
99	amine to amide.rxn	0.2253	0.6809
100	amine to amide.rxn	0.2472	0.7872
101	amine to amide.rxn	0.2355	0.6702
102	aro6 N 12 switch.rxn	0.2253	0.6667
103	aro6 N 13 switch.rxn	0.2217	0.6667
104	benzene to pyridine.rxn	0.2231	0.6667
105	benzene to pyridine.rxn	0.2200	0.6667
106	benzene to pyridine.rxn	0.2177	0.6667
107	benzene to pyridine.rxn	0.2221	0.6667
108	benzene to pyridine.rxn	0.2210	0.6667
109	benzene to pyridine.rxn	0.2063	0.6667
110	benzene to pyridine.rxn	0.2281	0.6667
111	benzene to pyridine.rxn	0.2229	0.6667
112	benzene to pyridine.rxn	0.2096	0.6667

113	benzene to pyridine.rxn	0.2117	0.6667
114	benzene to pyridine.rxn	0.2222	0.6667
115	benzene to pyridine.rxn	0.2087	0.6667
116	benzene to pyridine.rxn	0.1993	0.6667
117	benzene to pyridine.rxn	0.2022	0.6667
118	benzene to pyridine.rxn	0.2174	0.6667
119	benzene to pyridine.rxn	0.2209	0.6667
120	carbonyl to cyclooxime.rxn	0.2929	0.6915
121	carbonyl to cyclooxime.rxn	0.2947	0.6915
122	carbonyl to cyclooxime.rxn	0.2924	0.6915
123	carbonyl to isooxazole3.rxn	0.3356	0.7872
124	carbonyl to isooxazole3.rxn	0.2776	0.7872
125	carboxylate to CF3.rxn	0.2298	0.6596
126	carboxylate to acylsufonamide.rxn	0.2612	0.6907
127	carboxylate to sufonamide.rxn	0.2386	0.7128
128	carboxylate to tetrazole.rxn	0.2396	0.7158
129	ester to oxadiazole.rxn	0.3979	0.7872
130	ester to oxazole. rxn	0.3890	0.7872
131	hom [NOS]CH2.rxn	0.3232	0.6702
132	hom [NOS]CH2.rxn	0.3067	0.5745
133	hom [NOS]CH2.rxn	0.2946	0.5638
134	hom [NOS]CH2.rxn	0.2745	0.6702
135	hom [NOS]CH2.rxn	0.2730	0.6702

136	hom [NOS]CH2.rxn	0.2702	0.6702
137	hydroxy to chlorine.rxn	0.2136	0.6774
138	methoxy to CF3.rxn	0.2481	0.5474
139	methoxy to CF3.rxn	0.2514	0.5474
140	methoxy to chlorine.rxn	0.2229	0.6630
141	methoxy to chlorine.rxn	0.2275	0.6630
142	methoxy to cyano.rxn	0.2491	0.5591
143	methoxy to chlorine.rxn	0.2453	0.5591
144	methylate N.rxn	0.2125	0.6702
145	methylate N.rxn	0.2607	0.6702
146	methylate [OS] inv.rxn	0.2175	0.6630
147	methylate [OS] inv.rxn	0.2204	0.6630
148	phenyl to indole.rxn	0.3069	0.6771
149	phenyl to indole.rxn	0.3136	0.6771
150	phenyl to indole.rxn	0.3137	0.6771
151	phenyl to indole.rxn	0.3336	0.6771
152	phenyl to indole.rxn	0.3269	0.6771
153	phenyl to indole.rxn	0.3940	0.6771
154	phenyl to indole.rxn	0.3961	0.6771
155	phenyl to indole.rxn	0.4014	0.6771
156	phenyl to indole.rxn	0.3925	0.6771
157	phenyl to indole.rxn	0.3937	0.6771
158	phenyl to indole.rxn	0.4046	0.6771

159	phenyl to indole.rxn	0.3888	0.6771
160	phenyl to indole.rxn	0.3954	0.6771
161	phenyl to indole.rxn	0.4028	0.6771
162	phenyl to indole.rxn	0.3513	0.5833
163	phenyl to indole.rxn	0.3363	0.6771
164	phenyl to indole.rxn	0.3277	0.6771
165	phenyl to indole.rxn	0.3468	0.5729
166	phenyl to indole.rxn	0.3359	0.6771
167	phenyl to indole.rxn	0.3745	0.6771
168	phenyl to indole.rxn	0.3704	0.6771
169	phenyl to indole.rxn	0.3868	0.6771
170	phenyl to indole.rxn	0.3703	0.6771
171	phenyl to indole.rxn	0.3748	0.6771
172	phenyl to indole.rxn	0.3767	0.5833
173	phenyl to indole.rxn	0.3401	0.5625
174	phenyl to indole.rxn	0.3374	0.5625
175	phenyl to indole.rxn	0.3508	0.5625
176	phenyl to indole.rxn	0.3410	0.5729
177	phenyl to indole.rxn	0.3359	0.5729
178	phenyl to indole.rxn	0.3475	0.5729
179	phenyl to indole.rxn	0.3351	0.6771
180	phenyl to indole.rxn	0.3317	0.6771
181	phenyl to indole.rxn	0.3424	0.6771

182	phenyl to indole.rxn	0.3270	0.6771
183	phenyl to indole.rxn	0.3176	0.6771
184	phenyl to indole.rxn	0.3435	0.6771
185	phenyl to indole.rxn	0.3302	0.5729
186	phenyl to indole.rxn	0.3292	0.5729
187	phenyl to indole.rxn	0.3408	0.5729
188	phenyl to oxime 1.rxn	0.2402	0.6556
189	phenyl to oxime 1.rxn	0.2553	0.6556
190	phenyl to oxime 1.rxn	0.2157	0.6556
191	phenyl to thiophene 2.rxn	0.2332	0.6630
192	phenyl to oxime 2.rxn	0.2380	0.6630
193	phenyl to oxime 2.rxn	0.2403	0.6630
194	phenyl to oxime 2.rxn	0.2275	0.6630
195	phenyl to oxime 2.rxn	0.2273	0.6630
196	phenyl to oxime 2.rxn	0.2518	0.6630
197	phenyl to oxime 2.rxn	0.2495	0.6630
198	phenyl to oxime 2.rxn	0.2615	0.6630
199	phenyl to oxime 2.rxn	0.2593	0.6630
200	phenyl to oxime 2.rxn	0.2489	0.6630
201	phenyl to oxime 2.rxn	0.2434	0.6630
202	phenyl to oxime 2.rxn	0.2671	0.6630
203	phenyl to oxime 2.rxn	0.2768	0.6630
204	phenyl to oxime 2.rxn	0.2993	0.6630

205	phenyl to oxime 2.rxn	0.3105	0.6630
206	phenyl to oxime 2.rxn	0.2298	0.6630
207	phenyl to oxime 2.rxn	0.2042	0.6630
208	phenyl to oxime 2.rxn	0.2310	0.6630
209	phenyl to oxime 2.rxn	0.2323	0.6630
210	phenyl to oxime 2.rxn	0.2199	0.6630
211	phenyl to oxime 2.rxn	0.2232	0.6630
212	phenyl to oxime 2.rxn	0.2320	0.6630
213	phenyl to oxime 2.rxn	0.2466	0.6630
214	phenyl to oxime 2.rxn	0.2008	0.6630
215	phenyl to thiophene 3.rxn	0.2563	0.6630
216	phenyl to thiophene 3.rxn	0.2508	0.6630
217	phenyl to thiophene 3.rxn	0.2594	0.6630
218	phenyl to thiophene 3.rxn	0.3528	0.6630
219	phenyl to thiophene 3.rxn	0.3488	0.6630
220	phenyl to thiophene 3.rxn	0.3466	0.6630
221	phenyl to thiophene 3.rxn	0.3615	0.6630
222	phenyl to thiophene 3.rxn	0.3518	0.6630
223	phenyl to thiophene 3.rxn	0.3374	0.6630
224	phenyl to thiophene 3.rxn	0.3212	0.5326
225	phenyl to thiophene 3.rxn	0.3204	0.5326
226	phenyl to thiophene 3.rxn	0.3280	0.5326
227	phenyl to thiophene 3.rxn	0.3483	0.5326

228	phenyl to thiophene 3.rxn	0.3268	0.5326
229	phenyl to thiophene 3.rxn	0.3217	0.5326
230	phenyl to thiophene 3.rxn	0.3242	0.5326
231	phenyl to thiophene 3.rxn	0.3112	0.5326
232	phenyl to thiophene 3.rxn	0.3062	0.5326
233	phenyl to thiophene 3.rxn	0.2931	0.6630
234	phenyl to thiophene 3.rxn	0.2774	0.6630
235	phenyl to thiophene 3.rxn	0.2656	0.6630
236	phenyl to thiophene 3.rxn	0.3181	0.5870
237	phenyl to thiophene 3.rxn	0.2990	0.5870
238	phenyl to thiophene 3.rxn	0.2864	0.5870
239	phenyl to thiophene 4.rxn	0.3561	0.6630
240	phenyl to thiophene 4.rxn	0.3367	0.6630
241	phenyl to thiophene 4.rxn	0.3470	0.6630
242	phenyl to thiophene 4.rxn	0.2995	0.6630
243	phenyl to thiophene 4.rxn	0.2930	0.6630
244	phenyl to thiophene 4.rxn	0.2971	0.6630
245	pyridine to benzene.rxn	0.2058	0.6667
246	urea close 5.rxn	0.2138	0.6667
247	urea to guanidine.rxn	0.2879	0.6737
248	urea to guanidine.rxn	0.2769	0.6771
249	urea to guanidine.rxn	0.2266	0.6667
250	urea to guanidine.rxn	0.2216	0.6667

251	urea to guanidine.rxn	0.2423	0.6667
252	urea to guanidine.rxn	0.2639	0.6667
253	urea to guanidine.rxn	0.2347	0.6667
254	urea to guanidine.rxn	0.2454	0.6667
255	urea to guanidine.rxn	0.2714	0.6667
256	urea to guanidine.rxn	0.2624	0.6667
257	urea to guanidine.rxn	0.2625	0.6667
258	urea to guanidine.rxn	0.3056	0.6667

Database Viewer : $DESKTOP/TF3SPIROLIGOZIM_ITERATION2.mdb

File Edit Display Compute Window Help SVL DBV MOE Cancel

	outmol	rule	inmol	mseq	# trans	RMSD	rsynth
1	15b.pdb	C=O_to_C=S.rxn	15b.pdb	1	1	0.2285	0.6774
2	15b.pdb	C=O_to_C=S.rxn	15b.pdb	2	1	0.2340	0.6774
3	15b.pdb	C=O_to_C=S.rxn	15b.pdb	3	1	0.2220	0.6774
4	15b.pdb	C=O_to_C=S.rxn	15b.pdb	4	1	0.2433	0.6667
5	15b.pdb	C=O_to_C=S.rxn	15b.pdb	5	1	0.2553	0.6774
6	15b.pdb	C=O_to_C=S.rxn	15b.pdb	6	1	0.2373	0.6774
7	15b.pdb	C=O_to_C=S.rxn	15b.pdb	7	1	0.2301	0.6667
8	15b.pdb	C=O_to_C=S.rxn	15b.pdb	8	1	0.2687	0.6667
9	15b.pdb	C=O_to_C=S.rxn	15b.pdb	9	1	0.2213	0.6774
10	15b.pdb	C=O_to_SO2.rxn	15b.pdb	10	1	0.1584	0.6702
11	15b.pdb	C=O_to_SO2.rxn	15b.pdb	11	1	0.1526	0.6702
12	15b.pdb	C=O_to_SO2.rxn	15b.pdb	12	1	0.1768	0.7766
13	15b.pdb	C=O_to_SO2.rxn	15b.pdb	13	1	0.1630	0.6702
14	15b.pdb	C=O_to_SO2.rxn	15b.pdb	14	1	0.2255	0.7553
15	15b.pdb	C=O_to_SO2.rxn	15b.pdb	15	1	0.2165	0.7447
16	15b.pdb	C=O_to_SO2.rxn	15b.pdb	16	1	0.1843	0.6702
17	15b.pdb	C=O_to_SO2.rxn	15b.pdb	17	1	0.1739	0.6702
18	15b.pdb	C=O_to_SO2.rxn	15b.pdb	18	1	0.1508	0.7128
19	15b.pdb	CF3_to_carboxyl	15b.pdb	19	1	0.2342	0.6630
20	15b.pdb	CF3_to_chlorine	15b.pdb	20	1	0.0499	0.6556
21	15b.pdb	CF3_to_cyano.rx	15b.pdb	21	1	0.1362	0.5275
22	15b.pdb	CF3_to_methoxy.	15b.pdb	22	1	0.0904	0.6593
23	15b.pdb	CF3_to_methoxy.	15b.pdb	23	1	0.0908	0.5385
24	15b.pdb	CF3_to_methoxy.	15b.pdb	24	1	0.1483	0.5385
25	15b.pdb	C[CNOSFClBrI]_t	15b.pdb	25	1	0.1093	0.6702
26	15b.pdb	C[CNOSFClBrI]_t	15b.pdb	26	1	0.0920	0.6702
27	15b.pdb	C[CNOSFClBrI]_t	15b.pdb	27	1	0.1522	0.6702
28	15b.pdb	C[CNOSFClBrI]_t	15b.pdb	28	1	0.1062	0.6809
29	15b.pdb	C[CNOSFClBrI]_t	15b.pdb	29	1	0.1265	0.6809
30	15b.pdb	C[CNOSFClBrI]_t	15b.pdb	30	1	0.1843	0.6809
31	15b.pdb	C[CNOSFClBrI]_t	15b.pdb	31	1	0.0699	0.6702
32	15b.pdb	C[CNOSFClBrI]_t	15b.pdb	32	1	0.0859	0.6702
33	15b.pdb	C[CNOSFClBrI]_t	15b.pdb	33	1	0.1706	0.6702
34	15b.pdb	C[CNSFClBrI]_to	15b.pdb	34	1	0.2260	0.6667

8411 entries, 0 selected, all visible. 7 fields, 0 selected, all visible.

Figure A.1. Database of 8411 derivatives of TF3 spiroligozyme obtained by iteration 2